ANTHROPOGENIC IMPACTS ON THE LANDSCAPE:

INVESTIGATIONS IN WATER QUALITY AND

CHANNEL STABILITY

By

SAGAR NEUPANE

Bachelor of Civil Engineering
Pokhara University
Kaski, Nepal
2006

Master of Science in Civil Engineering
University of Idaho
Boise, Idaho
2012

Submitted to the Faculty of the
Graduate College of the
Oklahoma State University
in partial fulfillment of
the requirements for
the Degree of
DOCTOR OF PHILOSOPHY
July, 2016

ANTHROPOGENIC IMPACTS ON THE LANDSCAPE:

INVESTIGATIONS IN WATER QUALITY AND

CHANNEL STABILITY

Dissertation Approved:

Dr. Jason R. Vogel

Dissertation Adviser

Dr. Daniel E. Storm

Dr. Garey A. Fox

Dr. Gregory G. Wilber

ACKNOWLEDGEMENTS

I am very thankful to my parents who inspired, supported and encouraged me to complete my higher studies. I would like to express my sincere gratitude to my major advisor Dr. Jason Vogel, for his continuous support, guidance, encouragement, motivation, inspiration and mentorship for my doctoral studies as well my professional career. I would like to express my special thanks to my committee members, Dr. Daniel Storm, Dr. Garey Fox and Dr. Gregory Wilber for their guidance on developing my research projects and timely support as well as constructive feedback on my dissertation and teaching me scientific skills. I am highly indebted for the support of Dr. Bill Barfield and Dr. Stephanie Vogel for her support in technical writing.

My research projects were supported by funding from Oklahoma Department of Transportation, Oklahoma Transportation Center, US Department of Transportation and Woolpert, Inc. I am thankful to all research funding agencies. My sincere appreciation goes to Professor John Phillips, Monty Ramming, Dr. Patrick Starks and Dr. Russell Dutnell for providing me information and data. I am thankful to Dr. Aaron Mittelstet, Magen Kegley, Riley Jones, Hanna Huling, and Alex McLemore for their assistance in field data collection and laboratory experiments.

I am grateful to my office Stantec for providing me flexible working hours during dissertation writing. Finally, I would like to thank my wife and all my family and friends for their patience, constant support and love.

Acknowledgements reflect the views of the author and are not endorsed by committee members or Oklahoma State University.

Name: SAGAR NEUPANE

Date of Degree: JULY, 2016

Title of Study: ANTHROPOGENIC IMPACTS ON THE LANDSCAPE: INVESTIGATIONS ON IN STREAM WATER QUALITY AND CHANNEL STABILITY

Major Field: BIOSYSTEMS AND AGRICULTURAL ENGINEERING

Abstract: The natural landscape has been impacted by human settlement, development and agricultural practices. One of the major impacts of these anthropogenic activities is excessive upland soil erosion. During runoff events, eroded soil, or sediment, is transported to surface-water bodies and may impair water quality. To evaluate water-quality impairments, turbidity, suspended sediment, color and dissolved organic carbon have been commonly monitored in surface waters. In this study, water-quality and channel-stability parameters were evaluated in three parts. The objective of the first part was to develop a turbidity prediction methodology which can be integrated into existing runoff-erosion models. Based on the soil primary-particle sizes (sand, silt and clay), a turbidity prediction methodology was developed and applied to selected soils from Oklahoma and South Carolina. The methodology can be an add-on tool to runoff-erosion models to predict turbidity. The objective of the second part was to predict the water color of water samples with heterogeneous organic sources. Results showed a high correlation (R^2 = 0.99 and Nash-Sutcliffe efficiency = 0.95) between predicted and measured color for multiple sources in a laboratory study. The results of this study could be useful to predict water color in runoff from field-scale watersheds. The objective for the third part was to develop and apply an integrated approach to evaluate channel planform stability in an agricultural watershed with limited field data using historical records such as plat maps, aerial images, flow records, and relevant historical events. The approach has been applied in the Cobb Creek watershed in west-central Oklahoma. The results of the third part showed the length of the stream-channel network increased between 1873 and 2013 in the watershed and also found a decreasing trend in channel lateral migrations and planform stability in the mainstem of Cobb Creek since 1940. Overall, the methodologies and findings presented in this dissertation are useful for modeling and assessing the impacts of anthropogenic activities on water quality in runoff and streams and can be useful tools in shaping future watershed-management decisions.

TABLE OF CONTENTS

LIST OF TABLES

Table Page

LIST OF FIGURES

CHAPTER I

INTRODUCTION

More than 50% of the earth's landscape has been degraded, altered, modified, and disturbed by anthropogenic impacts (Hooke et al 2012). Such anthropogenic impacts are the results of a wide range of human activities in the landscape. Agricultural practices, grazing, irrigation, deforestation, construction activities, dam operations, and urban developments are some of the human activities that may degrade earth's landscape. Tillage and application of fertilizers and soil amendments are common in agricultural, gardening, and large-scale nurseries. The biodiversity of global ecosystems have been impaired by such anthropogenic activities (MEA 2005; Morris 2010). To minimize the human impacts on landscapes, best management practices (BMPs) may be implemented. Soil conservation practices and channel restoration in the river landscape are commonly used to reduce erosion, maintain water quality, and improve channel stability. Such practices are monitored and assessed using water-quality parameters such as turbidity, color, dissolved organic matter, and suspended sediment concentration (Gergel et al. 2002; USEPA 2009). In addition, channel stability and associated historic channel morphological changes may be evaluated to help guide future sustainable river management methodologies (Brierley and Hooke 2015).

In this dissertation, to assist future landscape and watershed management decisions, two indicators of anthropogenic impacts on landscape are investigated. The first investigation is using regression relationships to estimate turbidity and water color in hydrologic water-quality models, which is related to water-quality impairments due to soil erosion, sediment, and nutrients; the second investigation is that of the impacts of anthropogenic disturbances on fluvial system. Three different research projects are presented based on those two investigations.

The objective of the first research project was to develop a turbidity prediction methodology, which can be integrated into existing runoff-erosion models. Overall objective of the second research project was to predict water color on water samples with heterogeneous organic source. Similarly, the objective of third project was to develop and apply an integrated approach to evaluate channel planform stability in an agricultural watershed with limited field data using historical records such as plat maps, aerial images, and relevant historical events. In this chapter, background of the three research projects is presented.

Background on Research Project One

Eroded soil particles deposited into the landscapes and transported into surface waters are commonly called sediment (Julien 2010). Excessive sediment loading is a primary cause for the listing of surface waters on the USEPA 303(d) for impacted waters (USEPA 2009). The sediment transported into surface waters is often measured in terms of suspended sediment. Suspended sediment concentration (SSC) and related parameters have been used as indicators of water-quality impairment. Turbidity is one of the SSC-related parameters that is used an indicator. The relationship between SSC and turbidity has been extensively studied (Gippel 1995; Lewis 1996; Wass et al. 1997; Holliday et al. 2003; Zabaleta et al. 2007; Minella et al. 2008; Patil 2010; Williamson and Crawford 2011; Marttila and Kløve 2012; Line et al. 2013; Rügner et al. 2013; Perkins et al. 2014; Slaets et al. 2014).

The term turbidity originated in the literature by Parmelee and Ellms (1899). They first introduced turbidity as it related to suspended sediment. Today turbidity is well known as the light scattering property of water that resembles, to some extent, water clarity. Clarity and turbidity are two different parameters, but the terms are sometimes used interchangeable in a physical sense because highly turbid water decreases clearness, or increases the cloudiness of water by reducing light reflectance and penetration (Davies-Colley and Smith 2001; Kirk 1985). The turbidity theory, principles and measurements techniques are well defined and discussed in the literature (Sadar 1998; 2004; Lawer 2005; Omar and MatJafri 2009). Lawer (2005) has an in-depth description of turbidity, its effects on particle sizes, and applications. Turbidity is commonly measured in nephelometric turbidity units (NTU) with a turbidity meter (ASTM 2011; USEPA 1999; APHA et al. 2012).

Turbidity has been shown a proxy for several water-quality parameters. Rügner et al. (2014) demonstrated a strong relationship between turbidity and polycyclic aromatic hydrocarbons (PAHs) present in streams. PAHs are USEPA priority pollutants (Yan et al. 2004). Turbidity can also be a proxy for total nitrogen present in river water (Kim and Furumai 2013). In their study, Kim and Furumai developed a relationship that predicted total nitrogen based on turbidity and electrical conductivity in the Teguri River watershed, Japan. In addition to this, turbidity has been shown as an indirect measurement for particulate organic nitrogen and organic carbon in agricultural land in Vietnam (Slaets et al. 2014). Based on the studies in Utah and Minnesota watersheds, turbidity has been considered as a proxy measurement for total phosphorous and total suspended sediment (TSS) concentration (Jones et al. 2011; Ruzycki et al. 2014). Recent studies by Ruzycki et al. (2011) indicated a relationship between turbidity and total mercury levels in the Minnesota Rivers.

Besides nutrient pollutants, turbidity has often been used to evaluate the pathogen levels in surface water bodies (Brookes et al. 2005; Johnson et al. 2010; LeChevallier and Norton 1992; USEPA 1999). In addition to the pollutants and pathogens, turbidity can be a surrogate for evaluating the aquatic habitat potential in the surface waters. Hazelton and Grossman (2009) showed changes in foraging pattern of largemouth bass (Micropterus salmoides) at different turbidity levels. For a suitable fish habitat, optimum turbidity is required based on the species types (Lloyd 1987). The feedback between suspended sediment and turbidity on aquatic species have been discussed extensively in the literature (Kirk 1991; Vogel and Beauchamp 1999; Henley et al. 2000; Bilotta and Brazier 2008; Jönsson et al. 2013; Awata et al. 2011; Kemp et al. 2011; Jönsson et al. 2013; Rosewarne et al. 2013). Turbidity has also been shown to have a direct link to deterioration of aesthetic appearances of surface water bodies (Davies-Colley and Smith 2001; Pflüger et al. 2010).

In the USA, several runoff-erosion models have been developed to help erosion or sediment control BMPs in landscapes. For example the Sediment, Erosion and Discharge by Computer Aided Design (SEDCAD) by Warner et al. (1998), the Sedimentology by Distributed Modeling Techniques (SEDIMOT) by Barfield et al. (2006), and SEDPRO

(Harp et al. 2008) are widely used runoff-erosion models to manage sediment control BMPs (Hoomehr and Schwartz 2012). These models predict SSC based on the percent of silt, sand, and clay particles. However, these models to not currently have a method for predicting turbidity.

Background on Research Project Two

During runoff events, organic matter in various forms enters into receiving waters along with eroded soil and sediment. The dissolved portion of organic matter is commonly called dissolved organic carbon (DOC) (Thurman 1985; Collier 1987). The organic-matter containing runoff is often colored in the nature (APHA et al. 2012). DOC and the optical property of water called color are considered water-quality parameters. Aesthetic appearances and aquatic habitat are directly linked with water color (Davies-Colley et al. 1987; Smith et al. 1995; Wissel et al. 2003; Novoa et al. 2015). DOC is commonly measured to evaluate the carbon cycle and aquatic ecosystem functioning (Carter et al. 2012; Stasko et al. 2012; Peacock et al. 2014; Faithfull et al. 2015; Robidoux et al. 2015). Water color and DOC are shown to be impairments for drinking-water treatment processes (Ratnaweera et al. 1999; Shutova et al. 2014; Roccaro et al. 2015; Parry et al. 2015).

Color is considered a human perception and is composed of properties of light absorbance and reflectance. Humans perceive color in wavelengths associated with the visible spectrum, 400-800 nm. For example, at 420-470 nm, blue color is absorbed, and humans perceive orange color. The full descriptions of color and spectrophotometry are found in Resusch (1999), Hutchingd (2005), and Wordsfold (2005). In water chemistry, color is quantified with reference to platinum cobalt solution, commonly expressed in platinum cobalt unit (mg/L Pt-Co or PCU). The PCU of water color was developed by Allen Hazen in 1892 (Hazen 1892) and is also called a Hazen unit. Color is also referred to as yellow substance (Kirk 1976; Bricaud et al. 1981; Davies-Colley and Vant 1987). In natural waters, the common color-causing chemical agents are organic phenolic compounds, including vanillin, vanillic acid, syringic acid, carechol, resorcinol, protocatechuic acid, and 3,5-dihydroxybenzoic acid (Christman and Ghassemi 1966). Water color in general includes humic and fulvic acids (APHA et al. 2012.) Those humic matters are composed of complex chemical structures of carbohydrates and proteins of plant and animal origins (Mostafa et al. 2013). The complex chemical property of humic and fulvic acids content in organic matter vary with origins as well (Brezonik and William 2011; Mostofa et al. 2013).

In many studies, water color has been used as surrogate measurement for DOC (Molot and Dillon 1997; Worral et al. 2003; Ishikawa et al. 2006; Yallop and Clutterbuck 2009; Ishikawa et al. 2006). These studies showed the linear correlation between color and DOC. Molot and Dillon (1997) quantified the relationship between color and DOC in a peat dominated watershed in central Ontario, Canada. Their results indicated a strong linear relationship ($R^2 > 0.9$) between DOC and color. They reported variation on color to DOC ratio (slope of linear relationship) ranging from 3.3 to 9.9 in seven lakes and showed the variation caused by percent of peat cover in catchment areas. Christman and Ghassemi (1966) illustrated the color and DOC variation in a tree bark (Douglas fir) dominated watershed in western Washington, USA. Their results indicated the variation in color to DOC ratio 3.34 to 8.8. Worrall et al. (2003) studies showed the linear relationship between DOC and color ($R^2 > 0.8$) in peat dominated watershed in United Kingdom. Similarly, Yallop and Clutterbuck (2009) presented linear relationship between DOC and color ($R^2 > 0.9$) for peat dominated waters. Ishikawa et al. (2006) studies on rainforest-dominated watershed in Indonesia showed the linearity between DOC and Color ($R^2 > 0.9$). These color-DOC relationships are not uniform because of heterogeneous and complex chemical nature of source organic matter.

Background on Research Project Three

Anthropogenic factors such as impoundments, developments, and land use practices are reported as major factors for alteration of channel geomorphic functions (Hooke 2000; James and Marcus 2006; Gregory 2006; Hooke et al. 2012). Historic channel planform is often compared with existing planform to evaluate changes in channel geomorphic functions. Aerial photographs and maps are commonly used for spatial analysis of channel planform changes.

Gurnell et al. (1994) used geographic information system (GIS) techniques to analyze channel planform changes from 1876 to 1992 for the River Dee in the United Kingdom. Their findings showed the limited channel migration in the River Dee in 115 years because of flow regulations. Micheli and Kirchner (2002) used 1955-1995 aerial photographs for spatial analysis of channel lateral migration in Sierra Nevada, California. They digitized the channel centerlines for 1955, 1976, and 1995 and estimated channel migration rates based on eroded area polygon made by two channel centerlines divided by the elapsed time period in years. Heo et al. (2007) characterized channel meander migration for Sabine River in the southern USA. They analyzed the historical orthophotos to digitize channel centerlines from 1974 to 2004 in GIS. Yao et al. (2013) used similar GIS techniques to evaluate channel planform changes and migration rates in the Yellow River, China.

Numerous studies across the USA have demonstrated that BMPs and flow regulation can reduce lateral channel migration in fluvial systems (Shields et al. 2000; Ritter et al. 2007; Fremier et al. 2014). Fremier et al. (2014) demonstrated that the combined effects of BMPs on soil erosion and flow regulation or control reduced lateral channel migration by nearly 40% in the Sacramento River, California, USA. In west-central Ohio, soil conservation and river management activities helped to maintain geomorphic equilibrium for previously impacted channels (Ritter et al. 2007). Shields et al. (2000) showed significant reduction in downstream channel lateral migration after construction of dams in the Missouri River in Montana, USA.

More recently, Rhoads et al. (2016) evaluated changes in channel planform and watershed channel network from the 1820s to 2012 in the Sangamon River basin, Illinois, USA. They digitized the 1820s channel network from historic plat maps for the watershed and compared it with the 2012 channel network with reference to the USGS National Hydrography Dataset. Their results showed that the channel network in 2012 is almost three times larger than the 1820s channel networks. They reported that the majority of channel network expansion was due to the addition of agricultural drains in the watershed after European settlement.

In west-central Oklahoma, numerous studies have showed the reduction in watershed soil erosion, sediment yield from the watershed, and nutrient loading into the Fort Cobb reservoir due to USDA conservation practices (Simon and Klimetz 2008;

Garbrecht and Starks 2009; OCC 2009; Becker and Steiner 2011; Garbrecht 2011; Moriasi et al. 2011; Steiner et al. 2014). However, those studies have only attempted limited investigation of channel geomorphic changes over the long term. This background revealed a research gap for historic channel form and channel network assessment related to the effect of conservation practices implemented in the Fort Cobb watershed.

CHAPTER II

DEVELOPMENT OF A TURBIDITY PREDICTION METHODOLOGY FOR RUNOFF-EROSIN MODELS[1]

Abstract

Surface water bodies can be impaired by turbidity and excessive sediment loading due to urban development, construction activities, and agricultural practices. Turbidity has been considered as a proxy for evaluating water quality, aquatic habitat and aesthetic impairments in surface waters. The United States Environment Protection Agency (USEPA) has listed turbidity and sediment as major pollutants for construction site effluent. Recently proposed USEPA regulations for construction site runoff led to increased interest in methods to predict turbidity in runoff based on parameters that are more commonly predicted in runoff-erosion models. In this study, a turbidity prediction methodology that can be easily incorporated into existing runoff-erosion models has been developed using fractions of sand, silt, and clay plus suspended sediment concentration of eight parent soils from locations in Oklahoma and South Carolina, USA.

Keywords: Turbidity, Suspended Sediment Concentration, Particle Size Distribution, Runoff-erosion Models.

---

[1] Published in *Water, Air & Soil Pollution*
To Cite: Neupane, S., Vogel, J.R., Storm, D.E., Barfield, B.J., & Mittelstet, A.R. (2015). Development of a turbidity prediction methodology for runoff-erosion models. Water, Air & Soil Pollution, 226(12), 1-14.

Introduction

Urban development, construction activities and agricultural practices contribute to increased sediment loading into rivers and lakes (USEPA 2009). Increased sediment loading increases the suspended sediment concentration (SSC) in the surface waters, which in turn often increases the turbidity levels in such water bodies. Turbidity is a light-scattering property of water and is often used as a relative measurement for water clarity (Parmelee and Ellms 1899; Kirk 1985; USEPA 1999; Davies-Colley and Smith 2001; ASTM 2011). The United States Environmental Protection Agency (USEPA) has listed sediment and turbidity as primary pollutants for construction site effluent in 40 CFR Part 450, 2014 final rule (USEPA 2014). Turbidity may be used as a surrogate for other contaminants for determining the efficacy of best management practices (BMPs) for construction site effluent and erosion control, and can also have direct impacts on aquatic organisms. As a result, interest has increased in methods to predict turbidity using erosion-runoff models. The predicted turbidity can be a reference to evaluate impairments in surface water bodies.

The USEPA (2009) estimated that more than 40,000 kilometers of streams, 4,000 square kilometers of lakes and reservoirs, and 600 square kilometers of bays and estuaries are impaired by turbidity in the US. Factors that have been shown to impact the turbidity of water include soil type and concentration, organic content, color, nutrients, algae, and bacteria (Holstrom and Hawkins 1980; Gippel 1995; Davies-Colley and Smith 2001; Bilotta and Brazier 2008). The associated factors create water quality, aquatic habitat and aesthetic impairments in surface-water bodies.

Relationships have been documented between turbidity and many pollutants, including total nitrogen (Kim and Furumai 2013), particulate organic nitrogen and carbon (Slaets et al. 2014), total phosphorus and total suspended solids (TSS) (Jones et al. 2011; Ruzycki et al. 2014), mercury (Ruzycki et al. 2011), polycyclic aromatic hydrocarbons (PAHs) (Rügner et al. 2014), pathogens (USEPA 1999; LeChevallier and Norton 1992; Brookes et al. 2005; Johnson et al. 2010), and various indices of aquatic habitat quality (Lloyd 1987; Kirk 1991; Henley et al. 2000; Bilotta and Brazier 2008; Hazelton and Grossman 2009). Besides water quality and aquatic habitat, turbidity has been often reported as an indicator of surface water's aesthetic appearances. Aesthetic quality of surface waters is mainly related to public visual perception based on the clearness of water. Pflüger et al. (2010) demonstrated that the public had the lowest preference for rivers where turbidity and SSC are high. Similarly, the relationship between degraded aesthetic quality of surface waters and suspended sediment or turbidity has been reported in the literature (Effler et al. 1992; Smith et al. 1995; Bernal et al. 1999; Bilotta and Brazier 2008).

Turbidity has been used to estimate SSC (Rügner et al. 2013; Ruzycki et al. 2014). Parmelee and Ellms (1899) used measured turbidity to estimate SSC using a platinum and copper wire as an indicator of turbidity. Since then, many others have utilized regression techniques to predict SSC from turbidity including Gippel (1995); Lewis (1996); Wass et al. (1997); Riley (1998); Brasington and Richards (2000); Sun et al. (2001); Zabaleta et al. (2007); Gao et al. (2008); Minella et al. (2008); Williamson and Crawford (2011); Marttila and Kløve (2012) and Line et al. (2013). In these studies, the SSC-turbidity relationships are mostly linear at low turbidity levels, with non-linear SSC-turbidity relationships reported for higher turbidities or in heterogeneous soil mixes. Several site-specific SSC-turbidity relationships and evaluation comparisons (R^2) are documented in the literature (Rügner et al. 2013; Slaets et al. 2014). In some regression models, SSC along with the known fraction of sand, silt and clay has been utilized as a predictor variable for turbidity (Holliday et al. 2003; Patil 2010; Perkins et al. 2014).

Existing runoff-erosion models may be applied to easily estimate SSC and particle size distribution (PSD), but have limited capabilities to predict runoff turbidity. In the United States, the Sediment, Erosion and Discharge by Computer Aided Design (SEDCAD) (Warner et al. 1998), the Sedimentology by Distributed Modeling Techniques (SEDIMOT) (Barfield et al. 2006), and SEDPRO (Harp et al. 2008) models are commonly used runoff-erosion models for predicting sediment in construction site runoff and designing sediment control BMPs (Hoomehr and Schwartz 2012). Warner and Sturm (2002) mentioned that SEDCAD 4 (the current version) can estimate SSC and PSD of runoff. They developed turbidity-SSC relationships for a few sediment control measures based on model predicted SSC for runoff samples; however, their relationship does not address the effect of PSD on turbidity prediction. SEDIMOT III evaluates construction site sediment control BMPs (Barfield et al. 2006). The SEDIMOT III and SEDPRO models have the capability to differentiate parent soil particles in five groups (sand, silt, clay, large aggregates and small aggregates) based on Foster et al. (1985) soil matrix particle size distributions. However, SEDIMOT III and SEDPRO do not currently have the ability to predict turbidity of construction site runoff.

Pavanelli and Bigi (2005) mentioned that turbidity values vary significantly with changes in particle size distribution, even at similar SSC levels. Similarly, Slaets et al.

(2014) demonstrated that turbidity varied significantly by changing the suspended sediment PSD at the same SSC. Gippel (1995) showed that clay dominated SSC can increase turbidity up to four times more than the silt dominated SSC. The amount of sand, silt and clay (called primary particles) in the soil or runoff control the turbidity, which is commonly determined by dispersing the soil or sediment with a dispersing agent (ASTM 2007). Besides primary particles, fractions of large and small aggregates are also found in undispersed soil or sediment. Quantification of such fractions using the method of Foster et al. (1985) requires large computations and approximations for several parameters; therefore, this method has not been widely implemented. Since runoff sediment is mostly found in the undispersed form in nature, field turbidity measurements are mostly related to the undispersed form of sediment, whereas most current models predict turbidity based on the SSC and PSD in the dispersed form. Therefore, in order to predict the turbidity from parameters that are predicted by existing runoff-erosion models, the relationship between dispersed and undispersed PSD, and turbidity needs to be developed. Only then can a turbidity prediction methodology be easily integrated into runoff-erosion models.

The primary goal of this study is to develop a turbidity prediction methodology that is easily incorporated into existing runoff-erosion models. The two main objectives for this study are: 1) develop a simple, reliable method to predict dispersed turbidity and 2) develop a simple, reliable method to predict undispersed turbidity. This paper presents the general methodology for dispersed and undispersed runoff turbidity prediction. The proposed methodology was calibrated for eight parent soils from Oklahoma and South Carolina, USA. If existing models can be utilized to predict turbidity based on SSC and

PSD, there may be potential to correlate turbidity to water quality, habitat potential and aesthetic appearances of the surface waters.

Materials and Methods

To predict undispersed runoff turbidity for a given parent soil, a systematic approach has been developed (Figure 2.1). The detail description of systematic approach has been described in subsequent subsections.

Soil Location and Characteristics

In this study, five parent soil samples (Kamie B, Norge B, Stephenville, Port A and Port B) from Oklahoma and three parent soils (Cecil C, Cecil B and Pacolet E) from South Carolina were selected based on availability from active construction sites in each area (Table 2.1). The parent soils represent a wide range of particle size distributions and soil horizons from two different areas of the United States, but are not meant to represent an exhaustive list of soils. The alphabetical character following these soil names describes the soil horizon. These parent soils were selected from active construction sites during the sample collection period. Figure 2.2 shows the general distribution in Oklahoma and South Carolina of the soil series used in this study, and the exact county of soil sample collection is shown in Table 2.1.

A portion of all collected parent soils (2-3 kg of homogeneously mixed, air-dried for 2-3 weeks) were prepared using the classical coning and quartering method (Gerlach and Nocerino 2003) for PSD. The PSD was determined using the sedimentation method called pipette analysis (Gee and Bauder 1986) for Oklahoma soils, whereas PSD of South

Carolina soils were obtained from Patil (2010) hydrometer analysis based on ASTM (2007). Fractions of sand, silt and clay for each of the eight soils obtained from pipette or hydrometer analysis were characterized according to USDA soil textural classification criteria (Soil Survey Division Staff 1993) (Table 2.1)USDA soil textural criteria classifies sand as 2 to 0.05 mm, silt as 0.05 to 0.002 mm and clay as less than 0.002 mm. All parent soils' PSD were site-specific measurements. Based on the soil formation, there were three general groups for studied parent soil series. The Port, Kamie, Norge soil series were formed from Pleistocene age loamy alluvium deposits (NCSS 2000; NCSS 2004a; NCSS 2004b); Stephenville soil series were formed by weathering Permian age sandstone (NCSS 2014), and Cecil and Pacolet soil series were formed from weathered igneous and metamorphic rocks (NCSS 2007; NCSS 2008).

Predictive Relationships for Turbidity

In this study, linear and power relationships between turbidity and SSC were investigated. Turbidities of each suspended-sediment particles classes (clay, silt and sand) in the linear relationship are defined as,

$$DT_{L,cl} = k_{1L}[Clay];\ DT_{L,si} = k_{2L}[Silt] \text{ and } DT_{L,sa} = k_{3L}[Sand] \qquad (1)$$

where, $DT_{L,cl}$, $DT_{L,si}$ and $DT_{L,sa}$ are turbidities due to clay, silt and sand, respectively, in dispersed suspended sediment water samples in Nephelometric Turbidity Unit (NTU); [Clay],[Silt] and [Sand] are dispersed suspended-sediment concentrations of clay-, silt- and sand-sized sediment, respectively, in mg/l; and, k_{1L}, k_{2L} and k_{3L} are turbidity coefficients (NTU-L/mg) for clay-, silt- and sand-sized sediment, respectively, in the linear relationship. The combined predictive linear relationship for dispersed turbidity is

$$DT_L = DT_{L,cl} + DT_{L,si} + DT_{L,sa} \quad (2)$$

Similarly, a second predictive relationship for dispersed turbidity is defined as non-linear power function (power relationship hereafter) between turbidity and each SSC particle-size class, which is defined as,

$$DT_{P,cl} = k_{1P}\ [Clay]^a\ ;\ DT_{P,si} = k_{2p}[Silt]^b \text{ and } DT_{P,sa} = k_{3p}[Sand]^c \quad (3)$$

where $DT_{P,cl}$, $DT_{P,si}$ *and* $DT_{P,sa}$ are dispersed turbidities due to clay-, silt- and sand-sized sediment, respectively, in NTU in the power relationship, respectively; and k_{1P}, k_{2P} and k_{3P} are turbidity coefficients (NTU-L/mg) for clay-, silt- and sand-sized sediment, respectively.

Similarly, a, b and c are turbidity exponents clay-, silt- and sand-sized sediment, respectively, in the power relationship. The combined predictive power relationship for dispersed turbidity is

$$DT_P = DT_{P,cl} + DT_{P,si} + DT_{P,sa} \quad (4)$$

Since a runoff sample would nearly always be in an undispersed form, a proposed predictive relationship for undispersed runoff turbidity is

$$UT = \alpha\ (DT) + \beta\ [Clay] + \gamma\ [Silt] + \omega\ [Sand] \quad (5)$$

where *UT* is turbidity for undispersed soil (NTU), [*Clay*]; [*Silt*] and [*Sand*] are dispersed suspended-sediment concentrations of clay-, silt- and sand-sized sediment, respectively, in mg/l; α is dispersed turbidity factor (unit-less); and β, γ and ω are concentration factors (NTU-l/mg) for clay-, silt- and sand-sized sediment, respectively. *DT* is dispersed turbidity of the sample obtained from equation (2) or (4) whenever applicable.

Laboratory Separation of Sand, Silt and Clay

To separate the sand, silt and clay fraction of each soil, 2-3 kg of homogeneously mixed, air-dried parent soil was collected using the classical coning and quartering method for homogeneous mix (Gerlach and Nocerino 2003). The sample was then sieved through a 2 mm opening, ASTM No. 10 sieve (ASTM 2013) to remove gravel-size and larger particles. As per ASTM (2007), the sample passing through the No. 10 sieve was then soaked with 125 ml sodium hexametaphosphate (SHMP) solution (40 g/l concentration) per 50 g of soil sample for 16 hours to disperse the soil particles. After the soaking period, the sample was sieved through a No. 270 sieve (53 µm opening) to remove sand-sized particles, resulting in silt and clay-sized particles only. Note that the soil passed through No. 270 sieve is the portion of silt and clay according to the USDA classification (50 µm, cutoff for silt and clay), which is a different sieve size specification than described by ASTM (2007). During the sieving process, 40 g/l SHMP solution was used instead of water to maintain a constant 40g/l concentration of SHMP in silt and clay slurry. The retained sample (sand) on the No. 270 sieve was washed with reverse osmosis (RO) water 5-6 times to minimize the SHMP residuals present. The sand portion was oven dried at 90oC to constant mass in a pre-weighed polypropylene jar. The organics and minerals present in the soil sample may affect the turbidity of soil sample; therefore, a lower temperature than the ASTM (2007) recommendation of 110ºC was used for sample drying to prevent combustion or volatilization of any organic matter present. The organic matter content present in the soil sample was not measured.

Since separation of silt cannot be separated from clay by sieve analysis, a centrifugation method was utilized for this purpose. A Beckman GP centrifuge (Beckman

Instruments 1988) was used to separate silt and clay from the sample. The soil slurry passed through the No. 270 sieve was divided into four 750-ml centrifuge bottles and centrifuged for 1 minute and 42 seconds at 1000 RPM based on rotor's specifications of Beckman Coulter (2007) and using the relationship developed by Hathaway (1956). After centrifuging, the bottles were carefully removed from the centrifuge and approximately 80% of the supernatant was decanted from each bottle. This decanted volume was transferred to pre-weighed polypropylene jars for oven drying at 90o C to constant mass. The particles in the decanted portion were clay-sized particles and SHMP (40 g/l concentration), which made a hard clod after drying. Clay and SHMP were broken up using an electric spice grinder (Warning Commercial WSG30, CT, USA), resulting in final product of powdered clay and SHMP.

The SHMP concentration and resulting mass was recorded in each soil sample. The remaining 20% soil slurry in the centrifuge bottles was mainly silt-sized particles, a small amount of clay-sized particles, and SHMP. A sufficient amount of RO water was used to refill the bottles, mixed thoroughly, and the centrifuge run was repeated up to 13 times until there was a reasonably clear suspension (can see objects across the sample bottle easily with naked eye as shown in Figure 2.3) in the bottles to represent when all clay-sized particles had been removed by the SHMP slurry. The remaining soil slurry in the centrifuge bottle was silt, which had only a very small residual of SHMP as a result of the multiple decanting and dilutions. The silt slurry was transferred to pre-weighed polypropylene jars for oven drying at 90^{o}C to constant mass.

Sample Preparation and Turbidity Measurement

Turbidity measurements were completed for each dispersed primary particle fraction (sand, silt and clay) for each soil using a Hach Hydrolab MS5 Sonde (OTT Hydromet, Colorado, USA) (called turbidity meter hereafter), which has a maximum reading of 3000 NTU. The turbidity meter was calibrated using Hach company's turbidity standard in 4 points (1, 100, 1000 and 3000 NTUs). Ranges of dispersed SSC concentrations (approximately 50, 100, 200, 400, 800, 1600, 3200 and 4000 mg/l) were selected for clay, silt and sand in each type of soil to determine turbidity constants (equation 1 and 3) for clay, sand and silt for each parent soil. Similarly, to test predictive relationship (equations 2 and 4), turbidity were measured for a range of combinations of sand, silt and clay for each soil. The sand, silt and clay combinations were random and ranged from 250 to 5000 mg/l concentration in total. For example; 48 mg of sand, 240 mg of silt and 212 mg makes 500 mg of mix. There were total 16 such combinations for each soil types. The turbidity for each of these samples was measured in a one-liter beaker filled with 750 mL RO water plus the appropriate mass of soil placed on a continuous magnetic stirrer (Model: S131125, Thermo Scientific Cimarec, USA) rotating at a constant speed of approximately 525 rpm (level 7 on the stirrer) to keep solution in suspension . For clay, these concentrations were adjusted appropriately to account for SHMP content. The turbidity probe was inserted into the sample beaker as per turbidity meter specifications (Hach 2006) and turbidity readings were recorded every minute for up to 15 readings. The first five minutes were considered as mixing time and median of the last five one-minute readings were considered as the turbidity of the sample. The methodology was adapted from USGS field protocol for turbidity, which explains that reported turbidity values as the median of three or more readings at ±10 percent error range (Anderson 2005).

For quality control, all measurements were completed for at least duplicate samples. If the second set of turbidity measurements were different than the first set (out of turbidity meter's error range: ±1% for 0-100 NTU, ±3% for 100-400 NTU, ±5% for 400-3000 NTU), a third set of measurement were conducted. The process was repeated for all concentrations (each clay, sand and silt fraction) of all eight soils.

To measure undispersed turbidity, separate soil samples (not used in dispersed turbidity measurement) were prepared for each of the eight parent soils. Approximately 250 g of oven-dried parent soil sample (oven dried at 90^{o}C to a constant mass) was collecting using the quartering and coning method (Gerlach and Nocerino 2003). Clods larger than approximately 2 mm were ground using a rubber pestle in a mortar. The sample was then sieved through a No. 10 sieve to remove gravel-size particles and stored in an air-tight container. From the sample container, two types of representative suspended-sediment samples were created. The first type of sample contained consisted of the entire sample (sand, silt and clay fractions), whereas the second type of sample was without sand (i.e., consisted of only the silt- and clay-sized sediment fractions) that was meant to approximate eroded particles.

For the first sample type, 12 sub-samples of different sediment mass (and therefore concentration) were prepared for the turbidity measurement in such that it represented low to high concentrations of suspended sediment (Kamie B: 473 – 5554 mg/l: Norge B: 285 – 4906 mg/l; Port A: 515- 4139 mg/l; Port B: 429 – 4515 mg/l; Stephenville B: 421 – 6693 mg/l; Cecil B: 205 – 1433 mg/l; Cecil C: 304 - 4890 mg/l and

Pacolet E: 144 – 1045 mg/l). A known sediment mass was put into a 1 liter beaker and 750 ml of RO water was added. The sample was continuously stirred with a magnetic stirrer (Thermo Scientific Cimarec) at speed 7 (about 525 rpm). This type of sample (without addition of SHMP) was termed as undispersed turbidity (*UT*). Turbidity was measured using the previously described techniques (taking the last 5 reading of 15 minutes reading from turbidity meter). These procedures were applied to all eight soils and samples. After 15 minutes (completion of turbidity measurement), 30 g of SHMP (to maintain 40 g/l concentration) was added and mixing with the magnetic stirrer was continued for 5 minutes, or until the SHMP crystals were completely dissolved). After SHMP addition, the sample was covered and stored at room temperature in a dark location for 16 hours. Turbidity was then measured again. This type of sample was termed as measured dispersed turbidity (DT_m).These procedures were applied to all eight soils. The *UT* and DT_m samples were used for validating equation 5 and used for the systematic procedure to predict runoff turbidity (Figure 2.1).

In addition to the parent soils, a second soil distribution meant to approximately represent the eroded suspended sediment distribution was analyzed for soil that was sieved through a No. 270 sieve to remove sand-sized particles. Turbidities were measured on 6 sub-samples of this silt- and clay-only soil in such a way that concentrations ranged lower to higher (Kamie B: 430 – 5335 mg/l: Norge B: 550 – 1903 mg/l; Port A: 667-2928 mg/l; Port B: 624 – 2887 mg/l; Stephenville B: 583 – 5236 mg/l; Cecil B: 205 – 1433 mg/l; Cecil C: 536 – 1849 mg/l and Pacolet E: 242 – 619 mg/l), with an upper turbidity slightly less than 3,000 NTU, which represented the upper range of the turbidity meter. The turbidity measurements for the clay and silt-only samples were similar as discussed above, and undispersed and dispersed turbidity measurements were completed similarly to the measurements for the first type.

Statistical Methods

Turbidity coefficients and exponents for equation 1 and 2 were determined by Microsoft Excel (Microsoft 2010) regression trend line with the intercept term set to zero. The coefficients of determination (R^2) values were reported for those relationships. Based on the turbidity coefficient, exponent and known concentration of [clay], [silt] and [sand], turbidities for linear and power relationships were predicted. The predicted turbidities in such relationships were compared with measured turbidities with reference to R^2, Nash-Sutcliffe efficiency (*NSE*), absolute percentage relative error (RE in %) for all eight soils. The *NSE* value (Nash and Sutcliffe 1970) was computed as

$$NSE = 1 - \left[\frac{\sum_{i=1}^{n}(Tm_i - Tp_i)^2}{\sum_{i=1}^{n}(Tm_i - Ta)^2}\right] \quad (6)$$

where Tm_i is measured turbidity in the i^{th} sample, Tp_i is predicted turbidity for the i^{th} sample and Ta is average turbidity of measured samples, n is the number of sample. The relative percentage error (RE) was evaluated as

$$RE = \frac{|Tm_i - Tp_i|}{Tm_i} \times 100 \quad (7)$$

where, Tm_i is measured turbidity in the i^{th} sample, Tp_i is predicted turbidity for the i^{th} sample.

To determine undispersed turbidity for runoff sample, the number of coefficients used in equation (5) was minimized by determining the insignificant variables with multiple regression analysis using Minitab statistical software (Minitab 2010).

Results and Discussion

Methodologies for predicting the turbidity of dispersed and undispersed runoff samples have been developed. The coefficients and parameters for best-fit predictive relationships (equation 1 to 5) were determined and undispersed runoff turbidities were estimated for the eight soils shown in Table 2.1.

Turbidity Constants and Dispersed Turbidity-SSC Relationship Validation

For each dispersed primary-particle type (clay, silt and sand) and soil, the turbidity constants and coefficients for the linear and power relationships (equations 1 and 3) varied as shown in Table 2.2. This table describes the parameters for equations 1 and 3; for example, for Kamie B soil, $DT_{L,cl}$ = 0.432 [clay] in the linear relationship and $DT_{p,cl}$ = 0.324 $[Clay]^{1.034}$ for the power relationship. For all eight soils, the relationship between dispersed turbidity and SSC for each of the primary-particle classes (clay, silt and sand) was strong (R^2 > 0.96) for both the linear and power relationships. Since the R^2 did not give strong evidence that one type of relationship is better than the other, other statistical results were evaluated. Based on equation 2 and 4 (parameters from Table 2.2), measured vs. predicted turbidity values were compared with reference to R^2, Nash-Sutcliffe efficiency (NSE) value, and average relative error (RE, in %) for all eight soils and both relationships. Table 2.3 shows that the NSE value for the power relationship is greater than or equal to the linear relationship for all eight soils and REs were usually less in the power relationships (except Cecil B and Cecil C).

It is important to note that the turbidity meter has instrument error ±1% for 0-100 NTU, ±3% for 100-400 NTU, ±5% for 400-3000 NTU). In addition to this, preparation and processing error may have also influenced turbidity measurements. The NSE and RE values showed that the power model has a smaller relative error; however, given instrument error, possible measurement errors, and precision goals of the study, a conclusion has been made that the linear model is sufficient for most uses. If site specific soils performed better in the power relationship than the linear and project objectives require that level of accuracy, the power relationship can be used to predict turbidity. However, for our objectives linear relationships are considered sufficient for dispersed turbidity prediction and used for undispersed turbidity prediction hereafter in this study.

Prediction of Undispersed Runoff Turbidity

The systematic approach has been followed to predict undispersed runoff turbidity for a given parent soil (Figure 2.1). The predicted dispersed linear turbidity (DT_L) and direct measurement of turbidity without separating primary particles (DT_m) were compared. The relationship between DT_L and DT_m was estimated using linear regression using Excel. (Table 2.4). However, the intercept term in the linear regression equation was determined to be insignificant ($p < 0.05$) for all soils tested, so the equations are presented without the intercept. An intercept of zero is expected since the measured and predicted turbidity of pure water would be expected to both be zero.

The coefficient term in DT_L was considered as a dimensionless correction factor (called c-factor hereafter) and is used to adjust the turbidity predicted from turbidity constants for each individual particle-size class that were estimated from particles that were separated by centrifuging of the parent soil, to approximately match the turbidity actually measured with the dispersed parent soil without centrifugation. This c-factor adjustment is likely associated with potential changes in particle shape, size and/or color during centrifuging. Studies have shown that turbidity can be affected by color and PSD of suspended sediment present in the water sample (Gippel 1995; Packman et al. 1999; Teixeira and Caliari 2005).

With reference to a known concentration of SSC for undispersed runoff samples, c-factor, DT_L, and primary-particle fractions (Table 2.1), undispersed turbidity model factors were estimated using multiple linear regression analysis with Minitab statistical software (Minitab 2010). These equations (Table 2.5) were matched with the predictive equation (5). The significant coefficients α, β, γ and ω factors for equation 5 were selected ($p<0.05$). Model equations that utilize dispersed turbidity, silt-fraction sediment concentration, and/or clay-fraction sediment concentration are compared in Table 2.5. For all soils, the factor 'ω' was insignificant (therefore considered zero) based on the regression analysis.

For each soil, best-fit model equations to predict undispersed turbidity for runoff samples were determined. The best-fit model equation, shown in bold for each soil in Table 2.5, was selected based on the values of p (< 0.05), R^2 (maximized) and SE (minimized). Model 1 (predictor variables: *DT* and [*Clay*]) had the best fit in Port A, Cecil B and Pacolet E soils, while Model 2 (predictor variables: [*Clay*] and [*Silt*]) had best fit for Kamie B, Norge B, Port A, Port B, Cecil C, and Stephenville B soils. Model 3 (predictor variable: *DT* only) was the best fit for only Cecil C soil amongst the eight soils analyzed. Best-fit model selections depended upon the individual soil characteristics. Effect of particle size and shape for turbidity estimation has been previously reported on the several studies (Gippel 1995; Pavanelli and Bigi 2005; Teixeira and Caliari 2005). Holstrom and Hawkins (1980), and the results from this study, indicate a decrease in turbidity with increase in predominant particle-size class (D_{50}). Any inconsistences in the model performances may be related with variations in runoff sample colors and organic matter present in the suspended sediment samples which were not considered in this study. Future research could explore the effect of color and variation of organic matter on turbidity prediction for runoff water.

Conclusions

The primary goal of this study was to develop a turbidity prediction methodology that can be easily incorporated into existing runoff-erosion models. To achieve this goal, a reliable method that uses the concentration of sediment in each primary particle fraction (sand, silt and clay) has been developed to predict dispersed and undispersed turbidity. This method was applied to eight parent soils from Oklahoma and South Carolina, USA. For broader use, as with any empirical model, relationships between the concentration of sediment in each primary particle fraction and turbidity for specific soils must be calibrated and validated using the methodology provided. The runoff turbidity prediction methodology presented in this study can easily be used to develop turbidity coefficients for any soil and can be used as an add-on, predictive tool using currently available runoff-erosion models.

Once the presented methodology integrated and validated in existing runoff-erosion models, such as SEDMOT III, SEDPRO and SEDCAD, turbidity can be predicted for runoff from disturbed landscapes including construction sites and tilled agricultural fields. Further, the proposed methodology can be potentially extended to make turbidity as an all-in-one surrogate measurement for evaluating and monitoring water quality, habitat potential and aesthetic appearances for surface waters. However, future research is required to minimize the compounding error since the proposed methodology requires several predicted parameters. In addition to this, exploring color and small and large aggregates of runoff suspended sediment samples can provide more reliable estimation of undispersed turbidity for runoff samples.

Acknowledgements

This research was funded in part by the Oklahoma Department of Transportation Research Program, the Oklahoma Transportation Center, and Woolpert, Inc. The authors would like to thank Magen Kegley, Riley Jones and Hanna Huling for assistance in data collection.

Tables

Table 2.1. Results of site specific measurements for percent of sand, silt and clay with soil type of textures. Classification was based on USDA textural soil classification criteria (Soil Survey Division Staff, 1993). The letters on the soil type indicate the soil horizon. Horizon depth sources: NCSS 2000; NCSS 2004a; NCSS 2004b; NCSS 2007; NCSS 2008; NCSS 2014.

Soil Type	County of Collection	Horizon Depth Range (cm)	Sand (%)	Silt (%)	Clay (%)	Texture
Kamie B	Tulsa County, OK	46-142	77	15	8	Sandy Loam
Norge B	Payne County, OK	46-168	63	17	20	Sandy Clay Loam
Port A	Noble County, OK	23-69	13	55	32	Silty Clay Loam
Port B	Noble County, OK	69-107	27	36	37	Clay Loam
Stephenville B	Payne County, OK	97-213	42	25	33	Clay Loam
Cecil B	Greenville County, SC	20-107	58	20	22	Sandy Clay Loam
Cecil C	Greenville County, SC	127-203	58	17	25	Sandy Clay Loam
Pacolet E	Greenville County, SC	8-74	52	24	24	Sandy Clay Loam

Table 2.2. Turbidity constants for all soils as described in equation 1 and 3. The letter after the soil type represents the soil horizon.

Soil Type	Turbidity Constants														
	Linear						Power								
	Clay		Silt		Sand		Clay			Silt			Sand		
	k_{1L}^*	R^2	k_{2L}^*	R^2	k_{3L}^*	R^2	k_{1P}^*	a**	R^2	k_{2P}^*	b**	R^2	k_{3P}^*	c**	R^2
Kamie B	0.432	0.996	0.202	0.999	0.030	0.986	0.324	1.034	0.999	0.209	0.993	0.999	0.045	0.940	0.992
Norge B	0.729	0.998	0.242	0.999	0.052	0.974	0.635	1.016	0.998	0.204	1.020	0.999	0.060	0.976	0.994
Stephenville B	0.578	0.987	0.256	0.999	0.056	0.997	0.340	1.063	0.998	0.202	1.028	0.999	0.050	1.003	0.998
Port A	0.595	0.995	0.354	0.998	0.036	0.992	0.379	1.063	0.999	0.285	1.024	0.999	0.038	0.998	0.995
Port B	0.659	0.996	0.232	0.999	0.091	0.998	0.453	1.042	0.999	0.209	1.010	0.999	0.103	0.984	0.997
Cecil B	0.643	0.988	0.660	0.998	0.061	0.995	0.457	1.041	0.998	0.537	1.024	0.999	0.035	1.069	0.997
Cecil C	0.777	0.998	0.490	0.998	0.035	0.988	0.597	1.037	0.999	0.359	1.042	0.997	0.070	0.914	0.993
Pacolet E	1.432	0.992	0.742	0.998	0.088	0.959	1.695	0.972	0.992	0.507	1.046	0.999	0.049	1.061	0.976

R^2: Coefficient of determination, * Turbidity coefficients (NTU-L/mg), ** Turbidity exponents (dimensionless)

Table 2.3. Linear vs. power model performance comparison in terms of coefficient of determination (R^2), Nash-Sutcliffe Efficiency (NSE) and percentage average relative error (RE).

Soil Type	Linear			Power		
	R^2	NSE	RE (%)	R^2	NSE	RE (%)
Kamie B	0.996	0.94	9.1	0.996	0.98	4.6
Norge B	0.997	0.99	6.3	0.997	0.99	4.1
Stephenville B	0.996	0.96	14.4	0.997	0.99	5.6
Port A	0.996	0.94	13.8	0.996	0.98	7.3
Port B	0.996	0.99	12.1	0.997	0.99	4.6
Cecil B	0.994	0.99	5.9	0.994	0.99	6.7
Cecil C	0.978	0.98	4.9	0.978	0.98	6.9
Pacolet E	0.996	0.98	9.3	0.996	0.99	5.7

Table 2.4. Regression equations to predict dispersed turbidity (NTU) based on linear dispersed turbidity (NTU) and c-factor. The c-factor associated with change in dispersed turbidity between direct measurement and model prediction. p-value (<0.05) represents the significant relationship between corrected dispersed turbidity (*DT*) and predicted linear turbidity (DT_L).

Soil Type	Regression Equation	c-factor	R^2	p-value
Kamie B	$DT = 1.31\ DT_L$	1.31	0.991	< 0.0001
Norge B	$DT = 1.50\ DT_L$	1.50	0.995	< 0.0001
Port A	$DT = 1.43\ DT_L$	1.43	0.984	< 0.0001
Port B	$DT = 1.28\ DT_L$	1.28	0.997	< 0.0001
Stephenville B	$DT = 1.50\ DT_L$	1.50	0.992	< 0.0001
Cecil B	$DT = 1.34\ DT_L$	1.34	0.976	< 0.0001
Cecil C	$DT = 1.73\ DT_L$	1.73	0.997	< 0.0001
Pacolet E	$DT = 1.23\ DT_L$	1.23	0.996	< 0.0001

Table 2.5. Undispersed turbidity model equations (related to Equation 5). The bold text in model column represents the good fit model to predict undispersed turbidity for a given soil. p-value represents the level of significance at 0.05, *UT* is undispersed turbidity in NTU, *DT* is corrected dispersed turbidity in NTU, [*Clay*] and [*Silt*] are concentrations in mg/l based on dispersed particle size distribution of the parent soil. SE represents standard error (NTU) and R^2 is coefficient of determination.

Soil Type	Model	Undispersed Turbidity (*UT*)	Model R^2	SE (NTU)	p-value	
					Coefficients	
					b_1	b_2
Kamie B	1	*UT* = 1.39 *DT* - 0.94 [*Clay*]	0.998	22	< 0.0001	0.021
	2	***UT* = 1.18 [*Clay*] - 0.12 [*Silt*]**	**0.998**	**22**	**< 0.0001**	**< 0.0001**
	3	*UT* = 0.63 *DT*	0.997	25	< 0.0001	-
Norge B	1	*UT* = 1.67 *DT* - 1.95 [*Clay*]	0.999	20	< 0.0001	< 0.0001
	2	***UT* = 0.45 [Clay] + 0.38 [Silt]**	**0.999**	**20**	< 0.0001	< 0.0001
	3	*UT* = 0.56 DT	0.970	117	< 0.0001	-
Port A	**1**	***UT* = 0.34 DT + 0.53 [Clay]**	**0.990**	**113**	**0.02**	**0.02**
	2	**UT = 0.66 [Clay] + 0.25 [Silt]**	**0.990**	**113**	**0.001**	**0.02**
	3	*UT* = 0.67 *DT*	0.986	130	< 0.0001	-
Port B	1	*UT* = 1.05 *DT* - 0.43 [*Clay*]	0.997	60	< 0.0001	0.13
	2	***UT* = 0.66 [*Clay*] + 0.20 [*Silt*]**	**0.997**	**60**	**< 0.0001**	**< 0.0001**
	3	*UT* = 0.71 *DT*	0.996	62	< 0.0001	-
Cecil C	1	*UT* = 0.58 *DT* - 0.02 [*Clay*]	0.992	29.5	< 0.0001	0.797
	2	***UT* = 0.91[*Clay*] + 0.38 [*Silt*]**	**0.992**	**29.5**	**< 0.0001**	**< 0.0001**
	3	***UT* = 0.57 *DT***	**0.992**	**28.7**	**< 0.0001**	**-**
Cecil B	**1**	***UT* = 2.52 *DT* - 3.58 [*Clay*]**	**0.999**	**35**	**< 0.0001**	**< 0.0001**
	2	*UT* = 0.002 [*Clay*] + 1.25 [*Silt*]	0.999	35	0.9720	< 0.0001
	3	*UT* = 0.66 *DT*	0.976	151	< 0.0001	-
Stephenville B	1	*UT* = 1.38 *DT* - 1.05 [*Clay*]	0.997	59	< 0.0001	0.011
	2	***UT* = 0.51 [*Clay*] + 0.24 [*Silt*]**	**0.997**	**59**	**< 0.0001**	**< 0.0001**
	3	*UT* = 0.58 *DT*	0.995	70	< 0.0001	-
Pacolet E	**1**	***UT* = 3.24 *DT* - 7.65 [*Clay*]**	**0.996**	**81**	**< 0.0001**	**< 0.0001**
	2	*UT* = 0.32 [*Clay*] + 1.45 [*Silt*]	0.996	81	0.094	< 0.0001
	3	*UT* = 0.64 *DT*	0.985	158	< 0.0001	-

Figures

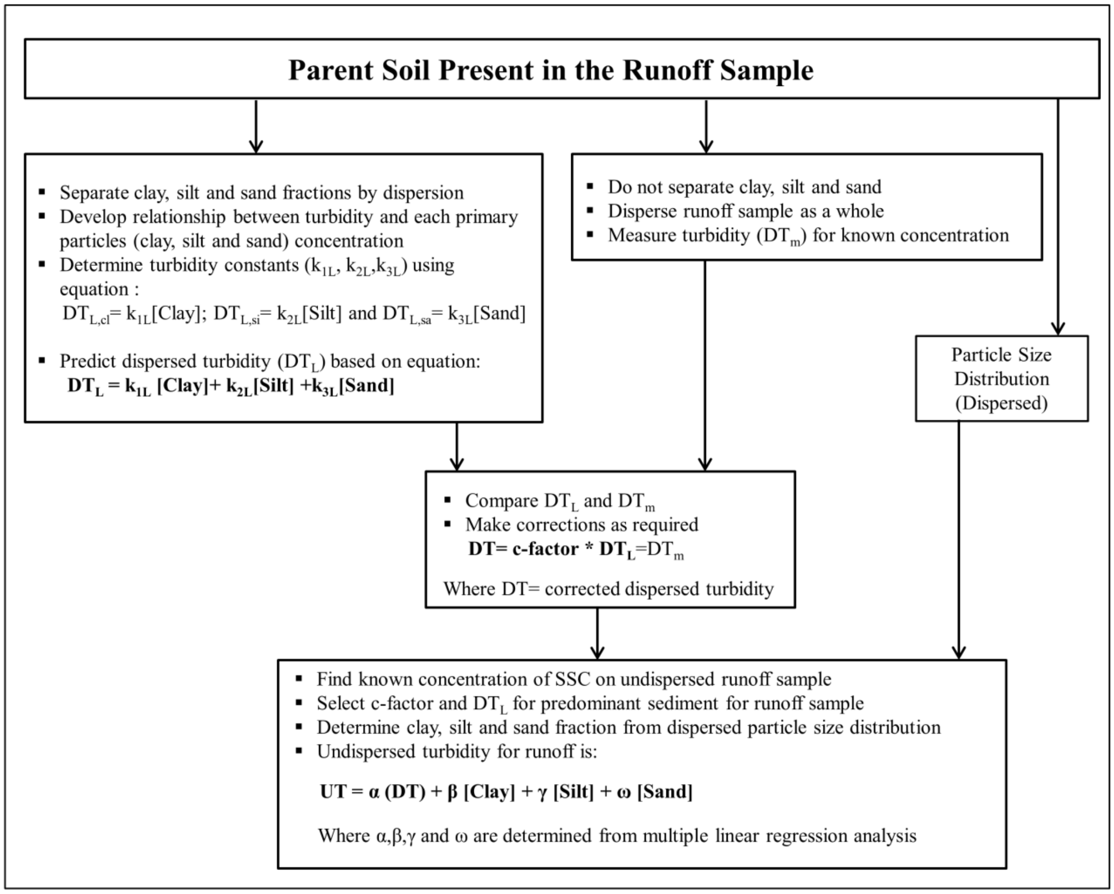

Figure 2.1. Flowchart for predicting undispersed turbidity based on suspended sediment concentration and particle size distribution for a given soil. $DT_{L,cl}$, $DT_{L,si}$ and $DT_{L,sa}$ are turbidities due to sand, silt and clay in dispersed suspended sediment water samples in Nephelometric Turbidity Unit (NTU); [*Clay*],[*Silt*] and [*Sand*] are concentrations of suspended sand , silt and clay-sized sediment in mg/l, respectively; and, k_{1L}, k_{2L} and k_{3L} are turbidity coefficients (NTU-l/mg)for sand, silt and clay in the linear relationship, respectively. D_{TL} is dispersed turbidity in linear relationship and DT_m is measured undispersed turbidity, c-factor is correction factor obtained from Table 2.4. Similarly, *UT* is turbidity for undispersed soil (NTU), [*Clay*]; [*Silt*] and [*Sand*] are dispersed suspended sediment concentrations, α is dispersed turbidity constant (unit-less), β, γ and ω are concentration factor (NTU-l/mg) for clay, silt and sand.

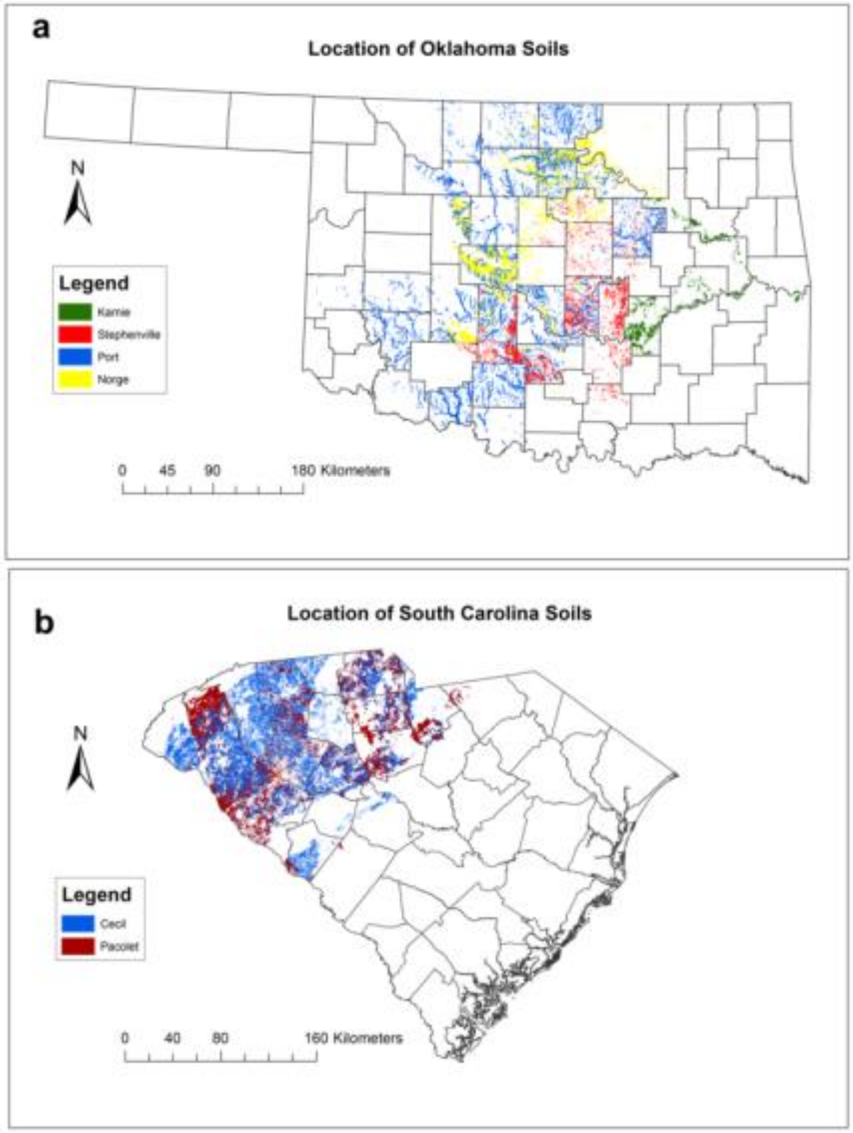

Figure 2.2. Study soil location map: a) studied soils distribution in Oklahoma, b) studied soil distribution in South Carolina (data source: Soil Survey Staff, 2011).

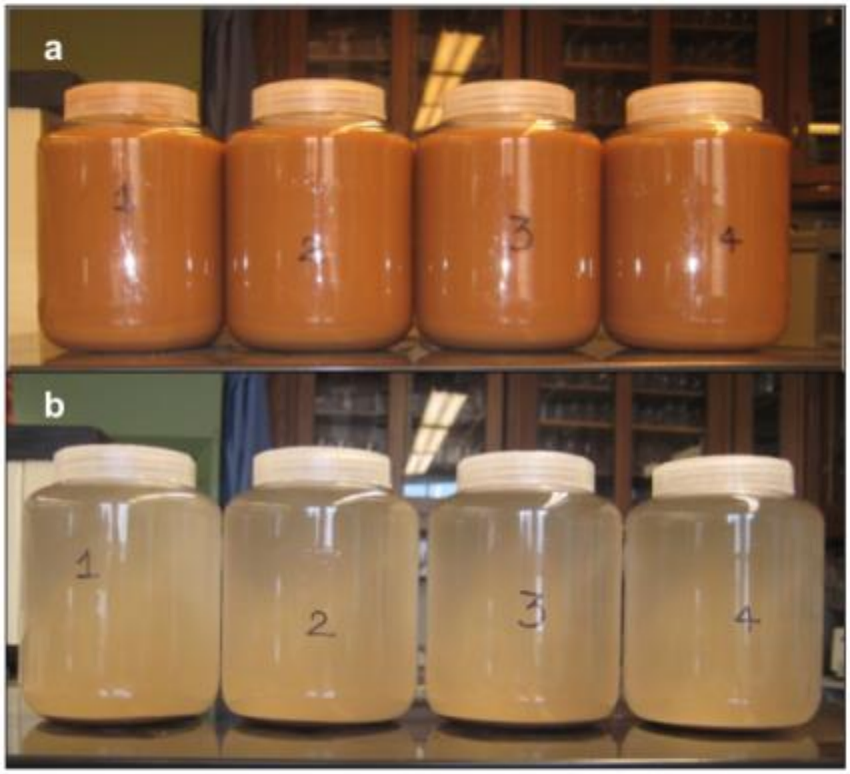

Figure 2.3. Samples in 750- ml centrifuge bottles: a) before the centrifuge runs b) after 13th centrifuge run, which were considered as clay-free samples.

CHAPTER III

QUANTIFYING THE RELATIONSHIP BETWEEN WATER COLOR AND DISSOLVED ORGANIC CARBON BASED ON ORGANIC MATTER SOURCE

Abstract

Water color is often used as a water-quality parameter to evaluate and assess aesthetic impairments, ecosystem functioning, and drinking water standards. Using dissolved organic carbon (DOC) for site-specific assessment of water color in surface waters has been attempted with mixed success, partially due to the complex nature of heterogeneous sources of organic matter. In this study, laboratory scale-based experiments were conducted using four types of homogeneous organic sources (peat moss, decomposing bark chips, cotton burr compost, and composted cow manure). The study objective was to develop a prediction equation to estimate water sample color with multiple sources of DOC. Results showed source-wise linear regression equations among water color and DOC were significantly different ($p < 0.05$). There was a high correlation ($R^2 = 0.99$ and Nash-Sutcliffe efficiency = 0.95) between predicted and measured color for heterogeneous sources. The results of this study could be useful to predict water color in runoff from field-scale watersheds.

Keywords: Water Color, Dissolved Organic Carbon, Organic Matter, Water Quality

Introduction

An application of organic matter as a soil amendment is common in agricultural, gardening, nursery, and landscaping activities. In large-scale plant nurseries, organic matter is used as potting media in nursery pots. As a result of plant nursery operations, dissolved organic residuals mixed with nursery effluent often ultimately enter into nearby surface and subsurface water bodies by means of irrigation and precipitation runoff (Huett et al. 2005). In addition, during large precipitation events, organic matter from upland areas are transported to surface waters through runoff (Morel et al. 2009; Sulzberger and Durisch-Kaiser 2009; Brezonik and William 2011; Kokorite 2012). The organic-matter containing runoff is often colored in nature due to presence of complex organic compounds from humic matter (APHA et al. 2012), including carbohydrates and proteins of plant and animal origins (Mostofa et al. 2013).

The nature and origin of water color in surface waters has been reported in the literature. Water color, also called yellow substance (Kirk 1976; Bricaud et al. 1981; Davies-Colley and Vant 1987), is an optical property of the water and is related to impairments in aesthetic quality as well as habitat potential in natural waters (Smith et al. 1995; Wissel et al. 2003; Novoa et al. 2015). It is commonly reported in Hazen Units (Hazen 1982) or Platinum-Cobalt Units (Pt-Co or PCU). When measured and reported in this manner, natural water color is measured by a spectrophotometer with reference to known standard color units of Platinum-Cobalt solution (Crowther and Evans 1981; Bennett and Drikas 1993; Hongve and Åkesson 1996; APHA et al. 2012). The color generally refers to the true color obtained by removing suspended sediment particles from the collected water sample. Christman and Ghassemi (1966) reported that water color was caused by the presence of organic phenolic compounds, including vanillin, vanillic acid, syringic acid, carechol, resorcinol, protocatechuic acid, and 3,5-dihydroxybenzoic acid.

The fraction of organic carbon that dissolves in water is called dissolved organic carbon (DOC). DOC is commonly measured as the fraction of organic carbon that passes through a 0.45 μm filter (Sulzberger and Durisch-Kaiser 2009). DOC in a surface water sample is commonly measured to evaluate the carbon cycle and aquatic ecosystem functioning (Carter et al. 2012; Stasko et al. 2012; Peacock et al. 2014; Faithfull et al. 2015; Robidoux et al. 2015). In addition to aesthetic and aquatic habitat, water color and DOC are closely related to water-quality impairments for drinking water. Drinking-water treatment often uses chlorination to remove water color and DOC, which may result in toxic by-products such as trihalomethane formation (Reckhow and Singer 1990; Morris et al. 1992; King and Marrett 1996; Magnus et al. 1999; Hwang et al. 2002; Kim et al. 2002; Mishra et al. 2014; Kumar et al. 2015). It has been reported that 50 to 75% of DOC in natural waters contain color-causing humic substances (Thurman 1985; Collier 1987). Recently, an increasing trend of DOC content in surface waters has been found in the literature (Worrall and Burt 2010; Filella and Rodriguez-Murillo 2014), which may result in an increase in the water color (Pagano et al. 2014).

In many studies, water color has been used as surrogate measurement for DOC (Molot and Dillon 1997; Worral et al. 2003; Ishikawa et al. 2006; Yallop and Clutterbuck 2009). These studies showed the linear correlation between color and DOC. Molot and

Dillon (1997) quantified the relationship between color and DOC in peat-dominated watershed in central Ontario, Canada. In this study, a strong linear relationship ($R^2 > 0.9$) between DOC and color was shown. Further, Molot and Dillon reported a variation in color to DOC ratio (slope of the linear relationship) ranging from 3.3 to 9.9 in seven lakes and showed the variation was correlated to the percent of peat cover in catchment areas. Christman and Ghassemi (1966) showed a color and DOC that varied from 3.34 to 8.8 in a tree bark (Douglas fir)-dominated watershed in western Washington, USA. Worrall et al. (2003) showed the linear relationship between DOC and color ($R^2 > 0.8$) in peat dominated watershed in the United Kingdom. Similarly, Yallop and Clutterbuck (2009) presented the linear relationship between DOC and color ($R^2 > 0.9$) for peat dominated waters. Ishikawa et al. (2006) studies on rainforest-dominated watershed in Indonesia indicated the linearity between DOC and Color ($R^2 > 0.9$).

In natural waters, DOC is a composite of heterogeneous sources of organic matter. Source-wise color-DOC relationships may help to predict natural water color in complex, heterogeneous surface waters, especially in field-scale modeling efforts of receiving waters where water color is of concern. If organic matter source or DOC is known, the water color in runoff from that source area can be measured before entering into receiving water bodies. To characterize the color-DOC interaction, a small laboratory-scale experiment was designed. Source-specific relationships between water color and DOC was developed based on sources of organic matter commonly found in surface waters. The specific objectives of the study were (1) to quantify the relationship between water color and DOC in water based on specific organic matter sources and (2) to test a method to predict the water color on water samples with multiple sources of DOC.

Methods

Organic Source Materials

To represent the common sources of DOC-containing runoff samples, four types of organic materials were collected (Figure 3.1): Sphagnum peat moss (PM), composted cow manure (CM), cotton burr compost (CC), and decomposing bark chips (BC). PM (Majestic Earth, Sun Gro Horticulture, Agawam, Massachusetts) and CC (Oldcastle Lawn and Garden, Inc., Georgia) were purchased in in Stillwater, Oklahoma. CM was obtained from a cattle farm in Gerty, Oklahoma. BC were collected from a tree service in Stillwater, Oklahoma.

Predictive Relationships between Color and DOC

Previous studies have demonstrated a linear relationship between water color and DOC in streams and lakes (Molot and Dillon 1997; Worral et al. 2003; Ishikawa et al. 2006; Yallop and Clutterbuck 2009; Ishikawa et al. 2006). Based on this previous research, the relationship between color and DOC for water samples with organic matter from a specific source was defined as:

$$Color = \beta\ [DOC] \qquad (1)$$

where *color* is in PCU, the coefficient β is called a color coefficient in (L/mg -PCU), and DOC is dissolved organic carbon (mg/L) present in the colored solution for that source of organic matter.

To predict the color-DOC relationship for water samples with heterogeneous sources of organic matter, the following relationship was proposed as:

$$Color = \sum_{i=1}^{n} \beta_i \, [DOC]_i P_i \qquad (2)$$

where n is number of individual *DOC* sources, and P_i is volumetric proportion of the ith color and *DOC* water source.

Water Sample Preparation

From each source of organic material, color-DOC solutions were prepared by soaking 2 kg of source material in deionized water (sufficient amount to saturate the source material) in a clean 5-gallon bucket for 16 hours. After several trials, 16 hours of soaking period was considered as a consistent color extraction time for all sources. After 16 hours, the soaked sample was filtered through 0.45 μm glass-fiber filter (DSC, Encino, CA). Filter clogging was common during the filtration process. To minimize clogging of the 0.45 μm filter paper, filters with larger pore sizes than the 0.45 μm filter paper were used as pre-filter. Coffee filter paper that was rinsed three times was used as pre-filter to avoid the residual DOC leaching. Khan and Subramania-Pillai (2006) showed that residual DOC may be released from unwashed filter papers. In this study, the filter paper was washed with 100-ml of deionized water prior to sample filtration to ensure the filter paper was free of any organic residuals. The filtered samples for each source were stored in a refrigerator at 4^0C. The stored samples were used for deriving the relationship for water color and DOC (equation 1 and equation 2) within 10 days of filtering.

From each filtered solution, 10 diluted sample solutions (100 ml each) were prepared from individual source samples. For quality control, there were duplicate dilutions for every other sample, which made 15 diluted samples for each source (Figure 3.2). A minimum sample size of 12 was estimated based on the peat moss color-DOC sample (n=30) using Minitab statistical software (Minitab 2010) with a 5% margin of error; therefore, the sample size of 15 was considered sufficient to develop the relationship between color and DOC.

Color and DOC Measurement

To analyze the linearity of color and DOC based on a homogenous source of organic matter (equation 1), 100 ml diluted samples were prepared for each source. Sample pH was recorded for each source sample using a benchtop pH meter. AHPA et al. (2012) reported that pH adjustments are required if sample pH is less than 4 or greater than 10. All source samples used in this study were within the APHA et al. (2012) recommended range, so pH adjustments were not required. For quality control, sub-samples for color and DOC measurements were taken from same batch of the 100 ml diluted sample.

Out of the 100 ml diluted sample, a 10 ml subsample was collected using a glass pipette and analyzed for color. Color measurements were performed on DR 6000 Spectrophotometer using Hach Company standard method of color measurement called Platinum-Cobalt Standard Method (Method 8025, Hach Company 2014a) at a wavelength of 455 nm (cell path length = 1 inch) and color units were reported in PCU. A blank sample of deionized (DI) water was used to define zero color. For quality control, 250 PCU solution was prepared with a 1:1 dilution of 500 PCU standard solution; all quality control color readings on the standard solution were within the 2% error range (245-255 PCU). For DOC measurement, a simple and direct method was selected from Hach's direct methods (Method 10129, Hach Company 2014b and Method 10173, Hach Company 2014c).

The Hach method is designed for total organic carbon (TOC) analysis. All the samples used in this study were filtered through 0.45 μm filter, so the measured TOC was considered as DOC. There are three types of standard procedures for this method based on the range of DOC concentration in the sample: low range (0.3 to 20 mg/L), mid-range (15 to 150 mg/L, and high range (100 to 700 mg/L). The method procedure differs based on the sample volume required for the test. In this study, low range (LR) and mid-range (MR) test procedures were followed for DOC measurements for diluted samples based on the trial test sample DOC measurement for each source. The detail description of Hach method is found in Hach Company, 2014b. In DR 6000 spectrophotometer, program 427 was selected for DOC test for LR samples and program 425 was selected for MR samples.

For accuracy check, 100 mg/L standard solution (for MR) and 50 mg/L (for LR) were prepared from Hach TOC standard (Potassium hydrogen phthalate, 1000 mg/L TOC), and measurements were checked for every source of samples. For quality control, every other sample was analyzed as duplicates and results were compared. If the duplicate DOC sample was more than 5%, test results were disregarded and a new test was performed. The measured color-DOC data for all four sources are presented in the Appendix (Table A.1 to A.5).

Validation

In order to validate equation 2, a range of heterogeneous solutions using four organic source materials were prepared in varying proportions (1:1, 1:1:1, and 1:1:1:1). Prior to making the heterogeneous combinations, the DOC for each homogeneous-source sample was measured and recorded. Equal volume (10 ml) of each filtered colored sample was taken and mixed well in a volumetric flask. Color measurements were performed for each heterogeneous source sample using a DR 6000 spectrophotometer. There were three sets of heterogeneous mixture (source combination), and each set had 11 combinations (Appendix: Table A.7 to A.10). Combination sets ranged from approximately 100 to 200 PCU (set-I), 200 to 400 PCU (set-II) and 400 to 500 PCU (set - III).

Statistical Methods

Color coefficients for equation 1 were determined by linear regression analysis using Minitab 16 (Minitab 2010). An analysis of covariance (ANCOVA) analysis was conducted to test differences between source-wise color-DOC relationships. In the ANCOVA tests, the response variable was '*Color*,' the covariate was '*DOC*,' and treatment was 'organic source.' Statistical results were reported based on APA (2010).

Based on the color coefficients and known DOC of individual source organic materials, water color for the heterogeneous mixture (equation 2) was predicted. The predicted color in each relationship was compared with measured colors with reference to R^2, Nash-Sutcliffe efficiency (NSE), and absolute percentage relative error (RE,%) for all combinations. The NSE value (Nash and Sutcliffe 1970) was computed as:

$$NSE = 1 - \left[\frac{\sum_{i=1}^{n}(Cm_i - Cp_i)^2}{\sum_{i=1}^{n}(Cm_i - Ca)^2}\right] \tag{3}$$

where Cm_i was measured color (PCU) in the ith mix-sample, Cp_i was predicted color for the ith mix-sample, Ca was average color (PCU) of measured samples, and n was the number of sample. The relative percentage error (RE) was evaluated as:

$$RE = \frac{|Cm_i - Cp_i|}{Cm_i} \times 100 \tag{4}$$

where Cm_i is measured color (PCU) in the ith sample, Cp_i is predicted color (PCU) for the ith sample.

Results and Discussion

A simple method that did not require detailed chemical analysis of organic matter to predict water sample color for known homogeneous sources of DOC has been developed and method was applied for multiple sources with defined proportions of selected organic sources. Further implications of this methodology are also discussed.

Individual Sources

The light absorbance capacity was hypothesized to be different for water with DOC from different organic material sources. Each source of organic matter had different physical and chemical characteristics. The complex chemical properties of humic and fulvic acids content in organic matter (Brezonik and William 2011; Mostafa et al. 2013) may vary by source and cause a range of color coefficients for each source. Variations of light absorbance in surface waters are a result of these physical and chemical properties of DOC in the water (Baricaud et al. 1981; Baker and Spencer 2004; Del Vecchio and Blough 2004; Helms et al. 2008; Sulzberger and Durisch-Kaiser 2009).

Linear relationships were developed between color and DOC for four sources of organic matter (Figure 3.3). The slope (color coefficient, β) was obtained from a linear regression analysis for each sources (Table 3.1). The intercept term in the linear regression was insignificant ($p < 0.05$) for all organic sources analyzed. A two-way ANCOVA showed the covariate, DOC was significantly related to the color, $F(1, 70) = 5418.3$, $p < 0.001$. There was a significant main effect of organic source on color after controlling for DOC, $F(3, 70) = 4.08$, $p = 0.01$. There was a significant interaction between DOC and source type $F(3, 70)= 510.48$, $p < 0.001$ (Table 3.2). Tukey pairwise comparison test showed that color was significantly different among four organic sources at $p < 0.05$. Among the four sources tested, CC had highest color coefficient followed by CM (Table 3.1). These two sources are well composted materials.

The PM color coefficient of 5.68 was within the range of 3.3 to 9.9 reported by Molot and Dillon (1997). Worrall (2003), and Yallop and Clutterbuck (2009) studies showed color/DOC ratio of almost 20 for peat-dominated area, which is greater than our reported ratio. The percent cover or extent of the peat present in the watershed is directly related to the DOC yield (Dillon and Molot 1997). BC color coefficient of 10.24 was slightly higher than 3.3 to 8.8 as reported by Christman and Ghassemi (1966). A color/DOC ratio for CM and CC were not found in literature.

The effects of pH on color measurements were reported in the literature (Chritman and Ghassemi 1966; Ishiawa et al. 2006). The PM sample was acidic (pH =

4.42) whereas other samples were neutral or slightly basic, with pH for undiluted CM, CC and decomposing BC of 7.79, 7.10 and 7.83, respectively. The electrical conductivity of lab-grade DI water was 1.6 micro-Siemens/cm and pH ranged from 5.1 to 6.5. pH measurements on a subset of test samples indicated that dilution with DI water did not change the pH of the diluted samples.

Multiple Sources

Based on the color coefficient and known DOC of individual organic sources, water color was predicted with reference to equation 2 for three combination sets (Appendix Table A7 to A10). The predicted versus measured comparison showed excellent results for combined set-I and set-II (R^2 = 0.99, NSE = 0.97 and relative absolute error = 5.4%, Figure 3.4), whereas set-III did not perform as well (R^2 = 0.84, NSE = -2.56 and relative absolute error = 12.0%, Appendix: Figure A.1). The set-III data had either measurement or instrument error that was likely a result of using Hach test kits that had been stored at too high of a temperature, so it was not included for relationship validation.

For a field-scale watershed, where the predominate proportion of source(s) of organic matter and runoff from source may be able to be more easily determined, color may be highly predictable. Studies have shown that DOC variation in runoff water can be quantified with reference to land-use practices (Larson et al. 2014; Gergel et al. 1999). In natural waters, the heterogeneous sources of organic matter may be determined using land-use practices and management records in the catchment area. For example, in production nurseries where application of organic matter and fertilizers is common and the receiving water body’s water color may be of concern, the color of runoff water from the site with a limited number of DOC sources can be determined as follows:

1. Dominant DOC sources can be determined based on potted fertilizer applications, organic matter applications, plant density, and/or other management records for specific areas/subwatersheds.
2. The proportion of DOC sources contributing to the watershed outlet can be estimated with reference to runoff volume and DOC concentrations derived from a hydrologic model, utilizing subwatersheds defined based on areas with a common dominant source(s).
3. With known DOC proportion and color coefficient, the color from a watershed could be estimated using Equation (2) and color coefficients determined in the laboratory for the dominant sources.
4. At the outlet of the watershed and each subwatershed, DOC, color and runoff volume can be measured for validation of the predicted values.

On a larger watershed scale, however, the application may be more difficult as the number and proportion of DOC sources would be much more difficult to accurately estimate. In addition, organic matter entering into the surface waters on a large scale with many DOC sources may create more complex chemical and physical properties of DOC (Massicotte and Frenette 2011; Nebbioso and Piccolo 2013) than is present in these laboratory experiments, and could potentially change the DOC-color relationships derived from single-source samples.

Further Applications

The methodology used in this study is applicable to predict water color based on DOC from a known source, assuming an absence of significant chemical or mineral interferences. There have been reported interferences of chemical agents or metals for DOC measurements, for example Fe inferences (Kritzberg and Ekström 2012). Future studies could include investigating the effects of chemical agents or minerals on heterogeneous sources of organic matter contained in colored-water samples.

Drinking water treatment depends upon the nature, source, and content of DOC (Volk et al. 2002; Matilainen et al. 2011). Coagulant dosing requirement is often determined by the amount of water color (Ratnaweera et al. 1999). The source-wise quantification of color and dissolved organic matter may also be useful for water treatment facilities (Volk et al. 2005; Kim and Yu 2005; Grayson et al. 2012; Parry et al. 2015), as well as management of DOC yield from drinking water catchment (Holden et al. 2012; Ritson et al. 2014; Bloodworth et al. 2015). Landscape-based management of organic materials and their sources can minimize the DOC yield into surface water. Proper quantification of the color-DOC relationship of source waters may help to determine chemical dosing for water treatment facilities, thereby minimizing the potential carcinogenic by-products in drinking water.

Based on the USEPA (2016) wadeable streams' water chemistry data (DOC and color from 2000-2004 throughout the conterminous United States), the relationship between color and DOC was determined by linear regression analysis in Minitab 16 (Minitab 2010). There was a significant linear relationship between color and DOC (R^2 = 0.68, and $p < 0.001$) (Figure 3.5). A possible contributing factor for the variation in this relationship may be the origin and spatial distribution of natural organic matters in these streams which ranged in size from first to fifth order (USEPA 2006). Decomposed vegetation, forest litters, human waste, animal manure, soil nutrients and, soil organic matter often originate from terrestrial landscapes whereas, decomposed aquatic plants or algal biomass may contribute organic matter directly in surface waters (Brezonik and William 2011, Mostofa 2013). Such variations in organic matters spatially would impact the physical and chemical properties of DOC in the stream at the watershed outlet. In addition, there could be industrial chemicals transported to the water bodies which would impact the water color in surface waters.

The color coefficient (slope) in Figure 5 for the stream water was lower than the samples analyzed in present study (Figure 3.3). The organic source samples used in present study were selected such a way that the water samples had concentrated color to develop color-DOC relationship. As discussed above, there are various sources organic matters in watersheds, which could have less color that were not analyzed in this study. Therefore, the color coefficients found for the sources analyzed in this study would likely be expected to be higher than the composite-source samples collected from natural streams shown in Figure 5.

Conclusions

The quantification of natural water color and DOC is important to evaluate aesthetic, aquatic habitat, ecosystem function, and drinking-water standards in natural waters. A color prediction methodology for single-source and heterogeneous organic matter present in water was developed and validated using laboratory-scale experiments. The study approach does not require separation of the complex chemical nature of organic matter. Results demonstrate that a linear relationship exists between water color and DOC in surface waters for specific DOC sources. This study also shows that water color for heterogeneous sources of organic matter content in surface waters can be predicted based on the proportion of various organic sources, at least for up to four defined sources of DOC.

The method used in this study will be especially useful to predict color based on sources and levels of organic matter for modeling of color in runoff from field-scale watersheds when predominant DOC sources are known (such as animal or plant based compost, manure, or potting soils). In larger watershed applications, future research will be required to test the applicability of the method to predict color for heterogeneous sources of organic matter.

Tables

Table 3.1. Regression equations to predict color for individual organic source. PM = sphagnum peat moss ; *CM* = composted cow manure; *CC* = cotton-burr compost ; BC = decomposing bark chips; *DOC* = dissolved organic carbon; R^2 = coefficient of determination; SE = standard error; PCU= Platinum-Cobalt Unit.

Source Type	Regression Equation	R^2	SE (PCU)	*p*-value
Peat Moss	$Color_{PM} = 5.68\ [DOC]_{PM}$	0.99	7	< 0.001
Composted Cow Manure	$Color_{CM} = 15.75\ [DOC]_{CM}$	0.98	14	< 0.001
Cotton-burr Compost	$Color_{CC} = 19.19\ [DOC]_{CC}$	0.97	24	< 0.001
Bark Chips	$Color_{BC} = 10.24\ [DOC]_{BC}$	0.99	10	< 0.001

Table 3.2 Analysis of covariance summary for color prediction by dissolved organic carbon (DOC) and organic source type. DF = degrees of freedom; SS = sum of squares and MS = mean squares; R^2 = coefficient of determination.

Term	Source of Variation	DF	SS	MS	F-value	*p*-value
Covariate	DOC	1	792954	792954	5418.3	<0.001
Intercept	Organic Source	3	1791	597	4.1	0.01
Slope	DOC* Organic Source	3	224122	74707	510.	<0.001
	Error	70	10244	146		

Note: S= 12.1; R^2 = 99.23%, adj. R^2 = 99.16%

Figures

Figure 3.1. Types of source organic source materials used in this study.

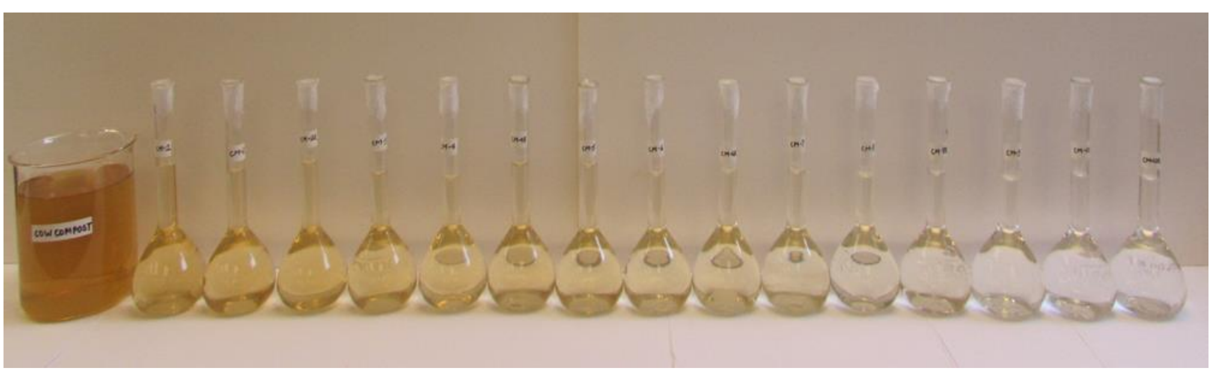

Figure 3.2. Example of 15 dilutions made for composted cow manure.

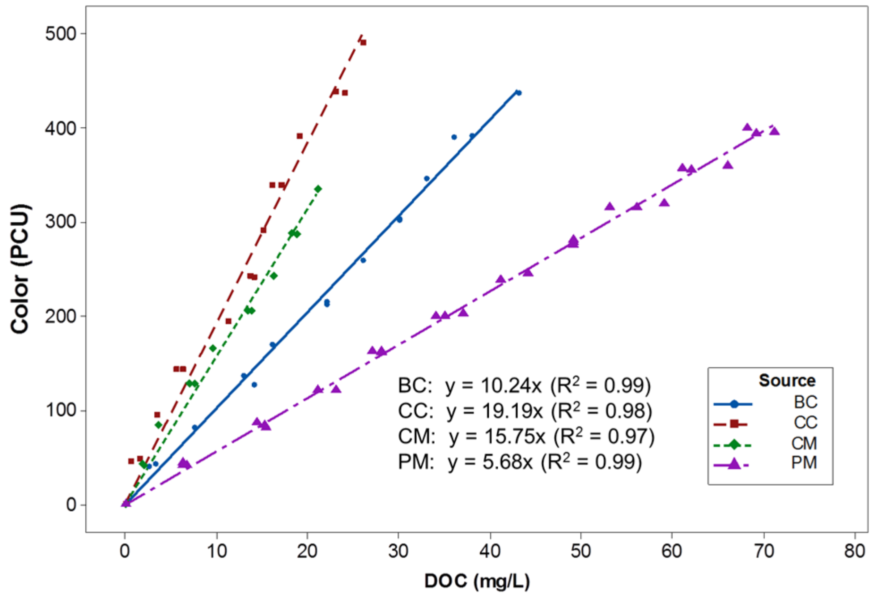

Figure 3.3. Linear relationships between color and dissolved organic carbon (DOC) for decomposing bark chips (BC), cotton burr compost (CC), cow compost (CM) and, Sphagnum peat moss (PM). The color unit is on Platinum Cobalt Unit (PCU). R^2 is coefficient of determination.

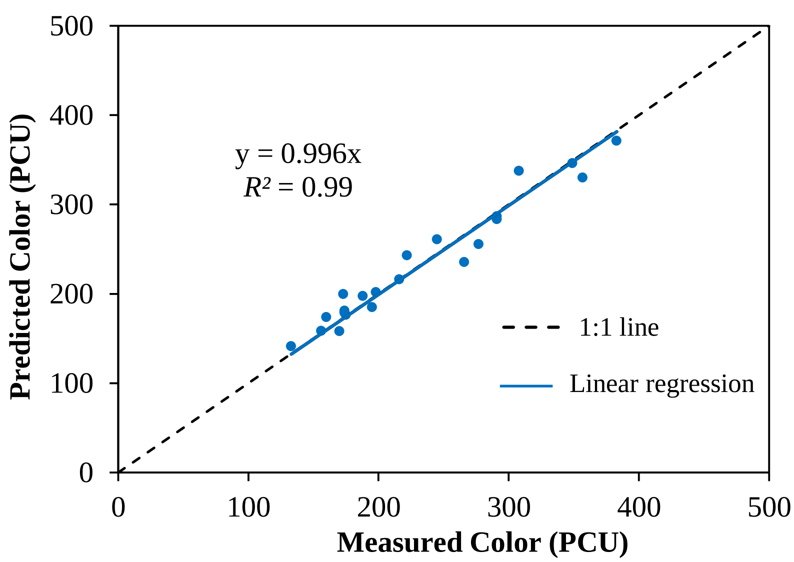

Figure 3.4. Comparison between measured color and predicted color for heterogeneous sources of organic matter contained in colored water samples. The color unit is on Platinum Cobalt Unit (PCU). R^2 is a coefficient of determination.

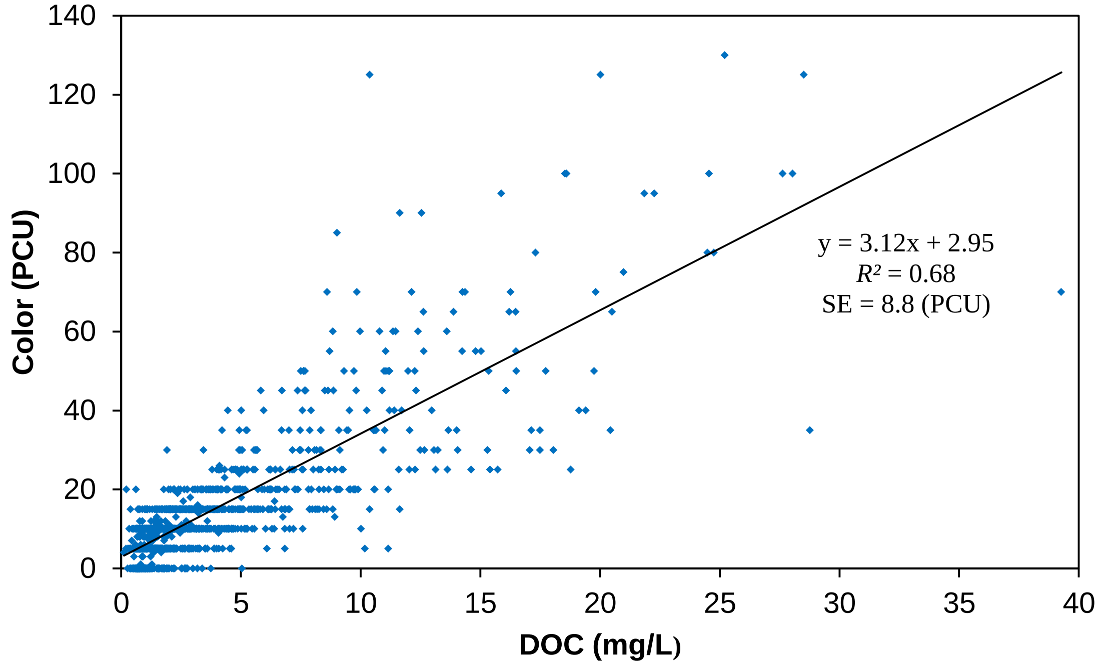

Figure 3.5. The relationship between color and dissolved organic carbon (DOC) for conterminous United States (data source: USEPA 2016). The color unit is on Platinum Cobalt Unit (PCU). R^2 = coefficient of determination; SE = standard error

CHAPTER IV

AN INTEGRATED APPROACH TO CHARACTERIZE LONG-TERM CHANNEL PLANFORM CHANGES IN AN AGRICULTURAL WATERSHED WITH LIMITED FIELD DATA

Abstract

Planform stability of stream channels can be impacted by anthropogenic factors such as settlement, agricultural practices, deforestation, construction activities, dam operations, and urban developments. However, most streams lack on-the-ground measurements over time to document these changes. Analysis of aerial images in geographic information system (GIS) is commonly used to determine changes in channel planform stability. Relevant historical events and records may be associated with the planform changes shown in aerial images. The objective of this study was to develop and apply an integrated approach to evaluate channel planform stability in an agricultural watershed using historical records such as plat maps, aerial images, and relevant historical events. The methodology has been applied in the Cobb Creek watershed in west-central Oklahoma. The Cobb Creek watershed channel networks in 1873 and 2013 were compared based on the total length of all channels in each network. Total channel length in 2013 network was almost 70% greater than in 1873 channel network, which was concurrent with settlement and associated erosion problems in the watershed that occurred during the early portion of this period. Further, a 31-km section of the main stem of Cobb Creek was selected and divided into 12 segments (SEGs) based on bridge constrictions on the channel. The channel migration rates were estimated for each SEGs and periods of 1940-1966, 1966-2003, and 2003-2013. Channel migration rates and cumulative effective stream power were normalized by average SEG's to compare historical planform changes for the period of 1966-2003 and 2003-2013. Channel migration was significantly decreasing from the period of 1940-1966 to 2003-2013. Based on the integrated approach framework developed in this study using only limited, on-the-ground field measurements, results indicated that the main stem of Cobb Creek had planform stability from 1940 to 2013. The approach presented in this paper could be applicable for other anthropogenically impacted agricultural watersheds.

Keywords: Channel migration, planform, historical changes, integrated method

Introduction

Natural geomorphic functions of streams and rivers are altered by anthropogenic factors such as impoundments, infrastructure development and land-use practices (Hooke 2000; James and Marcus 2006; Gregory 2006; Hooke et al 2012). Stream corridor restoration, planning and river management often require historical assessments of stream hydrology, climate, geological and geomorphological features, and land-use practices. Historical data can provide important information for changes in watershed hydrology and river morphology (Gurnell et al. 2003) which can, in turn, be utilized to develop future river management strategies (Brierley and Hooke 2015). Historical evaluations of changes in channel planform are useful to identify impacts of anthropogenic disturbances in natural streams and rivers (Benner and Sedell 1997; Trimble 2008; Lagasse et al. 2004; Erskine 2011; Deb and Ferreira 2014; Rhoads et al. 2016). Channel planform refers to the aerial or planimetric view of stream channel geometric features including sinuosity, meandering, channel width and centerlines. Historic channel planform is often compared with existing planform to evaluate changes in channel geomorphic functions.

In many studies, aerial photographs and maps have been used for spatial analysis of channel planform changes (e.g., Gurnell et al. 1994; Micheli and Kirchner 2002; Heo et al. 2009; Yao et al. 2013; Scorpio et al. 2015; Rhoads et al. 2016). Gurnell et al. (1994) investigated channel planform changes from 1876 to 1992 for the River Dee in the United Kingdom using historical aerial photographs and maps in geographic information system (GIS). In their study, limited channel migration was shown in the River Dee during the 115-year period because of flow regulations. Micheli and Kirchner (2002) used 1955-1995 aerial photographs for spatial analysis of channel lateral migration in Sierra Nevada, California. This study digitized the channel centerlines for 1955, 1976 and 1995 and estimated channel migration rates based on eroded area polygon made by two channel centerlines divided by the elapsed time period in years.

Heo et al. (2009) characterized channel meander migration for the Sabine River in the southern USA using historical orthophotos to digitize channel centerlines from 1974 to 2004 in GIS. Yao et al. (2013) used similar GIS techniques to evaluate channel planform changes and migration rates in the Yellow River, China. Scorpio et al. (2015) analyzed channel morphology for five rivers in Italy from 1869 to 2012 using aerial images and topographic maps. Their results showed that deforestation, agricultural practices and river training works were the primary causes of channel planform alteration.

More recently, Rhoads et al. (2016) evaluated changes in channel planform and the watershed channel network from the 1820s to 2012 in the Sangamon River basin, Illinois. In their study, the 1820s' channel network was digitized from historic plat maps for the watershed and was compared to the digitized 2012 channel network. Their results showed that the channel network in 2012 was almost three times larger in length than the 1820s' channel networks. Further, Rhoads et al. (2016) reported that the majority of channel network expansion was due to the addition of agricultural drains in the watershed after European settlement.

Digitized historical channel centerlines have been used to predict future channel flow path using channel migration models (e.g., Abad and Garcia 2008; Güneralp and Rhoads 2009; Motta et al. 2012; Chakraborty and Mukhopadhyay 2014). In valleys with stream channels that have exhibited historical stream migration, channel migration zones are identified by comparing spatial and temporal channel planform shape and patterns (Rapp and Abbe 2003). Channel migration zones are useful for flood management, potential infrastructure construction planning and damage prevention, conservation practices (CPs), and streambank erosion control.

Numerous studies across the USA have demonstrated that best management practices (BMPs) and flow regulation can reduce lateral channel migration in fluvial systems (Shields et al. 2000; Ritter et al. 2007; Fremier et al. 2014). Shields et al. (2000) showed significant reduction in downstream channel lateral migration after construction of dams in the Missouri River in Montana. However, studies showed that reservoirs could result in downstream incision (Kondolf 1997; Legleiter et al. 2015). In west-central Ohio, soil conservation and river management activities helped to maintain geomorphic equilibrium for previously impacted channels (Ritter et al. 2007). Fremier et al. (2014) demonstrated that the combined effects of BMPs on soil erosion and flow regulation or control reduced lateral channel migration by nearly 40% in the Sacramento River, California.

In the USA, many soil CPs have been implemented by farmers and ranchers with support from the United States Department of Agriculture (USDA) (Tomer and Locke 2011). In west-central Oklahoma, numerous studies have shown a reduction in upland soil erosion, sediment yield and nutrient loading into the Fort Cobb reservoir due to USDA soil CPs (Simon and Klimetz 2008; Garbrecht and Starks 2009; OCC 2009; Becker and Steiner 2011; Garbrecht 2011; Moriasi et al. 2011; Steiner et al. 2014). In 2010, the United States Geological Survey (USGS) published 10 scientific investigation reports for the Fort Cobb watershed focusing on evaluation of CPs, land use change, climate and water quality (Andrews et al. 2011; Becker 2011). More recently, authors from the USDA–ARS, Grazinglands Research Laboratory in El Reno, Oklahoma, published a series of 10 journal papers in a special section of the Journal of Environmental Quality (Volume 43, Issue 4, July-August 2014). These papers include up-to-date hydro-climatic, land use, geological and soil physiographic data for the Fort Cobb watershed (Steiner et al. 2014). However, those studies have only attempted limited investigation of channel geomorphic changes over the long term. To better understand these changes, relevant historical events and records associated with the planform changes in the watershed need to be evaluated.

The objective of this study was to develop and apply an integrated approach to evaluate channel planform stability in an agricultural watershed using historical records such as plat maps, aerial images, and relevant historical events. The methodology was applied in the Cobb Creek watershed in west-central Oklahoma.

Methods and Materials

Integrated Approach

For this integrated approach, channel planform characterization techniques have been coupled within a systematic framework that uses historic records and limited field data to describe long-term channel planform changes within a watershed. The framework for this approach included nine steps (Figure 4.1). These steps are described as follows.

1. **Historical Maps and Aerial Photographs.** The first step of integrated approach is gathering of survey plat maps, topographic maps, and aerial photographs from the area of interest. Rhoads et al. (2016) demonstrated that historical land-survey records and aerial images were useful in evaluating physical channel planform changes. In most watersheds, such maps and photographs are available. For example, in the USA, land aerial images are generally available from 1937 onward with varying degrees of temporal resolution (Trimble and Cooke 1991).
2. **Anthropogenic Impacts and Conservation Practices.** The second step is collecting historical records of anthropogenic impacts in the watershed. More than 50-percent of the earth’s landscape has been disturbed by anthropogenic impacts

(Hooke et al 2012). Agricultural practices, grazing, irrigation, deforestation, construction activities, dam operations, and urban developments are some of the human activities that may degrade watershed. In addition, information of conservation practices or best management practices should be collected that have been implemented in the watershed.

3. **Data Needs: Precipitation, Streamflow, and Representative Channel Survey**. In the third step, historical precipitation and streamflow records are required. Precipitation data can be obtained from government agency data archives. For example, in the USA, National Oceanic and Atmospheric Administration collects and archives precipitation records . Streamflow has been altered by dam operations and flood control impoundments in several watersheds. In many studies, effect of reservoir operation in downstream geomorphic changes have been evaluated (e.g., Shields et al. 2000; Kondolf 1997; Legleiter et al. 2015). In many streams, local agencies have recorded daily streamflows. For example, USGS has operated gaging stations at most of the streams in the USA. Acquire channel survey records for gage station or representative reaches survey records, otherwise, channel geomorphic serving is required to determine representative channel reaches in the watershed.
4. **Channel Network.** In the fourth step, the channel network should be digitized in GIS from maps and aerial images obtained from step 1. For the USA, channel flowlines for watersheds can be obtained from the USGS's Nation Hydrography Dataset in a shapefile format. While digitizing the channel network for the year of interest, NHD flowlines can be taken as a reference guide (Rhoads et al 2016).

With historic maps and aerial photographs, channel flowlines or centerlines are traced to determine the channel network and channel planform.

5. **Channel Segment Selection.** In the fifth step, select the representative channel reach length or section with reference to step 1 and step 2. Divide up the study channel reach into segments (SEGs) based on anthropogenic impacts and/or conservation practices implemented. Road bridge crossing locations are a convenient way to identify SEG since their location generally does not change over time. In this step, channel centerlines on each aerial images need to be accurately digitize with reference to channel banks.

6. **Segment-wise Streamflow and Power.** In the sixth step, mean daily streamflow and available stream power are required for each SEG. If there is not a gage site in each SEG, mean daily flows from gaged SEG could be transferred to the other segments (ungaged locations) using the drainage area ratio method assuming no major tributaries influences (Esralew and Smith 2009) as:

$$Q_{ug} = \frac{DA_g}{DA_{ug}}\ Q_g \tag{1}$$

where Q_{ug} is mean daily flow at ungaged site (m^3/s), DA_g is drainage area at gaged station(km^2), DA_{ug} is drainage area at ungaged site (km^2), and Q_g is mean daily flow at gaged site. Available stream power for each SEG and period should be estimated. Available power for channel work is defined by Leopold et al. (1964) as:

$$\Omega = \rho g S Q \tag{2}$$

where ρ is density of water (kg/m^3), g is acceleration due to gravity (m/s^2), S is channel slope and Q is discharge (m^3/s), which gives Ω in W/m.

7. **Channel Planform.** In the seventh step, estimate channel planform characteristics (SEG length, valley length, sinuosity) from channel digitized channel centerlines from step 5 in GIS.
8. **Lateral Channel Migration.** In the eighth step, lateral channel migration is estimated between time periods. With reference to step 1, 2, and 3, years can be grouped into periods. For example, if historical records have 1940, 1950, 1980 and 2010 aerial images, the groups will be 1940-1950 and 1980-2010. The channel lateral migration can be estimated for each period from digitized channel centerlines for each SEG and period.
9. **Historical Channel Planform Characterization and Comparison**. After quantifying and evaluating step 1 to 8 (Figure 4.1), historical channel planform characterization and comparison of study watershed can be completed in the last step. In this step, statistical comparisons between various parameters that control channel planform changes such as year, period, SEG and, stream power are completed. If parametric statistical tests are use, channel migration and stream power could be normalized with SEG channel lengths.

Application of Integrated Approach

Study Area

The 426-km2 Cobb Creek watershed is located in west-central Oklahoma (Figure 4.2). The watershed includes all or parts of Caddo, Custer and Washita counties in Oklahoma that drain to Fort Cobb Reservoir. In 1958-1959, the U.S. Bureau of Reclamation (USBR) constructed a reservoir on Cobb Creek called the Fort Cobb

Reservoir (Garbrecht 2011). The 31.4-km long segment of the main stem of Cobb Creek was selected for channel planform and lateral migration studies.

The watershed has various types of geological formations. The area is comprised of 58 percent Rush Springs Sandstone, 24 percent Cloud Chief rock, 15 percent Weatherford Gypsum and 3 percent alluvium deposits (Cederstrand 1996; Starks et al. 2011a; USDA-ARS 2013a; Moriasi et al. 2014a). The corridor along the study section is alluvial deposits and surrounded by the Rush Springs Sandstone formation. The Rush Springs Sandstone is a major rock formation that extends up to 102 m deep (Starks et al. 2011a).

The soils are primarily fine sandy loam based on USDA Natural Resources Conservation Services (NRCS) State Soil Geographic database (STATSGO) soil mapping unit of OK110 (Starks et al. 2011a; Moriasi et al. 2014a). The most recently compiled data for land use are from 2001 and 2005 (Storm 2003; Starks et al. 2011b). In 2001, about 51 percent of the Fort Cobb watershed was covered by cultivated crops, 40 percent by pastureland and 7 percent by forest land (Storm et al. 2003). In 2005, the cultivated land area was 56 percent, whereas pastureland was 34 percent and forest land was 5 percent (Starks et al. 2011b). In addition, there was 5 percent road in 2005 which was undetected in 2001 land use analysis because of spatial resolution (Storm et al. 2003). Yue (2006) reported that the Cobb Creek watershed has about 86 percent agricultural land, 14 percent pastureland and 0.1 percent forest land.

Approximately 29 percent of the watershed's contributing drainage area has NRCS regulated reservoirs (USDA-ARS 2013b, USGS 2016a). There are six flood control dams in the watersheds (Figure 4.2) which were constructed during the late 1950s

(Moriasi et al. 2014b). The study watershed has an active USGS stream gage station near Eakly, Oklahoma (USGS 07325800, Figure 4.2), which has flow record available from 1969 to the present. Average annual precipitation was 690 mm/year from 1895-1970, 773 mm/yr from 1970-2000, and 716 mm/yr from 2000-2012 (Garbrecht et al. 2014).

The application of the previously described integrated approach to the Cobb Creek watershed is described as follows.

Step 1: Historical Maps and Aerial Images

All available historical maps and aerial images information including historical for the Cobb Creek watershed were collected. The earliest available maps for the watershed are from 1873. The U.S. Bureau of Land Management, General Land Office (BLM-GLO) was established on April 12, 1812, and started record keeping survey plats (township and range) as per the Land Ordinance Act of May 20, 1785 (BLM-GLO 2016). In this study, the earliest detailed historical survey maps were obtained from BLM-GLO (2015). The BLM-GLO collection of plat maps for the study watershed were surveyed between October and November 1873 (approved in March 1874), hereafter referred to as the “1873 plat map.”

The plat maps obtained from BLM-GLO (2015) had 12 townships and ranges (8N 13W to 12N 13 W, 9N 14W to 12N 14W and, 10N 15W to 12N 15W). Collected plat maps were georectified with four known vertices of townships and ranges in ArcGIS 10.0 (ESRI 2010). The average georectification root mean squared error (RMSE) in georectified plat map was 6.7 m at first-order polynomial transformation. The coordinate system was on the North American Datum (NAD) of 1983 in Universal Transverse Mercator (UTM).

The earliest available aerial images for the watershed are from 1940. In order to evaluate historic channel planform changes in the watershed, aerial images of 1940, 1966, 2003 and 2013 were selected based on availability. The 1940 and 1966 images were obtained from USDA-ARS, Grazinglands Research Laboratory, El Reno, Oklahoma. Aerial images of 2003 and 2013 were obtained from the Agriculture Imagery Program (NAIP) (USDA-FSA 2003, 2013). Based on personal communication with Dr. Patrick Starks (USDA-ARS, EI Reno, February 10, 2016), USDA-ARS used a "rubber-sheet" method whereby individual black-and-white images were "stretched" to match a basemap with a RMSE value as close to 1 as possible. The rubber-sheet is a method of geometric transformation in GIS while georeferencing a target raster layer to base map raster layer (ESRI 2010). The aerial imagery obtained from USDA-ARS had incomplete coverage for 1966 photographs of the watershed. The incomplete sections for the watershed images were filled with 1966 aerial photographs obtained from ASCS (1966) and georeferenced in ArcGIS 10.0 (ESRI 2010) with seven to eight known ground control points. The NAIP 2003 and 2013 images were georectified to the NAD 1983 in UTM coordinate system (USDA-FSA 2003, 2013).

Step 2: Anthropogenic Impacts and Conservation Practices

Historically, the study watershed was impacted by soil erosion that resulted from agricultural practices. Historical events related to settlement, soil erosion, CPs, and relevant studies in the watershed were determined, and with details of these events are listed in Table 4.1. Five time periods, pre-1873, 1873-1940, 1940-1966, 1966-2003, and 2003 - 2013, were chosen based on availability plat maps, aerial images, and historical events. CPs refer to the soil erosion protection measures that have been implemented by farmers and ranchers. Based on the BMPs spatial dataset provided by the Oklahoma Conservation Commission (OCC) in January 2016, common CPs for erosion control were gully shaping, terrace removal or addition, cross-fencing, grade-stabilization structures, diversions, grassed waterways, critical area planting, and no-tillage.

Step 3: Precipitation, Streamflow, and Representative Channel Survey

Garbrecht et al. (2014) developed a weather dataset from 1949 to 2012 for the watershed with reference to nearby weather stations and available databases. The study watershed has only one gage station (USGS 07325800) (Figure 4.2), which has continuous daily stream-flow record available from 1969 to present. In 1959, a dam was constructed at Crowder Lake, the upstream-most section of the study stream (Figure 4.2). Flow records prior to water year 1969 were not available for the watershed. Daily flows for water year 1966 to water year 1968 were determined by a second-order polynomial relationship between three-day cumulative daily precipitation and daily mean flows for water year 1969 to 2012 (R^2 = 0.21). Precipitation data was obtained from Garbrecht et al. (2014). Considering the temperature, vegetation types, soil, runoff time and associated infiltration effects, three-day cumulative precipitation was correlated with daily average flow. The hydrograph of simulated daily mean flows for 1969 to 1968 gaged daily mean flows for 1968-2003 and 2003-2013 at the gaged site is shown in Figure 4.3.

As part of the present study, a channel cross-section and profile survey was conducted at a site on the mainstem of the Cobb Creek in July 27, 2015. The surveyed cross-section ($35^{o}17'28.8''$, $98^{o}35'38.9''$) was approximately 64-m upstream from the USGS gage station (USGS 07325800) (Figure 4.2). The water surface elevation and time of the survey were recorded. In addition, sediments from the surface of the streambed were collected.

Step 4: Channel Network

The 1873 channel network was digitized in a georectified plat map for the study watershed in ArcGIS 10.0 (ESRI 2010). In discussing the guidelines for defining the characteristics of water bodies on the 1873 plat maps, the General Land Office (GLO) manual of surveying instructions (GLO 1871) explicitly instructed the surveyors to note extent of streams and other water bodies up to the head water and origin. In addition, surveyors had well documented field notes for each of the townships and ranges (BLM-GLO 2015). Surveyors were instructed to note intersection of lines by water bodies (BLM-GLO 1871, p18). The lines described in survey notes were the section lines in 1873 plat maps. Surveyors followed the township section lines while recording the extent of streams (GLO 1871). If it is assumed that the surveyors followed the survey guidelines as described by the GLO, then the likely delineated the extent of stream up to the headwater.

The 2013 channel network for the Cobb Creek watershed was digitized in a 1-m resolution NAIP 2013 aerial imagery. Rhoads et al. (2016) digitized the 2012 channel network with reference to NHD flowlines in east-central Illinois. While digitizing the

Cobb Creek 2013 channel network, 2015 NHD flowlines (USGS 2015) layer was overlaid to the 2013 aerial images as a reference guide. The 2013 channel network was extended up to the headwater. The grass channels observed in the 2013 aerial image were not included, and offset-flowlines in the 2015 NHD were corrected to match the channels in the 2013 aerial image. The lengths of the total channel segments on the 1873 and 2013 channel networks were measured in NAD 1983 UTM coordinate system.

Step 5: Channel Segment Selection

In this study, 31.4 km (based on NAIP 2013 aerial imagery) of the main stem of Cobb Creek was considered as a study-channel section for channel planform characterization. The section extends from the outlet of Crowder Lake to approximately 2.5 km upstream from Fort Cobb Reservoir (Figure 4.2). Twelve channel segments in the main stem were defined to analyze the channel planform changes using the bridge locations as upstream and downstream end points of each segment (Figure 4.4). Full descriptions of the SEG endpoints are listed in Table 4.2. Most of the bridge structures were visible in the 1940 aerial imagery, except at the segment 2 and 3 boundary and the segment 6 and 7 boundary which were constructed in 1976 and 1950, respectively (ODOT 2016). The surveyed section and gage station is in SEG-5.

Channel Centerline Digitization

The channel centerlines in the main stem of Cobb Creek in 1940, 1966, 2003 and 2013 were digitized with ArcGIS software (ESRI 2010). To interpolate the channel centerline, an ArcGIS add-in called “Channel Planform Statistics” developed by Lauer

(2006) was used. This tool interpolates and creates a smooth channel centerline with reference to the right and left channel bank. Lauer and Parker (2008) demonstrated that channel centerline digitization may not be accurate if digitized by only considering the channel thalweg because streamflow and width varies with flow events. It was recommended to use the right and left bank of the stream to locate the channel centerline because banks, especially with vegetation, are easier to identify than the channel centerline. The digitized channel centerlines for 1940, 1966, 2003 and 2013 were used to estimate lateral channel migration. Note that the channel centerline digitized for the main stem of Cobb Creek was different than the channel network digitization in 2013. Channel networks were digitized with reference to NHD flowlines, not the banklines.

Step 6: Segment-wise Streamflow and Stream Power

Mean daily flows from SEG-5 were transferred to the other segments using equation (1). Drainage area of each SEG was determined from StreamStats Version 3.0 (USGS 2016b). The recurrence flood events of 2-yr, 10-yr, and 50-yr were determined using USGS flood-frequency analysis software called *PeakFQ Version 7.1* (Flynn et al. 2006). The estimated 2-yr, 10-yr and 50-yr flood events at SEG-5 were 55 m^3/s, 187 m^3/s and 385 m^3/s.

Stream power is often related with channel migration (Larsen et al. 2006). The available power for channel work is defined in equation (2). Larsen et al. (2006) introduced the term instantaneous effective stream power (Ω_e) as:

$$\Omega_e = 0 \ (\text{if } Q_d \leq Q_{d,\ \text{threshold}})$$

$$= \rho g S Q_d \ (if\ Q_d > Q_{d,threshold}) \tag{3}$$

where Ω_e is in W/m, Q_d is mean daily discharge (m^3/s). Larsen et al. (2006) defined a lower threshold discharge to initiate the bank erosion. In addition, they defined upper threshold discharge as discharge that overtops the bank. Their results showed no significant difference between with or without the upper threshold discharge. In this study, threshold discharge was estimated with reference to critical shear stress criterion (discussed in next section). Further, cumulative effective stream power (Ω_{ce}) was estimated by a similar procedure from Larsen et al. (2006) as:

$$\Omega_{ce} = \sum_{t_1}^{t_2} \Omega_e \tag{4}$$

where t_1 is starting time and t_2 is ending time in seconds for the period of interest (1966-2003 and 2003-2013). Cumulative effective stream power was estimated for two periods 1966-2003 and 2003-2013 for all SEGs except SEG-7.

A new concept of normalized cumulative stream power was introduced. The normalized cumulative effective (NCE) stream power per period (Ω_{nce}) was determined as:

$$\Omega_{nce} = \Omega_{ce}\ L_{avg} \tag{5}$$

where L_{avg} was each period's average SEG's channel length (m) which gives Ω_{nce} in Watts. Further, in order to compare NCE stream power with normalized migration rate, NCE stream power by year ($\Omega_{nce,y}$) was determined as:

$$\Omega_{nce,y} = \Omega_{nce} / n \tag{6}$$

where n was number of years in each period of interest, which gives $\Omega_{nce,y}$ in W/yr. $\Omega_{nce,y}$ NCE stream power per year ($\Omega_{nce,y}$) was estimated to for two periods 1966-2003 and 2003-2013 for all SEGs except SEG-7.

Threshold Discharge

Stream power is often related to bed shear stress (Larsen et al. 2006) as:

$$\Omega = \tau_b \, v \, w \tag{7}$$

where τ_b is bed shear stress (N/m^2), v is channel flow velocity (m/s), w is channel width (m), which gives Ω in W/m. Bed shear stress is defined as:

$$\tau_b = \rho \, g \, R \, S \tag{8}$$

where ρ is density of water (kg/m^3), g is acceleration due to gravity (m/s^2), R is hydraulic radius (m) and S is channel slope (m/m), which gives τ_b in N/m^2. Critical bed shear stress is normally estimated with reference to Shields-stress criterion (Shields 1936) for initiation of particle in motion (Buffington and Montgomery 1997) as:

$$\tau_c = {\tau_c}^*(\rho_s - \rho) g d_{50} \tag{9}$$

where τ_c is critical bed shear stress (N/m^2), τ_c* is dimensionless critical shear stress, g is acceleration due to gravity (m/s^2), ρ_s is density of sediment (kg/m^3), ρ is density of water (kg/m^3) and d_{50} is median grain size (m). The d_{50} was calculated as 0.5 mm from streambed surface sediment with hydrometer analysis based on ASTM (2007) at surveyed reach.

The Hydrologic Engineering Center’s River Analysis System (HEC-RAS) (USACE 2010) was used to determine hydraulic depth and shear stress parameters in steady state condition. Manning’s ‘n’ was calibrated with known discharge at the surveyed cross-section. Stream discharge at USGS gage station (USGS 07325800) was reported as 0.34 m^3/s (USGS 2016c) during survey time. No tributaries existed between the surveyed cross-section and gage station, so the same discharge was assumed for the surveyed section.

Using Shields curve (Vanoni 1964), τ_c* was estimated at 0.032 and critical bed shear stress (τ_c) was calculated from equation (10) as 0.26 N/m^2. Critical bed shear stresses for particle size 0.25-0.5 mm typically range from 0.194-0.27 (Berenbrock and Tranmer 2008, Julian 2010). The critical hydraulic radius corresponding to the critical shear stress was calculated from equation (9). With trial and error, the threshold discharge corresponding to the critical hydraulic radius was determined from HEC-RAS (USACE 2010) steady state simulation.

Step 7: Channel Planform

The channel planform characteristics of valley length, channel length and sinuosity were estimated for all SEGs and years 1940, 1966, 2003 and 2013. Valley length was kept constant for all periods because the SEG was bound by bridge structures. Channel sinuosity was estimated as the ratio of channel length to the valley length (Schumm 1963).

Step 8: Lateral Channel Migration

Lateral channel migration has been estimated by a method called "Eroded Area Polygons" (e.g., Kirchner et al. 1998; Micheli and Kirchner 2002; Wallick et al 2006; Constantine et al. 2009). In this method, channel centerlines are digitized for years of interest and a polygon is created by joining the two centerlines. Legg et al. (20014) developed an ArcGIS tool called "The Channel Migration Toolbox." The toolbox calculates total channel centerline migration (m) by dividing the eroded area polygon by the user defined reach length. In this study, the reach length was considered as half of the perimeter of eroded-area polygons as recommended by Wallick et al. (2006). Net lateral channel migration area between three periods 1940-1966, 1966-2003 and 2003-2013 for each SEG were estimated by the Channel Migration Toolbox. The lateral channel migration rates (*LCM*) (m/yr) were obtained by dividing the net channel lateral migration by the elapsed time (yr) for each time period and SEG. The SEGs were not equal in length. In order make fair comparison between segments, LCM for each period were normalized as:

$$\text{Normalized migration rate} = LCM^* \, L_{avg,SEG} \tag{10}$$

where LCM is in m/yr, $L_{avg,SEG}$ is the average SEG's channel length (m) for each period, which gives normalized migration rate in m^2/yr.

Errors on Lateral Channel Migration

The 1940 and 1966 aerial images were in black and white, whereas the NAIP 2003 and 2013 aerial images were color with 1 m resolution. Registration error is often used as spatial error between two aerial images (Perroy et al. 2010; Tobergte 2012). In the proximity of the main stem of the Cobb Creek, 12 feature points (buildings, road centerline, permanent landmark) were selected in 2013 aerial images and the distance between 2003 and 2013 feature points were measured as registration error using the UTM coordinate system.

The registration error was not calculated for 1940-1966 and 1966-2003. There were not distinguishable and comparable features such as buildings and permanent landmark within proximity to the main stem of the Cobb Creek in the 1940 and 1966 aerial images. In addition, those images were black and white, and the resolutions were not consistent between two years. Micheli and Kirchner (2002) used a similar geo-rectification technique and estimated spatial error as ± 5.4m for such historical aerial images in California. Further, Hughess et al. (2005) estimated ± 5.0 m spatial error for historic aerial images in Oregon.

Step 9: Historical Channel Planform Characterization and Comparison

In this study, channel planform condition in Cobb Creek was characterized in two parts based on availability of historical records such as plat maps, aerial images, and relevant historical events within the framework of integrated approach (Figure 4.1) and outline of historical events (Table 4.1). In the first part, stream channel network in 1873 plat maps was compared with 2013 channel network. In the second part, planform characteristics of valley length, channel length and sinuosity were characterized for 1940, 1966, 2003 and 2013. Further, lateral channel migration rates were estimated for the period of 1940-166, 1966-2003 and 2003-2013. In addition, lateral channel migration rates for the period of 1966-2003 and 2003-2013 were coupled with stream power.

Statistical test were conducted to compare various parameters of channel planform characteristics with year, period, and SEG as factors. One-way analysis of variance (ANOVA) was performed at $\alpha = 0.05$ level using sinuosity as response variables and year as the factor. Similarly, one-way ANOVA was conducted to determine significant differences in annual precipitation between three periods (1949-1966, 1966-2003 and 2003-2013) and the mean annual stream flow between two periods (1966-2003 and 2003-2013) at $\alpha = 0.05$ level. A two-way ANOVA without intercept was conducted to evaluate year-and SEG-wise significant differences in channel length. Similarly, a two-way ANOVA was conducted to evaluate the difference between normalized migration rates among the period and SEGs. In addition, a two-way analysis of covariance (ANCOVA) test was performed to determine the effects of stream power on channel migration using normalized channel migration as a response variable, period and segment as factors, and NCE stream power per year as a covariate at $\alpha = 0.1$. All statistical analysis were performed with Minitab statistical software, version17 (Minitab 2016), and test statistics reporting was based on APA (2010).

Results and Discussion

Channel Network Comparison

The Cobb Creek watershed channel networks in 1873 and 2013 were compared based on total channel segment length in each year. The total channel lengths in 1873 and 2013 channel network were 233 km and 393 km, respectively. The Cobb Creek channel network had expanded nearly 70% over the period (Figure 4.5). The accuracy of hand drawn plat maps was unknown; however, the 1873 survey guidelines (GLO 1871) indicated that surveyors had most likely correctly delineated the extent of the stream. Although direct causation of increasing channel length between 1873 and 2013 cannot be demonstrated from these data, the potential channel network expansion was concurrent with settlement and associated erosion problems in the watershed that occurred during this period (Table 4.1).

In Oklahoma, non-Native American settlement began with the 1889 Land Run (Hoig 2009). Wilson (2009) reported that Caddo County (almost half of the Cobb Creek watershed) was extensively occupied by settlement, and, as a result, 80 percent of the land had been converted to farmland at the time of Oklahoma statehood in 1907. In Oklahoma, due to the effects of human settlement and agricultural practices, extensive gully erosion was noted to begin around 1914 and had become a major issue by the 1920s (Phillips and Harrison 2004). In 1931, the first soil erosion survey was conducted in Oklahoma, which showed more than 80 percent of agricultural land was impacted by soil erosion (Phillips and Harrison 2004). A plausible conclusion is that the longer extent of the channel network in 2013 compared to1873 was likely a result, at least in part, by anthropogenic disturbances (agricultural practices and associated erosion problem) that occurred in the watershed during this time period.

Channel Planform, Lateral Migration and Stream Power Characterization and Comparison

Channel Planform Characterization

Several road bridge crossings were observed on the mainstem (Figure 4.4). Centerlines were not offset at those bridge structures when compared between years 1940, 1966, 2003 and 2013. Therefore, an assumption was made that the road bridge crossings created constraints to the lateral channel migration at those specific locations, which supports the selection of segment breakpoints at the bridges.

The estimated channel morphological characteristics for each segment (valley length, channel length, sinuosity and slope) are shown in Table 4.3. Eight of the segments (SEG-1, SEG-2, SEG-5, SEG-6, SEG-10, SEG-11, and SEG-12) exhibited relatively constant sinuosity from 1940 to 2013. The most sinuous channel segments were SEG-5 and SEG-7. For the relatively short channel segments (SEG-3 and SEG-4), channels tended to straighten from 1966 to 2013. The channel length and sinuosity sharply decreased from 1966 to 2003 in SEG-7 and remained constant from 2003 to 2013. Aerial images showed a channel cutoff that occurred in this segment sometime between 1966 and 2003 (Figure 4.6). The SEG-7 was considered as outlier because of this channel cutoff and excluded from statistical analysis.

A two-way ANOVA without the intercept term was conducted to compare the main effects of year and segment on channel length. The year factor included 1940, 1966, 2003 and 2013 whereas segment factor consisted of SEG-1 to SEG-12 except SEG-7. There were significant effects of year, $F(3, 30) = 4.08$, $p = 0.015$, and segment $F(10, 30) = 1475.88$, $p < 0.001$ on channel length. Tukey's pairwise comparison of mean channel length among year and segment factors is shown in Figure 4.7. A one-way ANOVA was conducted to evaluate year wise significant differences in sinuosity. The year factor included 1940, 1966, 2003 and 2013. The ANOVA revealed that the channel sinuosity was not significantly different year-wise, $F(3, 40) = 0.04$, $p = 0.989$; at $\alpha = 0.05$.

Lateral Channel Migration Rates

For 2003-2013, spatial (registration) error was 1.6 m for the period of 2003 to 2013 (Table 4.4). By dividing 1.63 m by 11 years, spatial error in lateral migration rate was estimated as ± 0.1 m/yr for 2003-2013. As there was insufficient information to estimate spatial error for the period of 1940-1966 and 1966-2003, spatial error estimated by Micheli and Kircher (2002) was applied in the present study. By dividing the spatial error of ± 5.4 m by 27 and 11 years, spatial error in lateral channel migration was estimated as ± 0.2 m/yr and ± 0.1 m/yr for 1940-1966 and 1966-2003, respectively. The estimated channel migration rate (m/yr) with spatial error for each period and segment is shown in Table 4.5.

All channel migration rates are at or below the estimated error, except SEG-2 and SEG-6 in period 1940-1966 (Table 4.5). However, these two SEGs were included in statistical analysis. This was similar to Tobergte (2012), which did not exclude channel migration rates below the spatial error, considering aerial images had not detected small changes in fluvial erosion. A two-way ANOVA was conducted to evaluate the difference between normalized migration rates among the period and segment. The period factor included 1940-1966, 1966-2003 and 2003-2013 whereas segment factor consisted of SEG-1 to SEG-12 except SEG-7. Note that normalized migration rate (m^2/yr) was determined using equation (10). The two-way ANOVA showed significant main effects for period, $F(2, 20) = 15.01$, $p < 0.001$, and segment, $F(10, 20) = 4.39$, $p = 0.002$ on normalized migration rate. Tukey's pairwise comparison of mean normalized migration rates among year and segment factors are shown in Figure 4.8. The mean of normalized migration rates in 1940-1966 was significantly different from 1966-2003 and 2003-2013 at $\alpha = 0.05$. In segment-wise, the mean of normalized migration rates in SEG-1, which was the longest SEG, (Figure 4.8) were significantly different compared to other SEGs, whereas means of normalized migration rates in other SEGs were not significantly different at $\alpha = 0.05$.

Precipitation and Streamflow

An one-way ANOVA was conducted to determine significant differences in annual precipitation (mm/yr) between three periods (1949-1966, 1966-2003 and 2003-2013) at $\alpha = 0.05$ level. The ANOVA revealed that annual precipitation (mm/yr) was not significantly different among the periods, $F(2,61) = 0.67$, $p = 0.517$. Similarly, a one-way ANOVA was performed to determine differences in the mean annual stream flow (m^3/s) between two periods (1966-2003 and 2003-2013) at $\alpha = 0.05$ level. Mean annual flow (m^3/s) was not significantly different between 1966-2003 and 2003-2013, $F(1, 47) = 0.03$, $p = 0.868$. This indicates that after constructing upstream reservoirs (Figure 4.2), the mean annual flow didn't change significantly in Cobb Creek.

Stream Power and Lateral Channel Migration

A HEC-RAS steady state (USACE 2010) simulated water surface elevation matched the measured water surface elevation of 25.19 m at surveyed cross-section (Table 4.6 and Figure 4.9). The calibrated channel manning's roughness parameter was 0.035 (Chow 1959). The estimated threshold discharge was 0.01 m^3/s. There was negligible difference (less than 0.05%) between Ω_{ce} for the period of 1966-2003 and 2003-2013 with and without considering the threshold discharge in SEG-5. Therefore, threshold discharge was not considered in the calculation of Ω_{ce} for all SEGs.

NCE stream power per year (W/yr) was estimated for periods 1966-2003 and 2003-2013 to all SEGs except SEG-7. A two-way analysis of covariance (ANCOVA) test was performed to determine the effects of stream power on channel migration using normalized channel migration (m^2/yr) as a response variable, period and segment as treatment variables, and normalized cumulative effective (NCE) stream power per year ($\Omega_{nce,y}$) as a covariate at $\alpha = 0.1$. There were significant main effects of NCE stream power per year (W/yr), $F(1,8) = 14.61$, $p = 0.005$; period, $F(1,8) = 4.55$, $p = 0.065$; segment, $F(10,8) = 2.63$, $p = 0.092$ on normalized migration rate (m^2/yr). There was no interaction between NCE stream power and segment; period and segment; and interaction between NCE stream power and period was insignificant, $F(1,8) = 2.48$, $p = 0.154$ (Table 4.7).

A significant linear relationship between normalized migration rate (m^2/yr) and NCE stream power per year (W/yr) was observed (Table 4.7 and Figure 4.10). However, parallel lines show that there was no significant difference in slope at $\alpha = 0.1$ (Table 4.7), which indicated that NCE stream power per year (W/yr) in 1966-2003 and 2003-2013 were not significantly different. Stream power is directly related to stream flow (Leopold et al. 1964). As there was no statistical difference in mean annual flow and annual precipitation between two periods (1966-2003 and 2003-2013), stream power was expected to follow a similar pattern. Tukey's pairwise comparison of mean normalized migration rate (as NCE stream power as a covariate) among year and segment factors are shown in Figure 4.11. In period wise, the means of normalized migration rate were significantly different between 1966-2003 and 2003-2013 at $\alpha = 0.1$.

Temporal Channel Planform Comparisons

The results of temporal comparison of channel planform in the study watershed are shown in Table 4.8. The channel network was 70% longer in 2013 than in 1873. The channel in the study reach was significantly longer in 1966 than in 1940 whereas the length in 2003 was not significantly longer than in 1966. There was similar results for the period of 2003-2013. While comparing channel sinuosity over time, the sinuosity was not significantly different compared to previous periods. Note that normalized migration rate in 1960-2003 was significantly lower than in 1940-1966 and similarly, significantly lower in 2003-20013 than in 1966-2003. This indicates that the overall channel migration rate has been decreasing from 1940 to 2013.

Planform Stability

In the study stream, climatic factors (precipitation and streamflow) and stream power didn't link with planform stability and channel migration reduction. One explanation for the lack of sinuosity change and lateral migration many of the segments is that bridge structures have acted as a fixed rigid boundary at each bridge section. Another potential explanation for that is flow controlled by impoundments (Figure 4.2) because mean annual flow were not changed significantly from 1949 to 2013. In the Cobb Creek watershed, after constructing upstream reservoirs (Figure 4.2), the frequency and timing of channel forming or peak flow were likely altered and the lateral channel migration thus reduced.

In discussing possible other factors in the watershed, CPs implemented in the watershed can be a major contributing factor. Normalized channel migration rate was decreasing from 1940-1966 to 2003-2013 in SEG-1, SEG-3, SEG-6 and SEG-11 where CPs were visible (Figure 4.12 and 4.13). However, there was no statistical evidence to differentiate the means of normalized migration rates Segment-wise with respect to CPs implemented areas. CPs implemented spatial data provided by the OCC in January 2016 included location but did not include temporal information on when the CPs were implemented.

Before 1940 there were minimum CPs in the watershed (Phillips and Harrison 2004). There have been numerous CPs implemented by farmers and ranchers after 1940 (Table 4.1). The normalized channel migration rate was significantly decreasing from 1940 to 2013, and channel sinuosity didn't change significantly in the main stem of Cobb Creek where continuous CPs were implemented. Vegetation planting along the stream banks, CPs might have helped to stabilize the bank and decreased the migration rate. Studies by Beeson and Doyle (1995) in British Columbia, Canada, indicated that non-vegetated channel banks significantly eroded compared with vegetated channel banks.

The results from aerial image interpretation of channel sinuosity changes and lateral channel migration characterization in the study section of Cobb Creek showed that the channel has stable planform. From an RGA study of Simon and Klimetz (2008), the majority of study segments in the main stem of Cobb Creek were in stage V (aggradation and widening) or stage VI (quasi-equilibrium). Their study indicated that those were stable channel segments. The present study agrees with these conclusions of Simon and Klimetz (2008).

Previous studies have shown a reduction in upland soil erosion and sediment loading to the Fort Cobb Reservoir due to CPs (Simon and Klimetz 2008; Garbrecht and Starks 2009; OCC 2009; Becker and Steiner 2011; Garbrecht 2011; Moriasi et al. 2011; Steiner et al. 2014). However, it is difficult to make the conclusion that reduction in channel migration by itself is an indicator of reduction in sediment loading to the reservoir without quantifying the in-channel aggradation and/or incision. In addition, assessment of channel planform changes in other tributaries and creeks of the Fort Cobb Reservoir would need to be evaluated.

Conclusions

In this study, channel planform characterization techniques have been coupled within an integrated, systematic framework that uses historic records and limited field data to describe long-term channel planform changes within a watershed. This integrated approach was then applied in the Cobb Creek watershed in west-central Oklahoma. The developed method integrates factors that control channel planform changes in the watershed. Segment-wise characterization and comparison between long-term channel planform changes can be completed to highlight the smaller-scale changes. The approach provides a step-by-step methodology to evaluate long-term channel planform changes in agricultural watershed in the absence of long-term streambank monitoring data.

Application of the integrated method in the Cobb Creek watershed determined that the total length in the channel network in 2013 was almost 70 percent greater than in 1873. In addition, channel planform (sinuosity) did not change significantly from 1940 to 2013. Two newly defined parameters, normalized channel migration and NCE stream power, were introduced to compare changes in historical lateral channel migrations. Mean annual streamflow and precipitation were not significantly different from 1966 to 2013, which has contributed to consistent NCE stream power per year in the main stem of Cobb Creek. Channel migration rates were significantly decreasing from the periods of 1940-1966 to 2003-2013. The decreasing trend of normalized channel migration rates and CPs implementation were concurrent. However, the present results cannot verify statistically that CPs helped to stabilize the channel in main stem of Cobb Creek. It could be a combination of flow and bridge structure constraints and CPs that created a fairly stable planform and channel migration reduction in the mainstem of Cobb Creek.

Future research could focus on bank-stability analysis with processed-based models and long-term bank erosion measurement using erosion pins at local reaches where bank erosion is of prime concern. Documentation and lessons learned on a historical time scale can help examine the implications of future natural resource management in the watershed (Brierley and Hooke 2015). In the planning stages of developing future river management, the integrated method used in this study can provide essential background information for natural resource management agencies to formulate necessary polices and recommendations for joint management of the stream channel and the overall watershed. In addition, the integrated approach presented can be used for planform stability assessment in other similar agricultural watersheds.

Tables

Table 4.1. Synopsis of settlement, soil erosion, conservation practices (CPs), and significant studies in the Fort Cobb watershed in Oklahoma

	Timeline	Notable Events
pre-1873	1803	Louisiana Purchase (with present day Oklahoma) from France (Mundende 2009)
	1820s-1830s	Native American-Choctaw and Chickasaw arrival (Wilson 2009)
	1862	Homestead Act of 1862, beginning of non-native settlement nationwide (Everett 2009)
	1867	Kiowa, Comanche and Apache settlement started in present day Caddo County (Wilson 2009)
	1869	Cheyenne and Arapaho settlement started in present day Washita County (O'Dell 2009)
1873-1940	1873	General map survey (plat maps) by General Land Office (BLM-GLO 2015)
	1883-1885	Native Indian land used for grazing cattle in present day Washita County (O'Dell 2009)
	1886	Cheyenne and Arapaho settlement began in present day Washita County (O'Dell 2009)
	1889	Non-native settlement began in Oklahoma including present day Caddo and Washita Counties (Everett 2009)
	1907	Oklahoma statehood
	1913-1914	Gulley erosion started (Phillips and Harrison 2004)
	1920	Gulley erosion became major issue in Oklahoma (Phillips and Harrison 2004)
	1920-1930	Minimum soil CPs (Phillips and Harrison 2004)
	1931	Soil erosion survey in Oklahoma, about 80% farmland impacted by erosion (Phillips and Harrison 2004)
	1933	Soil Erosion Service (SES) established
	1935	Oklahoma Dust bowl, Soil Conservation Service (SCS) established under the USDA (Phillips and Harrison 2004)
	1936	Soil Conservation and Domestic Allotment Act, establishment of Agricultural Conservation Program (ACP) (Phillips and Harrison 2004)
	1937	Soil conservation districts formation (Phillips and Harrison 2004)
1940-1966	1944	Flood Control Act of 1944 (PL 78-534) (Mundende 2009)
	1954	Watershed Protection and Flood Prevention Act of 1954 (PL 83-566) also called Small Watershed Program, began flood control dams constructions (Mundende 2009)
	1956-1959	Soil Conservation Service constructed flood control reservoirs (Garbrecht 2010)
	1956	Great Plains Conservation Program (GPCP), which resulted in development of conservation techniques (Mundende 2009)
	1961	Erosion and flood control monitoring started (Steiner et al. 2014)
1940-1966	1981	Water Quality Problem mainly suspended sediment, turbidity and nutrients detected in Ft. Cobb Reservoir (OCC 2009)
	1985	Food Security Act, which addressed conservation issues, followed by Farm Bill of 1990 (Mundende 2009)
	1990s	Active CPs (Mundende 2009)
	1996	Environmental Quality Incentives Program (EQIP) through Farm Bill of 1996
	1998	Fort Cobb watershed listed Clean Water Act section 303(d) as impaired water and sediment (Becker and Steiner 2011)
	2001	Oklahoma Conservation Commission started FY 2001 319 project (OCC 2009)
2003-2013	2003	Sediment, erosion, and nutrient modeling for the Fort Cobb watershed (Storm et al. 2003)
	2003	Fort Cobb watershed became Benchmark Watershed in Conservation Effectiveness Assessment Project (Becker and Steiner 2011)
	2005	Oklahoma Conservation Commission started FY 2005 319 project, focusing on no-tillage practices (OCC 2009)
	2011	US Geological Survey published special report on assessment of CPs in the Fort Cobb watershed (Becker 2011)

Table 4.2 . Physical location of study channel segments and their stability stages. SEG refers to the segment name followed by numerical value.

Segment Name	Boundary	
	Upstream End	Downstream End
SEG-1	E1210 Road	N2500 Road
SEG-2	Unnamed Road	E1210 Road
SEG-3	N2470 Road	Unnamed Road
SEG-4	State Hwy 152	N2470 Road
SEG-5	N2460 Road	State Hwy 152
SEG-6	N2450 Road	N2460 Road
SEG-7	N2440 Road	N2450 Road
SEG-8	N2430 Road	N2440 Road
SEG-9	E1150 Road	N2430 Road
SEG-10	E1140 Road	E1150 Road
SEG-11	E1130 Road	E1140 Road
SEG-12	Crowder Lake Outlet	E1130 Road

Table 4.3. Channel morphological characteristics (valley length, channel length and sinuosity) for study channel segments for year 1940, 1966, 2003 and 2013. Valley length is same for all years because upstream and downstream point of study channel segment has bridge as a boundary. SEG refers to the segment name followed by numerical value.

Segment Name	Slope (m/m)	Valley Length (km)	Channel Length (km)				Sinuosity (km/km)			
			1940	1966	2003	2013	1940	1966	2003	2013
SEG-1	0.0008	3.5	4.2	4.3	4.3	4.4	1.2	1.2	1.2	1.2
SEG-2	0.0009	2.6	3.1	3.2	3.2	3.2	1.2	1.2	1.2	1.2
SEG-3	0.0017	0.7	0.8	0.9	0.8	0.8	1.3	1.4	1.2	1.2
SEG-4	0.0015	0.6	0.8	0.7	0.6	0.6	1.4	1.2	1.0	1.0
SEG-5	0.0011	1.4	3.0	3.1	3.2	3.2	2.1	2.2	2.2	2.3
SEG-6	0.0009	1.8	2.3	2.4	2.4	2.4	1.3	1.3	1.3	1.3
SEG-7	0.0019	1.7	3.4	3.6	2.7	2.7	2.0	2.1	1.6	1.6
SEG-8	0.0010	2.5	3.6	3.8	3.7	3.8	1.4	1.1	1.1	1.1
SEG-9	0.0013	2.3	2.8	2.7	2.7	2.8	1.2	1.2	1.2	1.2
SEG-10	0.0014	1.7	2.1	2.2	2.2	2.2	1.3	1.3	1.3	1.3
SEG-11	0.0016	1.9	2.2	2.3	2.2	2.2	1.1	1.2	1.2	1.2
SEG-12	0.0018	2.1	2.9	3.1	3.1	3.1	1.4	1.5	1.4	1.5

Table 4.4. Registration error estimation for lateral channel migration between 2003 and 2013.

Feature Type	UTM Coordinate (2003)		UTM Coordinate (2013)		Difference (m)
	X (m)	Y (m)	X (m)	Y (m)	
Building	539259.21	3901974.10	539260.03	3901974.78	1.1
Building	537494.43	3902239.15	537495.21	3902239.37	0.8
Building	537446.02	3903944.44	537445.97	3903946.71	2.3
Road Intersection	537427.62	3905364.64	537426.25	3905365.80	1.8
Building	536993.25	3905667.96	536994.64	3905669.15	1.8
Building	534272.27	3907544.81	534272.49	3907544.95	0.3
Road Intersection	529395.71	3914948.66	529395.07	3914950.21	1.7
Building	528367.12	3915328.44	528365.56	3915328.14	1.6
Crowder Lake Outlet	527237.05	3916710.33	527236.13	3916711.03	1.2
Building	529318.22	3914221.37	529316.34	3914223.01	2.5
Building	537603.11	3902667.43	537604.35	3902666.70	1.4
Building	531152.28	3911478.37	531150.16	3911480.96	3.3
				Mean difference	**1.6**

Table 4.5. Lateral channel migration rate for individual channel segments for periods of 1940-1966, 1966-2003 and 2003-2013. SEG refers to the segment name followed by numerical value. Spatial error for 1940-1966 and 1966-2003 are based on Micheli and Kirchner (2002).

Segment Name	Channel Segment Migration Rate (m/yr)		
	(1940-1966)[a]	(1966-2003)[b]	(2003-2013)[c]
SEG-1	0.4	0.3	0.2
SEG-2	0.2	0.3	0.2
SEG-3	0.9	0.4	0.2
SEG-4	0.8	0.7	0.1
SEG-5	0.4	0.2	0.3
SEG-6	0.1	0.2	0.1
SEG-7	0.3	0.7	0.1
SEG-8	0.5	0.1	0.1
SEG-9	0.4	0.1	0.1
SEG-10	0.3	0.1	0.1
SEG-11	0.3	0.2	0.1
SEG-12	0.3	0.1	0.1

Error: a (± 0.2 m/yr), b (± 0.1 m/yr), and c (± 0.1 m/yr)

Table 4.6. Output from HEC-RAS (USACE 2010) simulation of known, maximum daily and threshold discharges and their corresponding hydraulic properties.

Profile	Discharge (m^3/s)	Water Surface Elevation (m)	Slope (m/m)	Hydraulic Radius (m)	Flow Area (m^2)	Shear Stress (N/m^2)
Known Discharge	0.34	25.19	0.00096	0.21	1.1	1.93
Maximum Daily Discharge	106.2	29.52	0.00096	2.44	66.2	22.98
Threshold Discharge	0.01	24.96	0.00096	0.03	0.07	0.26

Table 4.7. Two way-analysis of covariance summary table for normalized channel migration rate (m^2/yr) as normalized cumulative effective (NCE) stream power per year (W/yr) is a covariate among period and segment. Period group includes 1966-2003 and 2003 to 2013. Segment group includes SEG-1 to SEG 12 except SEG-7. DF= degrees of freedom; SS = sum of squares and MS = mean squares; S= standard error; R^2 = coefficient of determination.

Term	Source	DF	SS	MS	F	*p*
Covariate	NCE Stream Power (W/yr)	1	105046	105046	14.61	0.005
Intercept	Period	1	32729	32729	4.55	0.065
Intercept	Segment	10	189201	18920	2.63	0.092
Slope	NCE Stream Power (W/yr)* Period	1	17800	17800	2.48	0.154
	Error	8	57503	7188		
	Total	21	1530599			

S = 84.79, R^2 = 0.96 adj. R^2 = 0.90

Table 4.8. Results of temporal comparisons (NC = not calculated; CC = cannot compare to previous period with current information)

Segment	Parameter		
	Length	**Sinuosity**	**Normalized Migration Rate (NMR)**
Channel Network (1873-2013)	70% longer in 2013 than in 1873	NC	NC
Cobb Creek Study Reach (1940-1966)	Significantly longer in 1966 than in 1940 [Figure 4.7]	Not significantly different in 1966 than in 1940	CC
Cobb Creek Study Reach (1966-2003)	Not significantly longer in 2003 than in 1966 [Figure 4.7]	Not significantly different in 2003 than in 1966	Significantly lower NMR compared to previous period [Figure 4.8]
Cobb Creek Study Reach (2003-2013)	Not significantly longer in 2013 than in 2003 [Figure 4.7]	Not significantly different in 2013 than in 2003	Similar NMR compared to previous period, [Figure 4.8]; significantly lower NMR than previous period when NCE stream power is covariate [Figure 4.11]

Figures

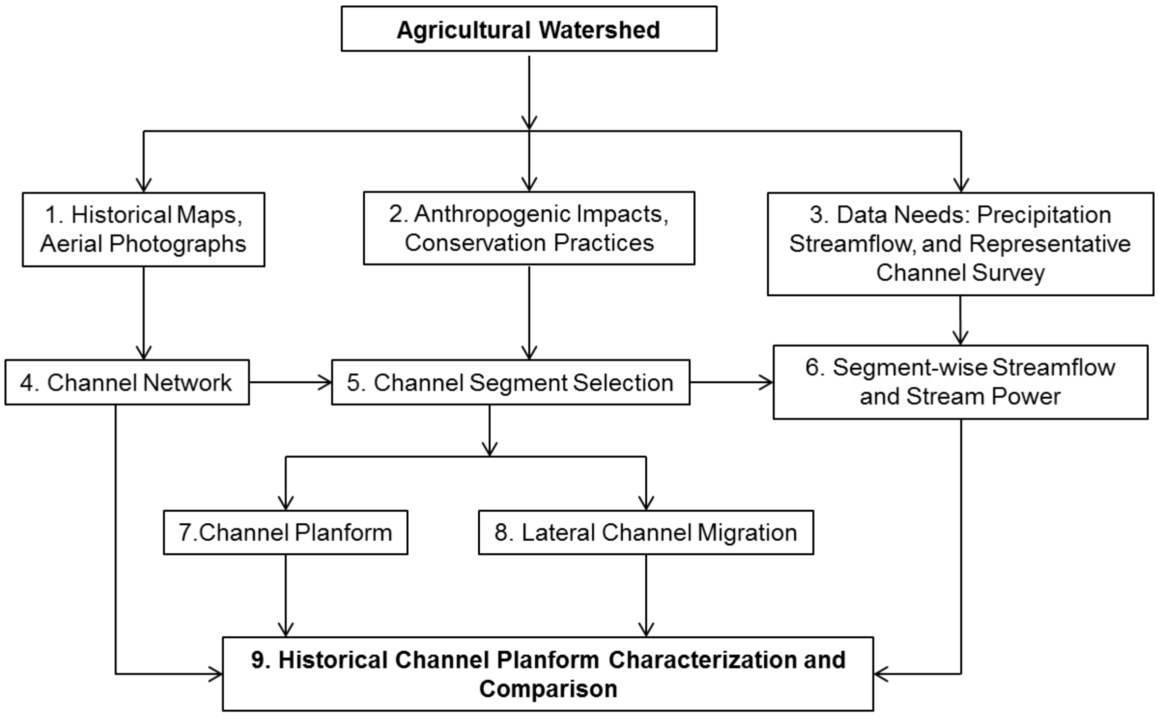

Figure 4.1. Framework for an integrated approach to characterize long-term channel planfrom changes in an agricultural watershed with limited field data.

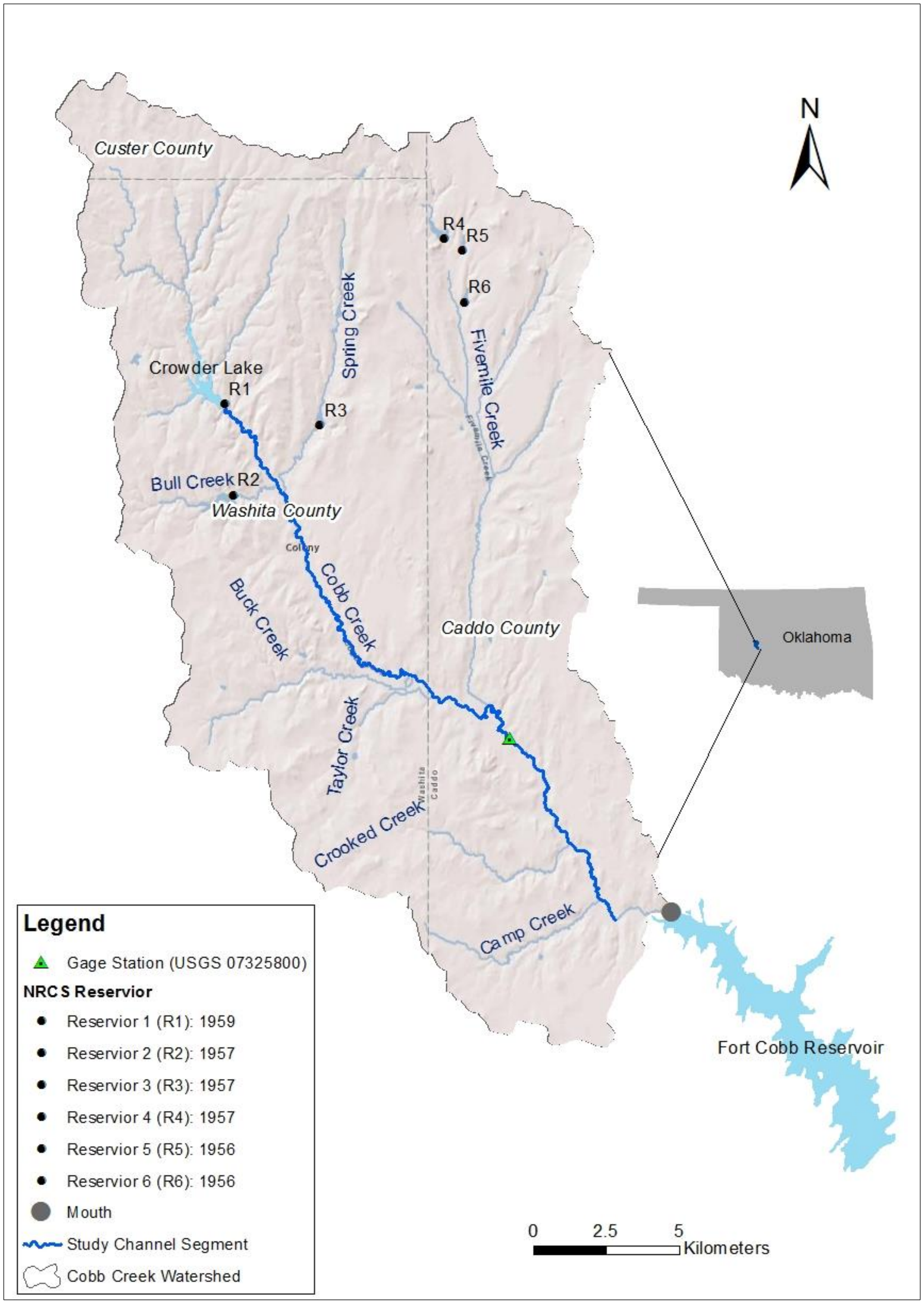

Figure 4.2. Map showing study location at Cobb Creek, Oklahoma, USA [Data source: base map (ESRI 2010), Reservoir (USDA-ARS 2013b)]. The reservoir built years (Moriasi et al. 2014b) are shown in the legend.

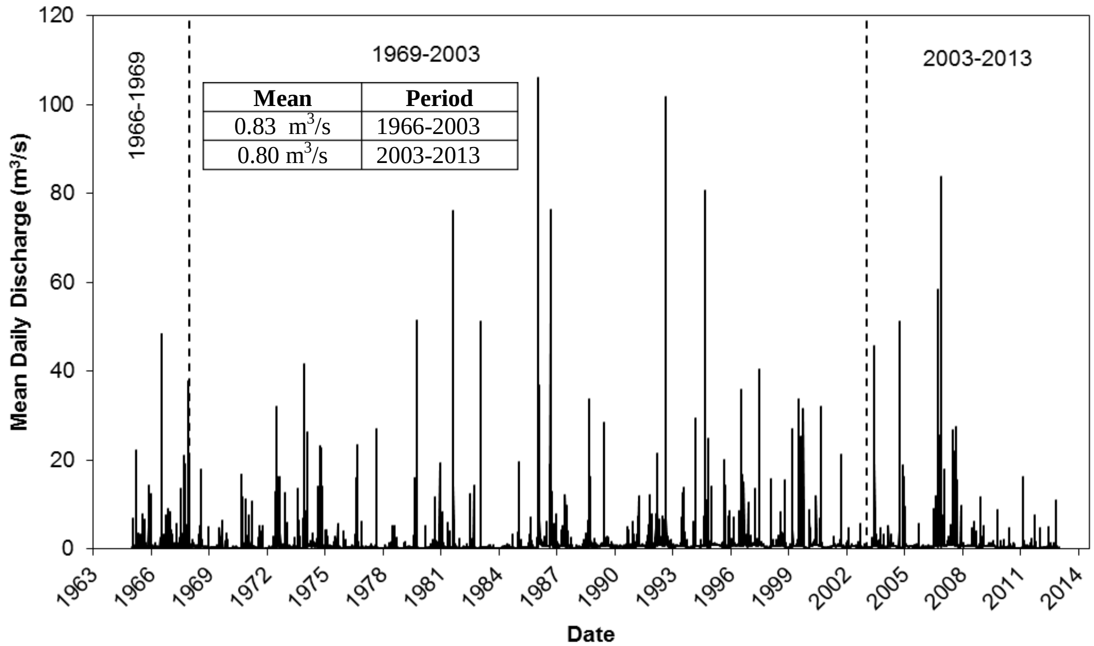

Figure 4.3. Hydrograph of daily mean flows for water year 1699 to1969 (simulated) and, 1969 to 2003, 2003-2013 (gaged data) at USGS 07325800 gage station, near Eakly, Oklahoma. Dash-line represents divided line between periods 1966-1969, 1966-2003, and 2003-2013.

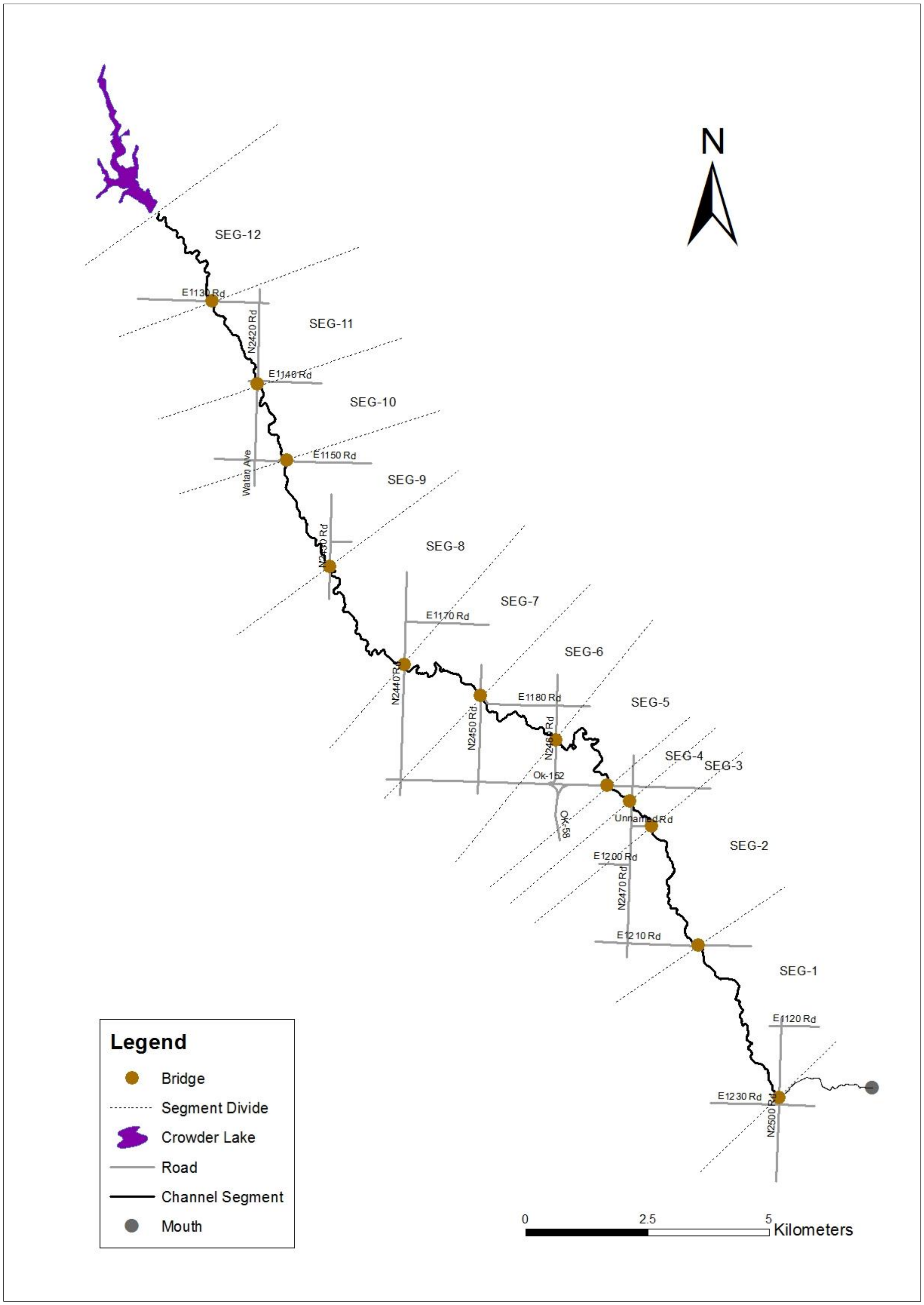

Figure 4.4. Map showing study segments for main stem of the Cobb Creek. The segment divide lines are shown to identify the channel segments (SEG). The bridge locations were identified from aerial photographs of 1940, 1966, USDA-FSA (2003, 2013) and verified with ODOT (2016). Road levels were identified with ERSI (2010) basemap layer.

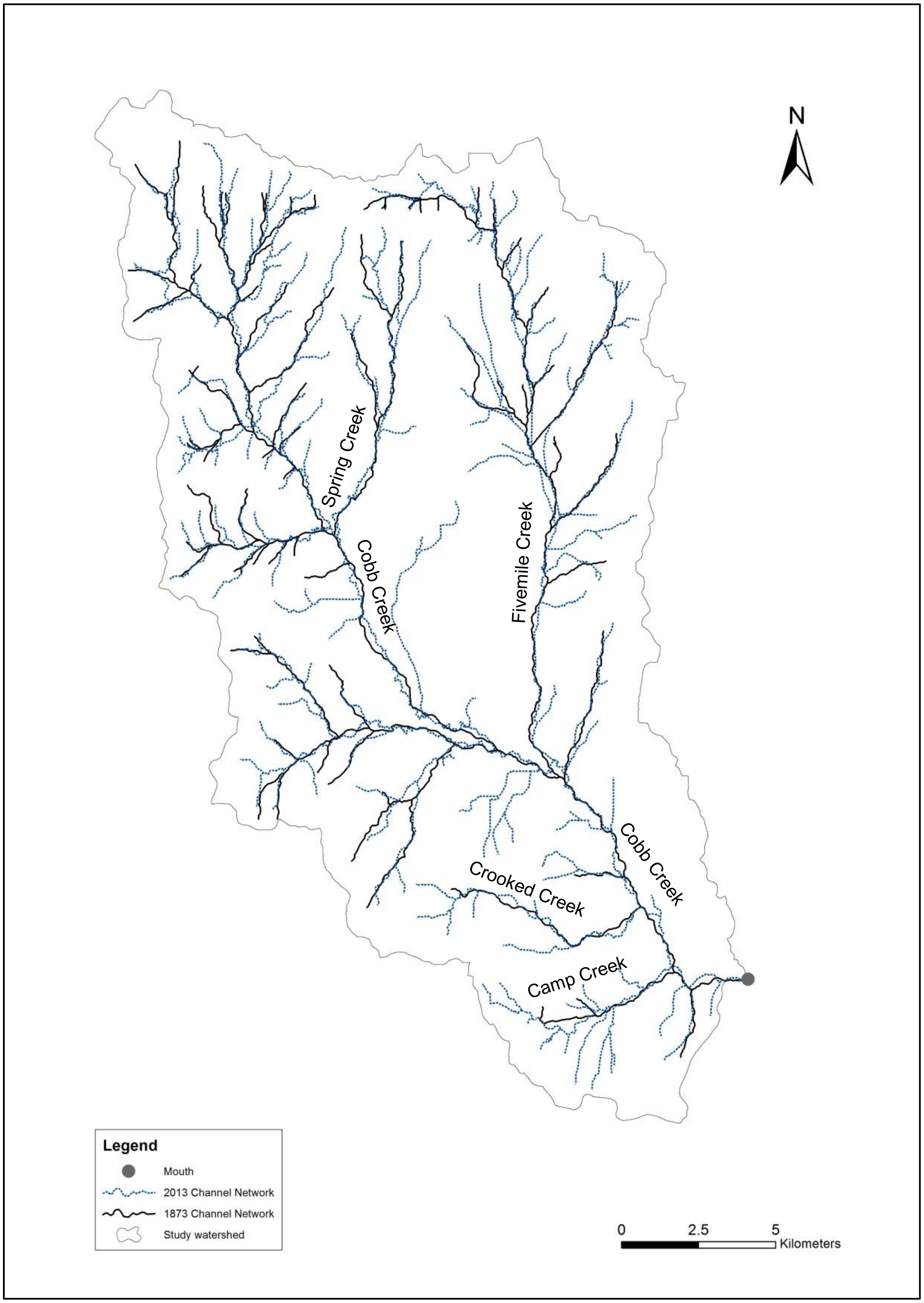

Figure 4.5. Map shows a comparison between 1873 and 2013 channel networks in Cobb Creek watershed. The1873 channel network was digitized on the 1873 plat maps (BLM-GLO 2015) and 2013 channel network was digitized on the NAIP 2013 aerial image (USDA-FSA 2013) with refrence to NHD flowlines (USGS 2015).

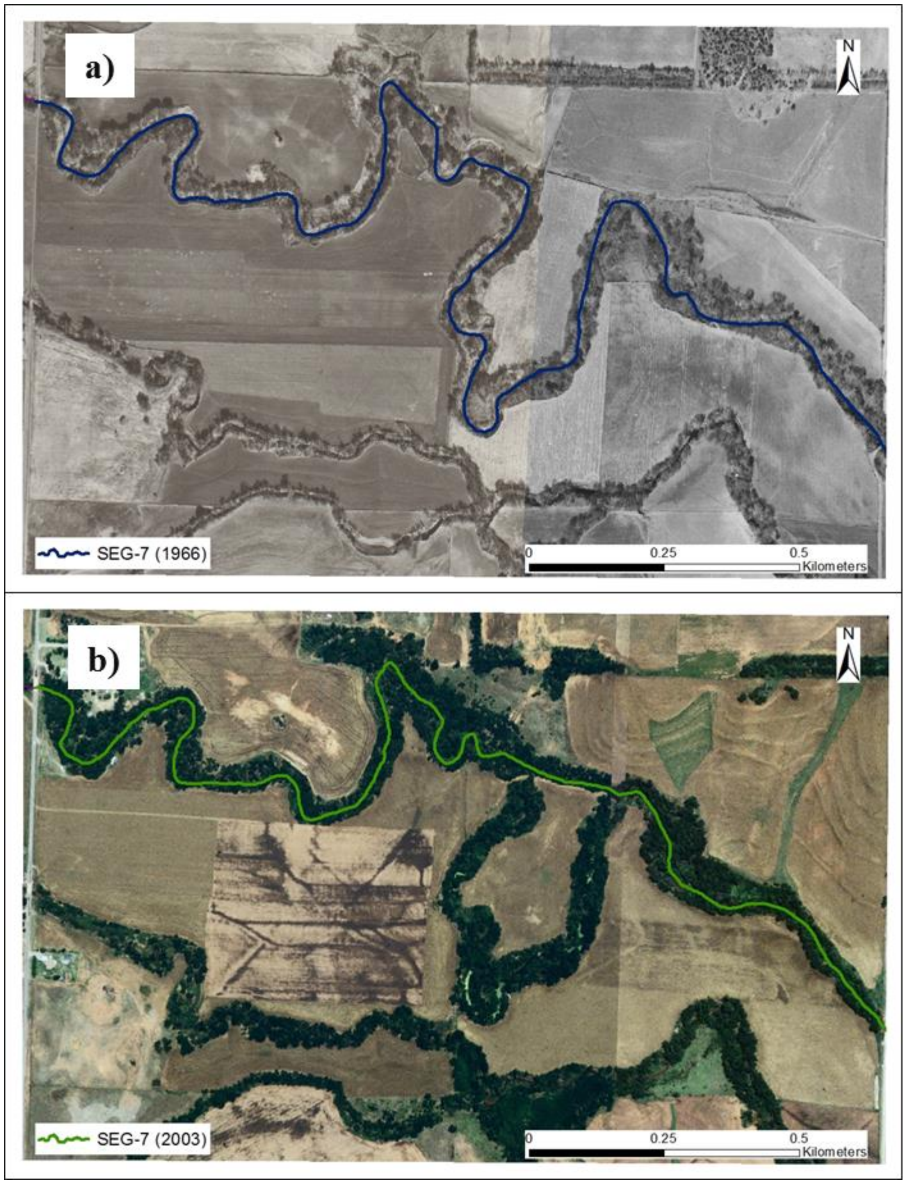

Figure 4.6. Channel cutoff between 1966 (a) and 2003 (b) in SEG-7 (ASCS 1966, USDA-FSA 2003). The cutoff channel segment is approximately 1 km in length.

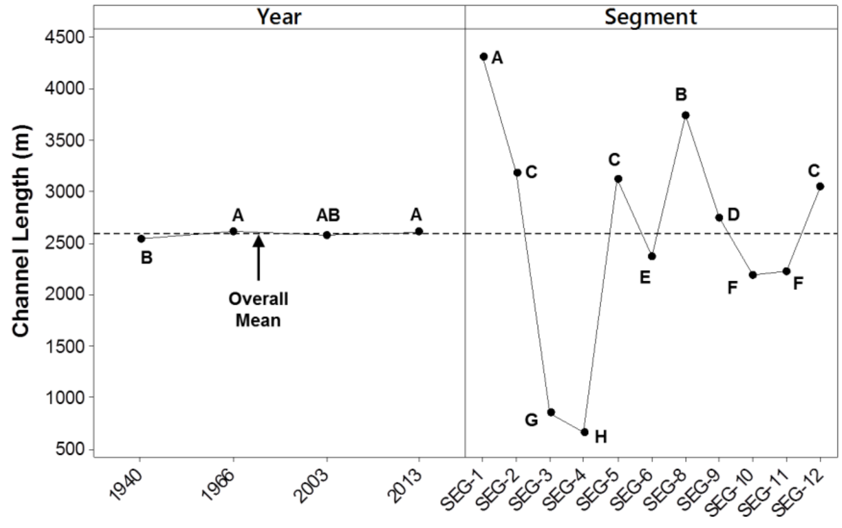

Figure 4.7. Two-way analysis of variance's main effects plot for channel length by year and segment. Means that do not share a letter are significantly different at α = 0.05 level using Tukey's pairwise comparisons. SEG refers to the segment name followed by numerical value.

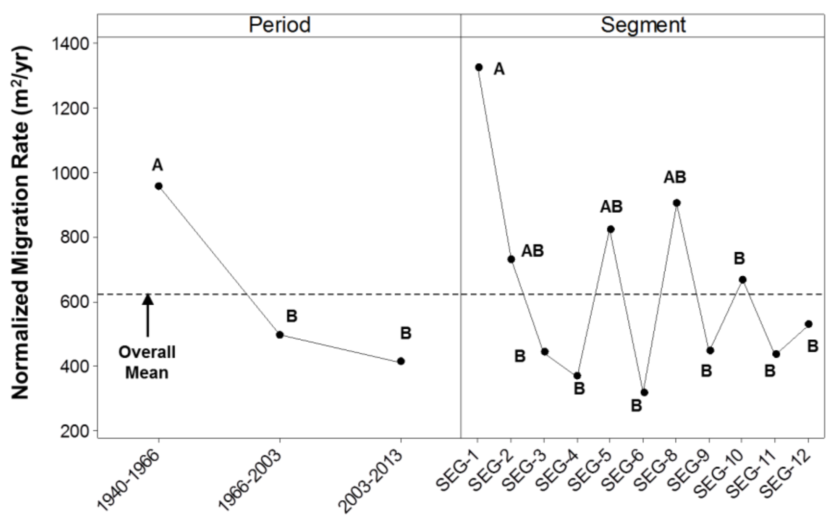

Figure 4.8. Two-way analysis of variance's main effects plot for normalized migration rate (m/yr) by period and segment. Means that do not share a letter are significantly different at α = 0.05 level using Tukey's pairwise comparisons. SEG refers to the segment name followed by numerical value.

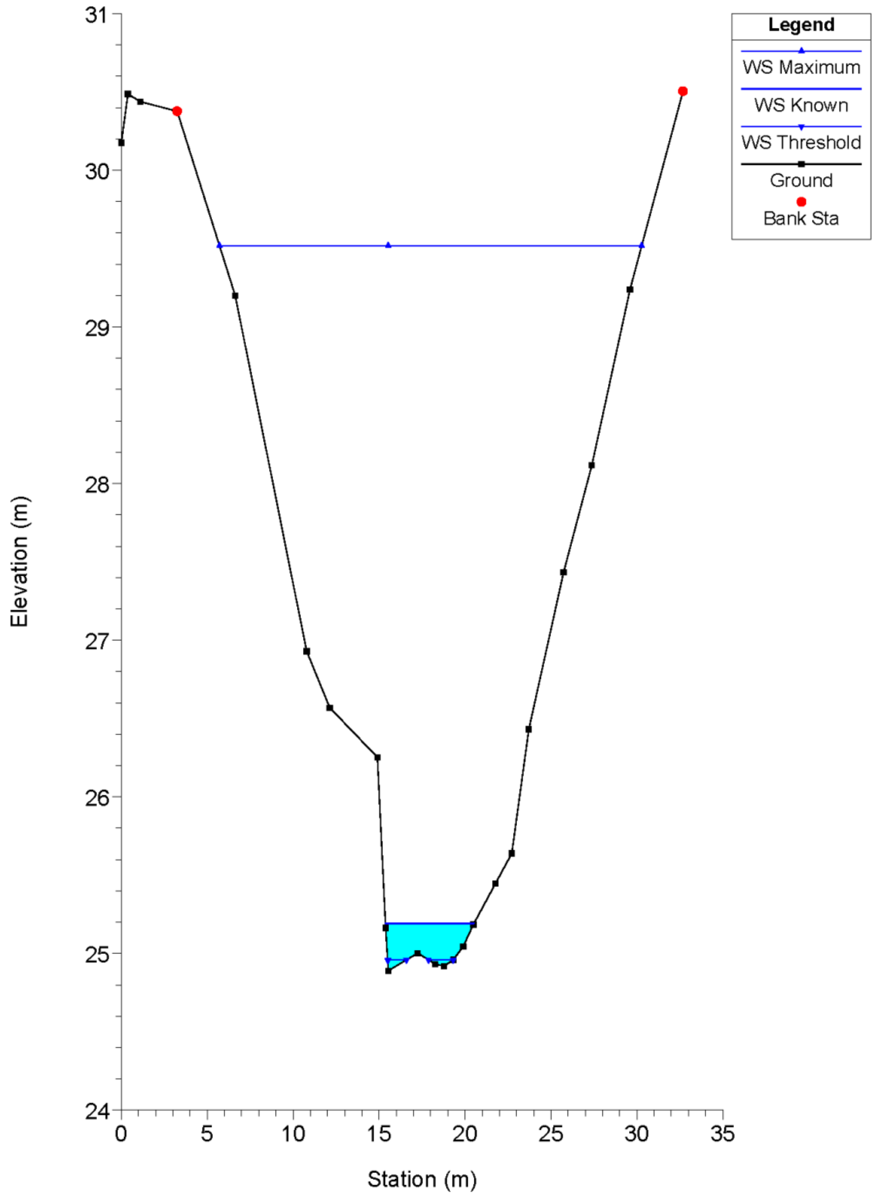

Figure 4.9. A surveyed cross-section at SEG-5 and HEC-RAS (USACE 2010) steady state simulation for water surface elevations at known, maximum, and threshold discharges (incipient motion for channel sediment particle).

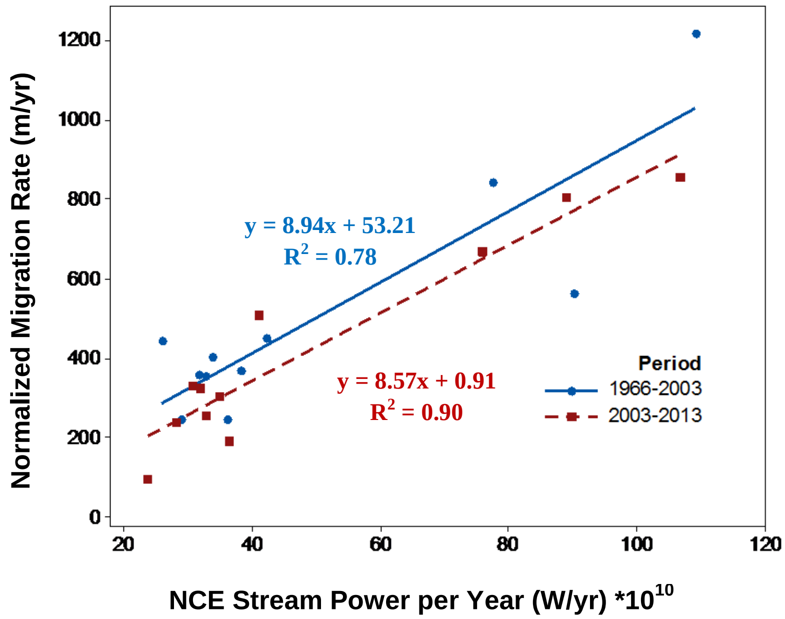

Figure 4.10. Relationship between normalized migration rate and normalized cumulative effective stream power per year. The slopes of regression lines were not significantly different whereas intercept was significantly different at $\alpha = 0.1$ based on two-way analysis of covariance (Table 4.6).

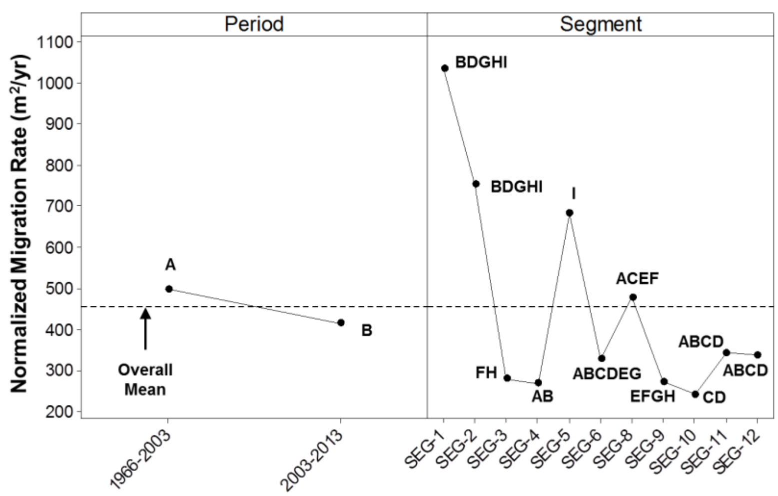

Figure 4.11. Two-way analysis of covariance’s main effects plot for normalized migration rate (m/yr) by period and segment as NCE stream power per year (W/yr) as covariate. Means that do not share a letter are significantly different at $\alpha = 0.05$ level using Tukey’s pairwise comparisons. SEG refers to the segment name followed by numerical value.

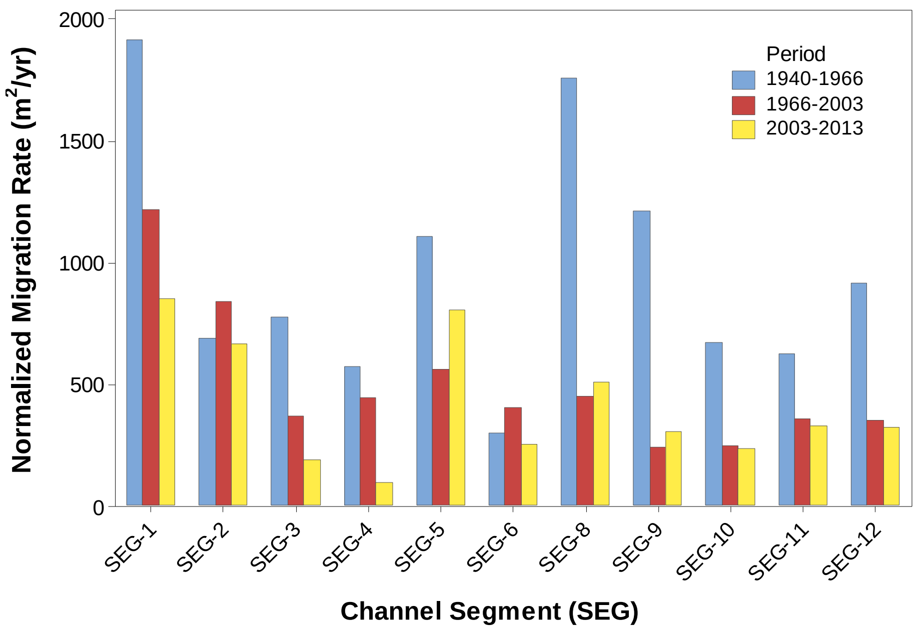

Figure 4.12. The chart shows the segment and period wise normalized migration rate (m/yr). SEG refers to the segment name followed by numerical value.

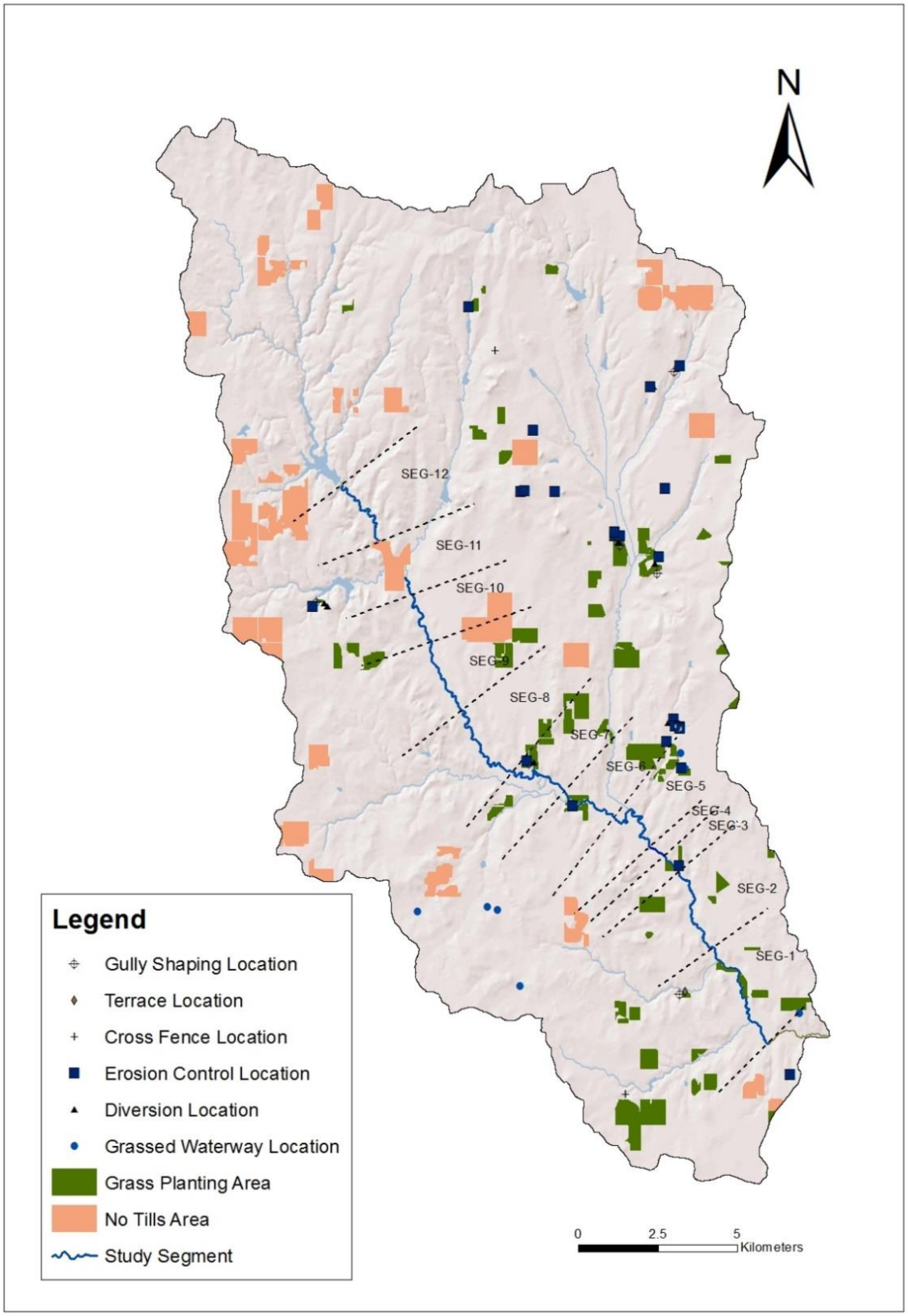

Figure 4.13. Best management practices implemented in the study watershed for the FY2001 Fort Cobb Watershed Implementation 319 Project funded by the US Environmental Protection Agency. Spatial data provided by Oklahoma Conservation Commision on January 21, 2016. Basemap source: ESRI (2010). SEG refers to the segment name followed by numerical value.

CHAPTER V

CONCLUSIONS AND RECOMMENDATIONS

Conclusions

The research findings from this dissertation may be applied to reduce environmental impacts from anthropogenic activities in several ways. In urban settings, water bodies are impaired by excessive suspended sediment loading due to development and construction activities. Agricultural streams are impaired due to suspended sediment and nutrients loading from agricultural fields. The turbidity prediction methodology can be applied to reduction of suspended sediment loading into surface water bodies as well as evaluate the effectiveness of BMPs in erosion reduction. The water-color prediction methodology can be applied to big plant nurseries and small watersheds, where the predominate source of organic matter and runoff measurement from that source is measurable. Aerial images and maps were shown to evaluate the impacts of conservation practices on channel stability.

Research Project One

The overall study goal of the first research project was to develop a turbidity prediction methodology for existing runoff-erosion models. The research objectives of this project were to (i) develop a simple, reliable method to predict dispersed turbidity and (ii) develop a simple, reliable method to predict undispersed turbidity. Based on the results of this project, the following conclusions were made:

- A simple method of turbidity prediction, which can be easily integrated into an existing runoff-erosion model, was developed based on percentage of soil particles and suspended sediment concentration.

- General methodologies to predict dispersed runoff turbidity were developed, which showed the mostly linear relationships between primary soil particles (sand, silt and clay) and turbidity.

- Undispersed runoff turbidity showed a function of dispersed turbidity and a percentage of sand, silt and clay in the runoff sediment samples.

- The results indicated the possibility of integrating various water quality parameters with turbidity and incorporating them with existing runoff erosion models, which help to estimate water quality parameters and runoff-erosion rates in the impacted landscape.

- Overall, the research findings indicated the importance of all-in-one surrogate measurement of turbidity and integration in runoff-erosion models to evaluate associated anthropogenic impacts on soil erosion and surface water quality.

Research Project Two

The overall goal of the second research project was to quantify the relationship between water color and dissolved organic carbon (DOC) based on the sources of organic matter. The specific objectives of the study were (i) to quantify the relationship between water color and DOC in water, based on specific organic matter sources and (ii) to test a method to predict the water color of water samples with multiple sources of DOC. Based on the results of this project, following conclusions were made:

- A small laboratory scale experiment was designed for this study. The source-specific relationship between water color and DOC was quantified based on sources of organic matter commonly found in surface waters.

- A methodology was developed that predicts water color without separating the complex chemical constituents and instead estimates water color based on DOC on organic matter in natural waters.

- Color prediction methodology for heterogeneous organic matter present in surface waters was developed and validated using laboratory scale-based experiments.

- Overall, the research findings indicated that the water color for heterogeneous sources of organic matter content in surface waters can be predicted based on the proportion of various organic sources.

Research Project Three

As an indicator of human impacts on riverine landscape, historic channel morphological changes were evaluated in the Cobb Creek watershed. The objective of this study was to develop and apply an integrated approach to evaluate channel planform stability in an agricultural watershed using historical records such as plat maps, aerial images, and relevant historical events. Based on the findings of this project, the following conclusions were drawn:

- The notable events related to settlement, soil erosion, conservation practices and significant studies in the Fort Cobb watershed were documented.
- The extent of the channel network from 1873 to 2013 reflected the land disturbance activities in the watershed occurred at the same time of channel network extension
- Results indicated that streamflow and precipitation were not changed over the periods that contributed to consistent stream power in the Cobb Creek.
- Lateral channel migration significantly decreased from 1940 to 2013.
- Overall, stable channel planform sinuosity, consistent average annual stream power and decreased lateral migrations indicated that the main stem of Cobb Creek tended to be stable in terms of aerial view.

Future Research Recommendations

As this dissertation has three research components based on surface water quality and stream channel stability parameters, possible future research recommendations are described in subsequent sub-sections.

Turbidity and Suspended Sediment Concentration

Based on the findings of the research project on turbidity and suspended sediment concentrations, future research recommendations identified for this subject are:

- The factors associated with the relationship between dispersed turbidity and predicted turbidity were unknown, and thereby were corrected with a c-factor. Future research may study possible factors including interactions between change in particle shape and size during the turbidity measurement and primary soil particles separation process.

- In addition, the findings of this research suggest the necessity of developing a link between turbidity, water color and particle size distributions in runoff.

- The present method does not require the separation of large and small particles beyond sand, silt and clay fractions in the runoff sediment sample to predict runoff turbidity. Future research could investigate the effects of small and large aggregates in turbidity prediction for runoff-erosion water samples.

Water Color and Dissolved Organic Carbon

Based on the laboratory based measurements and results analysis of color prediction for heterogeneous organic source in runoff samples, potential future research opportunities identified are:

- All the water color and DOC samples were prepared with lab-grade deionized water. The effect of pH on natural water samples needs to be evaluated. In natural systems, the temporal variation of pH in waters cannot be avoided. Therefore, the relationship between water color and pH variations should be investigated.

- The interferences of minerals on color-DOC measurements were not investigated in this study. Future studies could investigate such effects, which may help develop methods to measure water color more precisely than those presently available.

- This study was based on laboratory experiments; however, a small watershed scale study should be conducted to investigate whether water color for runoff can be predicted based on the proportion of various organic matters or not.

An Integrated Approach on Channel Planform Changes

Based on the aerial images and maps interpretation method to analyze channel planform and lateral migrations, several potential research areas are recommended:

- As channel stability itself cannot be addressed by channel planform changes or lateral migrations, there could be potential in-channel erosion such as channel incisions and bank failures. Future studies should focus on process-based channel stability assessment with reference to historic planform changes.

- Historic hydrological records for the watershed were not available before 1966. Future research should focus on reconstructing or generating historic flow patterns in the watershed.

- Channel geomorphic processes associated with changes in sediment supply regimes were not directly studied in this research. Assessment of channel sediment dynamics before and after soil conservation practices may address problems associated with streambank failures in the watershed.

REFERENCES

Abad, J. D. & Garcia, M. H. (2006). RVR Meander: A toolbox for re-meandering of channelized streams, *Computers & Geosciences 32*, 92-101.

Agricultural Stabilization and Conservation Service (ASCS).(1966). *Aerial Flyovers for Caddo and Washita County*. Edmon Low Library, Oklahoma State University. Map Room Collection.

Anderson, C. (2005). Turbidity 6.7 (Version 2.1, 9/2005). In F. D. Wilde (Ed.), *National Field Manual for the Collection of Water-Quality Data, Book 9, Handbooks for Water-Resources Investigations Chapter A6 Field Measurement*: U.S. Geological Survey.

Andrews, W.J., Becker, C.J., Steiner, J.L., Daniel, J.A., Garbrecht, J.D., Moriasi, D.N., Starks, P.J., Mladnich, C.S., Rao, Maheesh, Siewe, Siewe, Clark, R.N., Wise, R.A., Fairchild, J.F., Allert, A.L., & Smith, S.J. (2011). Synopsis of integrated science to support the assessment of conservation practices in the Fort Cobb Reservoir watershed, southwestern Oklahoma, chap. 10 of Becker, C.J., ed., Assessment of conservation practices in the Fort Cobb Reservoir watershed, southwestern Oklahoma: U.S. Geological Survey Scientific Investigations Report 2010–5257, 22p.

APA manual (publication manual of the American Psychological Association). Washington, DC: American Psychological Association.

APHA, AWWA & WEF. (2012). *Standard methods for the examination of water & wastewater*. 22nd Edition, American Public Health Association (APHA), American Water Works Association (AWWA), Water Environment Federation (WEF). American Public Health Association, Washington, DC.

ASTM. (2007). *ASTM D422 - 63 standard test method for particle-size analysis of soils.* West Conshohocken, PA: ASTM International.

ASTM. (2011). *D7726-11 Standard guide for the use of various turbidimeter technologies for measurement of turbidity in water* (p. 17). West Conshohocken, PA, USA ASTM International.

ASTM. (2013). *E11-13 Standard specification for woven wire test sieve cloth and test sieves*. West Conshohocken, PA: ASTM International.

Awata, S., Tsuruta, T., Yada, T., & Iguchi, K. I. (2011). Effects of suspended sediment on cortisol levels in wild and cultured strains of ayu Plecoglossus altivelis. *Aquaculture*, *314*(1), 115-121.

Baker, A., & Spencer, R. G. (2004). Characterization of dissolved organic matter from source to sea using fluorescence and absorbance spectroscopy. *Science of the Total Environment*, *333*(1), 217-232.

Barfield, B. J., Hayes, J. C., Stevens, E., Harp, S. L., & Fogle, A. (2006). SEDIMOT III Model. In V. P. Singh, & D. K. Frevert (Eds.), *Watershed Models* (pp. 381-398): CRC Press.

Becker, C. J. & Steiner, J. L.(2011). Integrated science to support the assessment of conservation practices in the Fort Cobb watershed, southwestern Oklahoma, in C. J. Becker (Ed.), Assessment of conservation practices in the Fort Cobb Reservoir watershed, southwestern Oklahoma, p. 4.

Becker, C.J.(2011).Assessment of conservation practices in the Fort Cobb Reservoir watershed, southwestern Oklahoma: Beckler, C.J. ed. U.S. Geological Survey Scientific Investigations Report 2010–5257, 10 chapters

Beckman Coulter. (2007). *Instructions for using the gh-3.8 swinging bucket rotor* (pp. 41). Fullerton, California, USA: Beckman Coulter, Inc.

Beckman Instruments. (1988). *Instructional manual gp tabletop centrifuge*. Palo Alto, California: Spinco Division of Beckman Instruments, Inc.

Beeson, C. E., & Doyle, P. F. (1995). Comparison of bank erosion at vegetated and non-vegetated channel bends. *JAWRA Journal of the American Water Resources Association*, *31*(6), 983-990.

Benner, P. A., & Sedell, J. R. (1997). Upper Willamette River landscape: a historic perspective. *River quality: dynamics and restoration*. CRC Press, Lewis Publishers, New York, 23-47.

Bennett, L. E., & Drikas, M. (1993). The evaluation of colour in natural waters. *Water Research*, *27*(7), 1209-1218.

Berenbrock, C., & Tranmer, A. W. (2008). Simulation of flow, sediment transport, and sediment mobility of the lower Coeur d'Alene River, Idaho. US Geological Survey.

Bernal, A., Cardenoso, R., Fabrellas, C., Matia, L., & Salvatella, N. (1999). An aesthetic quality index for Barcelona's water supply. *Water science and technology*, *40*(6), 23-29.

Bilotta, G. S., & Brazier, R. E. (2008). Understanding the influence of suspended solids on water quality and aquatic biota. *Water Research*, *42*(12), 2849-2861, doi:http://dx.doi.org/10.1016/j.watres.2008.03.018.

BLM-GLO (2016). Our Record Keeping History. US Department of the Interior, Bureau of Land Management, General Land Office Records. Available from : http://www.glorecords.blm.gov/reference/default.aspx#id=01_GLO_Records|01_Our_Record_Keeping_History (Accessed on March 3, 2016).

BLM-GLO. (2015). Survey Plats and Field Notes for Oklahoma (Caddo, Custer and Washita County). Available from: https://www.glorecords.blm.gov/default.aspx (Accessed May 17, 2015)

Bloodworth, J. W., Holman, I. P., Burgess, P. J., Gillman, S., Frogbrook, Z., & Brown, P. (2015). Developing a multi-pollutant conceptual framework for the selection and targeting of interventions in water industry catchment management schemes. *Journal of Environmental Management, 161,* 153-162.

Brasington, J., & Richards, K. (2000). Turbidity and suspended sediment dynamics in small catchments in the Nepal Middle Hills. *Hydrological Processes, 14*(14), 2559-2574, doi:10.1002/1099-1085(20001015)14:14<2559::AID-HYP114>3.0.CO;2-E.

Brezonik, P. L., & Arnold, W. A. (2011). *Water chemistry: An introduction to the chemistry of natural and engineered aquatic systems*. Oxford University Press, USA.

Bricaud, A., Morel, A. and Prieur, A. (1981) Absorption by dissolved organic matter of the sea (yellow substance) in the UV and visible domains. *Limnology and Oceanography 26*, 43-53.

Brierley, G. and Hooke, J. (2015). Emerging geomorphic approaches to guide river management practices, *Geomorphology*, Volume 251, 15 December 2015, Pages 1-5, ISSN 0169-555X, http://dx.doi.org/10.1016/j.geomorph.2015.08.019.

Brookes, J. D., Hipsey, M. R., Burch, M. D., Regel, R. H., Linden, L. G., Ferguson, C. M., et al. (2005). Relative Value of Surrogate Indicators for Detecting Pathogens in Lakes and Reservoirs. *Environmental Science & Technology*, 39(22), 8614-8621, doi:10.1021/es050821+.

Buffington, J. M., & Montgomery, D. R. (1997). A systematic analysis of eight decades of incipient motion studies, with special reference to gravel-bedded rivers. Water Resources Research, 33(8), 1993-2029.

Carter, H. T., Tipping, E., Koprivnjak, J. F., Miller, M. P., Cookson, B., & Hamilton-Taylor, J. (2012). Freshwater DOM quantity and quality from a two-component model of UV absorbance. *Water Research, 46(14),* 4532-4542.

Cederstrand, J.R., 1996, Digital geologic map of Clinton Quadrangle, West-central Oklahoma: U.S. Geological Survey Open-File Report 96-373.

Chakraborty, S. & Mukhopadhyay, S. (2014). An assessment on the nature of channel migration of River Diana of the sub-Himalayan West Bengal using field and GIS techniques, *Arabian Journal of Geosciences, 1*-13.

Chang, H. H. (1979). Minimum stream power and river channel patterns. *Journal of Hydrology, 41(3),* 303-327

Chow, V.T. (1959). Open Channel Hydraulics, McGraw Hill Book Company, NY.

Christman, R. F., & Ghassemi, M. (1966). Chemical nature of organic color in water. *Journal (American Water Works Association)*, 723-741.

Collier, K. J. (1987). Spectral properties of some West Coast waters and their relationship with dissolved organic carbon. *Mauri Ora, 14,* 25-32.

Constantine, C. R., Dunne, T., & Hanson, G. J. (2009). Examining the physical meaning of the bank erosion coefficient used in meander migration modeling. *Geomorphology, 106*(3), 242-252.

Crowther, J. and Evans J. (1981). Estimating color in Hazen units by spectrophotometry. *Journal (American Water Works Association)* 265-270.

Davies-Colley, R. J. and Vant, W. N. (1987) Absorption of light by yellow substance in freshwater lakes. *Limnology and Oceanography 32,* 416-425.

Davies-Colley, R. J., & Smith, D. G. (2001). Turbidity suspended sediment, and water clarity: a review. *Journal of the American Water Resources Association, 37,* doi:10.1111/j.1752-1688.2001.tb03624.x

Deb, M., & Ferreira, C. (2015). Planform channel dynamics and bank migration hazard assessment of a highly sinuous river in the north-eastern zone of Bangladesh. *Environmental Earth Sciences*, *73(10)*, 6613-6623.

Del Vecchio, R., & Blough, N. V. (2004). On the origin of the optical properties of humic substances. Environmental Science & Technology, 38(14), 3885-3891.

Dillon, P. J., and L. A. Molot. (1997). Effect of landscape form on export of dissolved organic carbon, iron, and phosphorus from forested stream catchments. *Water Resources Research,* 33 (11), 2591-2600.

Effler, S. W., Johnson, D. L., Jiao, J. F., & Perkins, M. (1992). Optical impacts and sources of suspended solids in onondaga creek, U.S.A. *JAWRA Journal of the American Water Resources Association,* 28: 251–262. doi: 10.1111/j.1752-1688.1992.tb03991.x.

Erskine, W. D. (2011). Geomorphic controls on historical channel planform changes on the lower Pages River, Hunter Valley, Australia. *Australian Geographer, 42(3),* 289-307.

Esralew, R. A., & Smith, S. J. (2009). Methods for estimating flow-duration and annual mean-flow statistics for ungaged streams in Oklahoma. US Department of the Interior, US Geological Survey.

ESRI. (2010). ArcGIS Desktop. Release Version10.0. Environmental Systems Research Institute (ESRI): Redlands, CA.

Everett, D. (2009). Homestead Act (1862), Encyclopedia of Oklahoma history and culture. Available from: www.okhistory.org (Accessed on March 12, 2016).

Faithfull, C. L., Mathisen, P., Wenzel, A., Bergström, A. K., & Vrede, T. (2015). Food web efficiency differs between humic and clear water lake communities in response to nutrients and light. *Oecologia*, *177*(3), 823-835.

Filella, M., & Rodríguez-Murillo, J. C. (2014). Long-Term trends of organic carbon concentrations in freshwaters: Strengths and weaknesses of existing evidence. *Water, 6(5),* 1360-1418.

Flynn, K. M., W. H. Kirby, and Hummel, P.R.. (2006). User's manual for program PeakFQ, annual flood-frequency 655 analysis using Bulletin 17B guidelines. Techniques and Methods 4-B4, U.S. Geological Survey. Available online (

Foster, G., Young, R., & Neibling, W. (1985). Sediment composition for nonpoint source pollution analyses. *Transactions of the ASAE-American Society of Agricultural Engineers (USA)*.

Fremier, A. K., Girvetz, E. H., Greco, S. E., & Larsen, E. W. (2014). Quantifying process-based mitigation strategies in historical context: separating multiple cumulative effects on river meander migration. *PloS one*, *9*(6), e99736.

Gao, P., Pasternack, G., Bali, K., & Wallender, W. (2008). Estimating suspended sediment concentration using turbidity in an irrigation-dominated southeastern california watershed. *Journal of Irrigation and Drainage Engineering, 134*(2), 250-259, doi:10.1061/(ASCE)0733-9437(2008)134:2(250).

Garbrecht, J. D.(2011).Effects of climate variations and soil conservation on sedimentation of a west-central Oklahoma reservoir, *Journal of Hydrologic Engineering 16,* 899-906.

Garbrecht, J. D., & Starks, P. J. (2009). Watershed sediment yield reduction through soil conservation in a West-Central Oklahoma watershed. *Ecohydrology, 2*(3), 313-320.

Garbrecht, J.(2010). Climate Variations, Soil Conservation, and Reservior Sedimentation. 2nd Joint Federal Interagency Conference, Las Vegas, NV, June 27-July 1, 2010.

Garbrecht, J.D., Zhang, X.C. and Steiner, J.L., 2014. Climate change and observed climate trends in the Fort Cobb experimental watershed. *Journal of environmental quality*, *43*(4), pp.1319-1327.

Gee, G. W., & Bauder, J. W. (1986). Particle-size analysis1. In A. Klute (Ed.), *Methods of Soil Analysis: Part 1—Physical and Mineralogical Methods* (pp. 383-411, SSSA Book Series): Soil Science Society of America, American Society of Agronomy.

Gergel, S. E., M. G. Turner, J. R. Miller, J. M. Melack, and E. H. Stanley. (2002). Landscape indicators of human impacts to riverine systems. *Aquatic Sciences 64*,118–128

Gergel, S. E., Turner, M. G., & Kratz, T. K. (1999). Dissolved organic carbon as an indicator of the scale of watershed influence on lakes and rivers. *Ecological Applications, 9(4)*, 1377-1390.

Gerlach, R. W., & Nocerino, J. M. (2003). *Guidance for obtaining representative laboratory analytical subsamples from particulate laboratory samples*: US Environmental Protection Agency, Office of Research and Development, National Exposure Research Laboratory, Environmental Sciences Division.

Gippel, C. J. (1995). Potential of turbidity monitoring for measuring the transport of suspended solids in streams. *Hydrological Processes, 9*(1), 83-97, doi:10.1002/hyp.3360090108.

GLO. (1871). Instructions to the surveyors general of public lands of the United States for those surveying districts established in and since the year 1850; containing, also a manual of instructions to regulate the field operators of deputy surveyors. John M. Moore, Principal Clerk of Surveys, General Land Office (GLO). Washington: Government Printing Office.

Grayson, R., Kay, P., Foulger, M., & Gledhill, S. (2012). A GIS based MCE model for identifying water colour generation potential in UK upland drinking water supply catchments. *Journal of Hydrology*, *420*, 37-45.

Gregory, K. J. (2006). The human role in changing river channels. *Geomorphology, 79*(3), 172-191.

Güneralp,I. and. Rhoads.B.L. (2009). Planform change and stream power in the Kishwaukee River watershed, Illinois: geomorphic assessment for environmental management. *Geological Society of America Special Papers 451*: 109-118.

Gurnell, A. M., Downward, S. R., & Jones, R. (1994). Channel planform change on the River Dee meanders, 1876–1992. *Regulated rivers: research & management*, *9*(4), 187-204.

Gurnell, A. M., Peiry, J. L., & Petts, G. E. (2003). Using historical data in fluvial geomorphology. In *Tools in Fluvial Geomorphology* (eds G.M. Kondolf and H. Piegay). John Wiley & Sons, Ltd.

Hach Company. (2014a). Color, True and Apparent (DOC316.53.01037, Edition 10),*Method 8025*: Hach company/Hach Lange Gmb.

Hach Company. (2014b). Organic Carbon, (Total DOC316.53.01093, Edition 9), *Direct method (US Patent 6,368,870), Method 10129*: Hach Company/Hach Lange Gmb.

Hach Company.(2014c).Organic Carbon, Total (DOC316.53.01094, Edition 9), *Direct method (US Patent 6,368,870), Method 10173*: Hach company/Hach Lange Gmb.

Hach, C. (2006). Hydrolab DS5X, DS5, and MS5 Water Quality Multiprobles, User Manual, Edition 3. (pp. 74). Ludwigstrasse 16, Germany: OTT Hydromet GmbH.

Harp, S. L., Barfield, B. J., Hayes, J. C., Yeri, S., & Chalavadi, M. (2008). *SEDPRO modeling of BMP effectiveness at construction sites.* Paper presented at the World Environmental and Water Resources Congress 2008: Ahupua'a, May 12, 2008 - May 16, 2008, Honolulu, HI, United States.

Hathaway, J. C. (1956). Procedure for clay mineral analysis used in the sedimentary petrology laboratory of the US Geological Survey. *Clay minerals bulletin, 3,* 8-13.

Hazelton, P. D., & Grossman, G. D. (2009). The effects of turbidity and an invasive species on foraging success of rosyside dace (Clinostomus funduloides). *Freshwater Biology, 54*(9), 1977-1989, doi:10.1111/j.1365-2427.2009.02248.x.

Hazen, A. (1892). A new color standard for natural waters. *American Chemical Journal*, 14:300.

Helms, J. R., Stubbins, A., Ritchie, J. D., Minor, E. C., Kieber, D. J., & Mopper, K. (2008). Absorption spectral slopes and slope ratios as indicators of molecular weight, source, and photobleaching of chromophoric dissolved organic matter. *Limnology and Oceanography, 53(3),* 955.

Henley, W., Patterson, M., Neves, R., & Lemly, A. D. (2000). Effects of sedimentation and turbidity on lotic food webs: a concise review for natural resource managers. *Reviews in Fisheries Science*, *8*(2), 125-139.

Heo, J., Duc, T. A., Cho, H. S., & Choi, S. U. (2009). Characterization and prediction of meandering channel migration in the GIS environment: A case study of the Sabine River in the USA. *Environmental monitoring and assessment, 152*(1-4), 155-165.

Hoig, S. (2009). Land Run of 1889. Encyclopedia of Oklahoma History and Culture, Available from: www.okhistory.org (Accessed March 24, 2016).

Holden, J., Chapman, P. J., Palmer, S. M., Kay, P., & Grayson, R. (2012). The impacts of prescribed moorland burning on water colour and dissolved organic carbon: a critical synthesis. *Journal of environmental management*, *101*, 92-103.

Holliday, C., Rasmussen, T. C., & Miller, W. P. (2003). Establishing the relationship between turbidity and total suspended sediment concentration. In *Proceedings of the 2003 Georgia Water Resources Conference,* (pp. 23-24): The University of Georgia, Institute of Ecology Georgia.

Holstrom, T. A., & Hawkins, R. H. (1980). Particle size distribution effects on turbidity. In *Symposium on Watershed Management, Boise, Idaho, 1980* (pp. 283-297): Committee on Watershed Management of the Irrigation and Drainage Division, American Society of Civil Engineers, New York, NY.

Hongve, D., & Åkesson, G. (1996). Spectrophotometric determination of water colour in Hazen units. *Water Research, 30(11),* 2771-2775.

Hooke, R. L. (2000). On the history of humans as geomorphic agents. *Geology*, *28*(9), 843-846.

Hooke, R. L., Martín-Duque, J. F., & Pedraza, J. (2012). Land transformation by humans: a review. *GSA Today*, *22(12)*, 4-10.

Hoomehr, S., & Schwartz, J. S. (2012). Evaluating SEDCAD model performance on reclaimed coal mine lands in East Tennessee. *Journal of Irrigation and Drainage Engineering*, 139(3), 261-266.

Huett, D., Morris, S., Smith, G. & Hunt, N.(2005). Nitrogen and phosphorus removal from plant nursery runoff in vegetated and unvegetated subsurface flow wetlands. *Water Research 39,* 3259-3272.

Hughes, M. L., McDowell, P. F., & Marcus, W. A. (2006). Accuracy assessment of georectified aerial photographs: implications for measuring lateral channel movement in a GIS. *Geomorphology*, *74*(1), 1-16.

Hutchings, J.B. (2005). Color measurement. In Encyclopedia of Analytical Science (Second Edition), edited by Paul Worsfold Alan Townshend Colin Poole, Elsevier, Oxford, 2005, Pages 198-208, ISBN 9780123693976, http://dx.doi.org/10.1016/B0-12-369397-7/00100-X.

Hwang, B. F., Magnus, P., & Jaakkola, J. J. (2002). Risk of specific birth defects in relation to chlorination and the amount of natural organic matter in the water supply. *American Journal of Epidemiology*, *156(4)*, 374-382.

Ishikawa, T., Trisliana, Yurenfrie, Ardianor & Gumiri, S.(2006). Dissolved organic carbon concentration of a natural water body and its relationship to water color in Central Kalimantan, Indonesia. *Limnology 7,* 143-146.

James, L. A., & Marcus, W. A. (2006). The human role in changing fluvial systems: Retrospect, inventory and prospect. *Geomorphology*, *79*(3), 152-171.

Johnson, C., Flowers, A., Noriea, N., Zimmerman, A., Bowers, J., DePaola, A., et al. (2010). Relationships between environmental factors and pathogenic Vibrios in the Northern Gulf of Mexico. *Applied and Environmental Microbiology*, 76(21), 7076-7084.

Jones, A. S., Stevens, D. K., Horsburgh, J. S. and Mesner, N. O. (2011). Surrogate measures for providing high frequency estimates of total suspended solids and total phosphorus concentrations. *JAWRA Journal of the American Water Resources Association*, 47: 239–253. doi: 10.1111/j.1752-1688.2010.00505.

Jönsson, M., Ranåker, L., Nilsson, P. A., & Brönmark, C. (2013). Foraging efficiency and prey selectivity in a visual predator: differential effects of turbid and humic water. *Canadian Journal of Fisheries and Aquatic Sciences*,*70*(12), 1685-1690.

Julien, P. Y. (2010). Erosion and sedimentation. Cambridge University Press.

Julien, Pierre Y.. (2010). Erosion and Sedimentation (2nd Edition). Cambridge University Press, UK.

Kemp, P., Sear, D., Collins, A., Naden, P., & Jones, I. (2011). The impacts of fine sediment on riverine fish. *Hydrological Processes*, *25*(11), 1800-1821.

Khan, E., & Subramania-Pillai, S. (2006). Effect of leaching from filters on laboratory analyses of collective organic constituents. *Proceedings of the Water Environment Federation, 2006(12),* 901-918.

Kim, H. C., & Yu, M. J. (2005). Characterization of natural organic matter in conventional water treatment processes for selection of treatment processes focused on DBPs control. *Water Research, 39(19),* 4779-4789.

Kim, J., & Furumai, H. (2013). Improved calibration of a rainfall-pollutant-runoff model using turbidity and electrical conductivity as surrogate parameters for total nitrogen. *Water and Environment Journal*, *27*(1), 79-85, doi:10.1111/j.1747-6593.2012.00328.x.

Kim, J., Chung, Y., Shin, D., Kim, M., Lee, Y., Lim, Y., & Lee, D. (2002). Chlorination by-products in surface water treatment process. *Desalination*, *151*(1), 1-9.

King, W. D., & Marrett, L. D. (1996). Case-control study of bladder cancer and chlorination by-products in treated water (Ontario, Canada). *Cancer Causes & Control, 7(6),* 596-604.

Kirchner, J. W., Micheli, L., & Farrington, J. D. (1998). Effects of herbaceous riparian vegetation on streambank stability. University of California Water Resources Center.

Kirk, J. O. (1985). Effects of suspensoids (turbidity) on penetration of solar radiation in aquatic ecosystems. *Hydrobiologia*, *125*(1), 195-208, doi:10.1007/BF00045935.

Kirk, J. T. O. (1976).Yellow substance (Gelbstoff) and its contribution to the attenuation of photosynthetically active radiation in some inland and coastal south-eastern Australian waters. *Marine and Freshwater Research 27*, 61-71.

Kirk, K. L. (1991). Suspended clay reduces Daphnia feeding rate. *Freshwater Biology*, *25*(2), 357-365, doi:10.1111/j.1365-2427.1991.tb00498.x.

Kokorite, I., Klavins, M., Rodinov, V., & Springe, G. (2012). Trends of natural organic matter concentrations in river waters of Latvia. *Environmental Monitoring and Assessment*, *184*(8), 4999-5008.

Kondolf, G. M. (1997). PROFILE: hungry water: effects of dams and gravel mining on river channels. *Environmental management*, *21*(4), 533-551.

Kritzberg, E. S. & Ekström, S. M. (2012). Increasing iron concentrations in surface waters - a factor behind brownification?. *Biogeosciences 9*, 1465-1478.

Kumar, S., Forand, S., Babcock, G., & Hwang, S. A. (2014). Total trihalomethanes in public drinking water supply and birth outcomes: a cross-sectional study. *Maternal and Child Health Journal*, *18*(4), 996-1006.

Lagasse, P. F., Spitz, W.J., Zevenbergen, L.W., Zachmann, D.W., Aown Ayres and Associates, Inc. (2004). Handbook for predicting stream meander migration (NCHRP Report No. 553). Transportation Research Board. Washington, D.C., USA.

Larsen, E. W., Premier, A. K. and Greco, S. E. (2006), Cumulative effective stream power and bank erosion on the Sacramento river, California, USA. *JAWRA Journal of the American Water Resources Association*, *42*: 1077–1097. doi: 10.1111/j.1752-1688.2006.tb04515.x

Larson, J. H., Frost, P. C., Xenopoulos, M. A., Williams, C. J., Morales-Williams, A. M., Vallazza, J. M., ... & Richardson, W. B. (2014). Relationships between land cover and dissolved organic matter change along the river to lake transition. *Ecosystems, 17(8),* 1413-1425.

Lauer, J. W., & Parker, G. (2008). Net local removal of floodplain sediment by river meander migration. *Geomorphology, 96*(1), 123-149.

Lauer, W.J. (2006). Channel Planform Statistics. NCED Stream Restoration Toolbox. National Center for Earth-Surface Dynamics. National Center for Earth-surface Dynamics Data Repository. Available from: http://www.nced.umn.edu/Data_Repository.html (Accessed February 22, 2016).

Lawler, D.M. (2005). Spectrophotometry-Turbidimetry and Nephelometry, In Encyclopedia of Analytical Science (Second Edition), edited by Paul Worsfold, Alan Townshend Colin Poole, Elsevier, Oxford, 2005, Pages 343-351, ISBN 9780123693976, http://dx.doi.org/10.1016/B0-12-369397-7/00718-4.

LeChevallier, M. W., & Norton, W. D. (1992). Examining relationships between particle counts and Giardia, Cryptosporidium, and turbidity. *Journal (American Water Works Association)*, 54-60.

Legg, N.T., Heimburg, C., Collins B.D. and Olson, P.L. (2014). The Channel Migration Toolbox, ArcGIS Tools for Measuring Stream Channel Migration. Publication no. 14-06-032. Shorelands and Environmental Assistance Program, Washington State Department of Ecology Olympia, Washington. Available from: https://fortress.wa.gov/ecy/publications/SummaryPages/1406032.html (Accesed on March 12, 2016).

Legleiter, C. J. (2015). Downstream effects of recent reservoir development on the morphodynamics of a meandering channel: Savery Creek, Wyoming, USA. *River Research and Applications, 31*(10), 1328-1343.

Leopold, L.B., M.G. Wolman, and J.P. Miller, (1964). *Fluvial Processes in Geomorphology*. W. H. Freeman and Company, San Francisco,California, 522 pp.

Lewis, J. (1996). Turbidity-controlled suspended sediment sampling for runoff-event load estimation. *Water Resources Research, 32*(7), 2299-2310, doi:Doi 10.1029/96wr00991.

Line, D., Hall, K., & Blackwell, J. (2013). Estimating suspended solids from turbidity in the robeson creek, NC watershed. *JAWRA Journal of the American Water Resources Association, 49*(6), 1412-1420.

Lloyd, D. S. (1987). Turbidity as a water quality standard for salmonid habitats in Alaska. *North American journal of fisheries management, 7*(1), 34-45.

Magnus, P., Jaakkola, J. J., Skrondal, A., Alexander, J., Becker, G., Krogh, T., & Dybing, E. (1999). Water chlorination and birth defects. *Epidemiology*,*10*(5), 513-517.

Marttila, H., & Kløve, B. (2012). Use of turbidity measurements to estimate suspended solids and nutrient loads from peatland forestry drainage. *Journal of Irrigation and Drainage Engineering, 138*(12), 1088-1096, doi:10.1061/(ASCE)IR.1943-4774.0000509.

Massicotte, P., & Frenette, J. J. (2011). Spatial connectivity in a large river system: resolving the sources and fate of dissolved organic matter. *Ecological Applications, 21*(7), 2600-2617.

Matilainen, A., Vepsäläinen, M., & Sillanpää, M. (2010). Natural organic matter removal by coagulation during drinking water treatment: A review. *Advances in Colloid and Interface Science*, *159*(2), 189-197.

MEA. (2005). Ecosystem services and human well-being: wetlands and water synthesis. Millennium Ecosystems Assessment. World Resources Institute, Washington, D.C., USA.

Micheli, E. R., & Kirchner, J. W. (2002). Effects of wet meadow riparian vegetation on streambank erosion. 1. Remote sensing measurements of streambank migration and erodibility. *Earth Surface Processes and Landforms, 27*(6), 627-639.

Microsoft (2010). Microsoft Excel (Vol. Service Pack 1): Microsoft Corporation.

Minella, J. P., Merten, G. H., Reichert, J. M., & Clarke, R. T. (2008). Estimating suspended sediment concentrations from turbidity measurements and the calibration problem. *Hydrological Processes, 22*(12), 1819-1830.

Minitab. (2010). *Minitab 16 Statistical Software*. Minitab, Inc. State College, PA.

Minitab. (2016). Minitab 17 Statistical Software. Minitab, Inc, State College, PA.

Mishra, B. K., Gupta, S. K., & Sinha, A. (2014). Human health risk analysis from disinfection by-products (DBPs) in drinking and bathing water of some Indian cities. *Journal of Environmental Health Science and Engineering*, *12*(1), 73.

Molot, L. A. & Dillon, P. J. (1997a). Colour-mass balances and colour-dissolved organic carbon relationships in lakes and streams in central Ontario. *Canadian Journal of Fisheries and Aquatic Sciences*, *54*, 2789-2795.

Morel, B., Durand, P., Jaffrezic, A., Gruau, G., & Molénat, J. (2009). Sources of dissolved organic carbon during stormflow in a headwater agricultural catchment. *Hydrological Processes*, *23*(20), 2888-2901.

Moriasi, D. N., Starks, P. J., Guzman, J. A., Garbrecht, J. D., Steiner, J. L., Stoner, J. C.,Allen, P.B. & Naney, J. W. (2014b). Upper Washita River Experimental Watersheds: Reservoir, Groundwater, and Stream Flow Data. *Journal of environmental quality*, 43(4), 1262-1272.

Moriasi, D. N., Starks, P. J., Steiner, J. L., Guzman, J. A., Allen, P. B., & Naney, J. W. (2014a). Upper Washita River experimental watersheds: Physiography data. *Journal of Environmental Quality*, *43*(4), 1298-1309.

Moriasi, D. N., Steiner, J. L., & Arnold, J. G. (2011). Sediment measurement and transport modeling: Impact of riparian and filter strip buffers. *Journal of Environmental Quality, 40*(3), 807-814.

Morris, R. D., Audet, A. M., Angelillo, I. F., Chalmers, T. C., & Mosteller, F. (1992). Chlorination, chlorination by-products, and cancer: a meta-analysis. *American Journal of Public Health, 82*(7), 955-963.

Morris, R. J. (2010). Anthropogenic impacts on tropical forest biodiversity: a network structure and ecosystem functioning perspective. Philosophical Transactions of the Royal Society of London B: *Biological Sciences, 365*(1558), 3709-3718.

Mostofa, K. M.G., Liu, C. Q., Mottaleb, M. A., Wan, G., Ogawa, H., Vione, D., ... & Wu, F. (2013). Dissolved organic matter in natural waters. In *Photobiogeochemistry of Organic Matter* (pp. 1-137). Springer Berlin Heidelberg.

Motta, D., Abad, J. D., Langendoen, E. J., & Garcia, M. H. (2012). A simplified 2D model for meander migration with physically-based bank evolution. *Geomorphology, 163*, 10-25.

Mundende, C.D. (2009). "Soil and Water Conservation, Encyclopedia of Oklahoma History and Culture, www.okhistory.org (accessed March 24, 2016).

Nash, J. E., & Sutcliffe, J. V. (1970). River flow forecasting through conceptual models part I A discussion of principles. *Journal of Hydrology, 10*(3), 282-290, doi:http://dx.doi.org/10.1016/0022-1694(70)90255-6.

NCSS (2000). Kamie series.National Cooperative Soil Survey, USDA Natural Resources Conservation Service, U.S.A. Available online: https://soilseries.sc.egov.usda.gov/OSD_Docs/K/KAMIE.html. Accessed 4 July 2015.

NCSS (2004a). Port series. National Cooperative Soil Survey, USDA Natural Resources Conservation Service, U.S.A. Available online: https://soilseries.sc.egov.usda.gov/OSD_Docs/P/PORT.html. Accessed 4 July 2015.

NCSS (2004b). Norge series. National Cooperative Soil Survey, USDA Natural Resources Conservation Service, U.S.A. Available online: https://soilseries.sc.egov.usda.gov/OSD_Docs/N/NORGE.html. Accessed 4 July 2015.

NCSS (2007). Cecil series. National Cooperative Soil Survey, USDA Natural Resources Conservation Service, U.S.A. Available online: https://soilseries.sc.egov.usda.gov/OSD_Docs/C/CECIL.html. Accessed 4 July 2015.

NCSS (2008). Pacolet series. National Cooperative Soil Survey, USDA Natural Resources Conservation Service, U.S.A. Available online: https://soilseries.sc.egov.usda.gov/OSD_Docs/P/PACOLET.html. Accessed 4 July 2015.

NCSS (2014). Stephenville series. National Cooperative Soil Survey, USDA Natural Resources Conservation Service, U.S.A. Available online: https://soilseries.sc.egov.usda.gov/OSD_Docs/S/STEPHENVILLE.html. Accessed 4 July 2015.

Nebbioso, A., & Piccolo, A. (2013). Molecular characterization of dissolved organic matter (DOM): a critical review. *Analytical and Bioanalytical Chemistry, 405*(1), 109-124.

Novoa, S., Wernand, M. R., & van der Woerd, H. J. (2014). The modern Forel-Ule scale: a 'do-it-yourself'colour comparator for water monitoring. *Journal of the European Optical Society-Rapid publications*, 9.

OCC. (2009). Watershed based plan for the Fort Cobb Watershed. June 2009 Update. Oklahoma Conservation Commission (OCC), Water Quality Division, Oklahoma City, Oklahoma, 186 pp.

O'Dell,L. (2009). Washita County, Encyclopedia of Oklahoma History and Culture, www.okhistory.org (accessed March 24, 2016).

ODOT. (2016). All bridges currently on the Oklahoma Highway System. Bridges ArcView Shape File. Oklahoma Department of Transportation. Available from: http://www.okladot.state.ok.us/maps/shp/index.htm (Accessed March 5, 2016).

Omar, B. A. F. and MatJafri, B.M. Z. (2009). Turbidimeter design and analysis: a review on optical fiber sensors for the measurement of water turbidity. *Sensors, 9*(10), 8311-8335.

Packman, J.J., Comings, K. J., & Booth, D. B.(1999). Using turbidity to determine total suspended solids in urbanizing streams in the Puget Lowlands: in *Confronting*

Uncertainty: Managing Change in Water Resources and the Environment, Canadian Water Resources Association annual meeting, Vancouver, BC, 27–29 October 1999, p. 158–165.

Pagano, T., Bida, M., & Kenny, J. E. (2014). Trends in levels of allochthonous dissolved organic carbon in natural water: a review of potential mechanisms under a changing climate. *Water, 6*(10), 2862-2897.

Parmelee, C. L., & Ellms, J. W. (1899). On rapid methods for the estimation of the weight of suspended matters in turbid waters. *Technology Quartery and proceedings of Society of Arts, XII*(2), 20.

Parry, L. E., Chapman, P. J., Palmer, S. M., Wallage, Z. E., Wynne, H., & Holden, J. (2015). The influence of slope and peatland vegetation type on riverine dissolved organic carbon and water colour at different scales. *Science of The Total Environment, 527,* 530-539.

Patil, S. S. (2010). Turbidity Modeling Based on the Concentration of Total Suspended Solids for Stormwater Runoff from Construction Sites. *Master's Thesis*, Oklahoma State University.

Pavanelli, D., & Bigi, A. (2005). Indirect methods to estimate suspended sediment concentration: reliability and relationship of turbidity and settleable solids. *Biosystems Engineering, 90*(1), 75-83, doi:http://dx.doi.org/10.1016/j.biosystemseng.2004.09.001.

Peacock, M., Evans, C. D., Fenner, N., Freeman, C., Gough, R., Jones, T. G., & Lebron, I. (2014). UV-visible absorbance spectroscopy as a proxy for peatland dissolved organic carbon (DOC) quantity and quality: considerations on wavelength and absorbance degradation. *Environmental Science: Processes & Impacts, 16*(6), 1445-1461.

Perkins, R., Hansen, B., Wilson, B., & Gulliver, J. (2014). Development and Evaluation of Effective Turbidity Monitoring Methods for Construction Projects,Bruce Wilson, Principal Investigator. In U. o. M. Departments of Bioproducts/Biosystems and Civil Engineering (Ed.), (pp. 158): Minnesota Department of Transportation.

Perroy, R. L., Bookhagen, B., Asner, G. P., & Chadwick, O. A. (2010). Comparison of gully erosion estimates using airborne and ground-based LiDAR on Santa Cruz Island, California. *Geomorphology, 118*(3), 288-300.

Pflüger, Y., Rackham, A., & Larned, S. (2010). The aesthetic value of river flows: An assessment of flow preferences for large and small rivers. *Landscape and Urban Planning, 95*(1), 68-78.

Phillips, D.F., and M.S. Harrison. (2004). Out of the dust: The history of conservation in Oklahoma in the 20th century. Oklahoma Assoc. of Conserv. Districts, Oklahoma City, OK.

Rapp, C.F., Abbe, T.B., 2003. A framework for delineating channel migration zones. Washington Department of Transportation, Department of Ecology Publication 03-06-027. 66 pp.

Ratnaweera, H., Hiller, N., & Bunse, U. (1999). Comparison of the coagulation behavior of different Norwegian aquatic NOM sources. *Environment International, 25*(2), 347-355.

Reckhow, D. A., & Singer, P. C. (1990). Chlorination by-products in drinking waters: from formation potentials to finished water concentrations. *Journal (American Water Works Association)*, 173-180.

Reusch, W. (1999). *Virtual textbook of organic chemistry*. Available from: http://www2.chemistry.msu.edu/faculty/reusch/virttxtjml/intro1.htm (Accessed March 18, 2016).

Rhoads , B. L., Lewis, Q. W., & Andresen, W. (2016). Historical changes in channel network extent and channel planform in an intensively managed landscape: Natural versus human-induced effects. *Geomorphology, 252*, 17-31.

Riley, S. (1998). The sediment concentration–turbidity relation: its value in monitoring at Ranger Uranium Mine, Northern Territory, Australia. *CATENA, 32*(1), 1-14.

Ritson, J. P., Bell, M., Graham, N. J., Templeton, M. R., Brazier, R. E., Verhoef, A.,Freeman, C. & Clark, J. M. (2014). Simulated climate change impact on summer dissolved organic carbon release from peat and surface vegetation: Implications for drinking water treatment. *Water research*, *67*, 66-76.

Ritter, J. B., Rumschlag, J. H., & Zaleha, M. J. (2007). Evaluating recent stream channel and pattern changes for stream resource protection and restoration: An example from west-central Ohio. *Journal of Great Lakes Research, 33*(sp2), 154-166.

Robidoux, M., del Giorgio, P. and Derry, A. (2015), Effects of humic stress on the zooplankton from clear and DOC-rich lakes. *Freshw Biol, 60*: 1263–1278. doi:10.1111/fwb.12560

Roccaro, P., Yan, M., & Korshin, G. V. (2015). Use of log-transformed absorbance spectra for online monitoring of the reactivity of natural organic matter. *Water Research, 84*, 136-143.

Rosewarne, P. J., Svendsen, J. C., Mortimer, R. J., & Dunn, A. M. (2014). Muddied waters: suspended sediment impacts on gill structure and aerobic scope in an endangered native and an invasive freshwater crayfish. *Hydrobiologia*, *722*(1), 61-74.

Rügner, H., Schwientek, M., Beckingham, B., Kuch, B., & Grathwohl, P. (2013). Turbidity as a proxy for total suspended solids (TSS) and particle facilitated pollutant transport in catchments. *Environmental Earth Sciences*, *69*(2), 373-380, doi:10.1007/s12665-013-2307-1.

Rügner, H., Schwientek, M., Egner, M., & Grathwohl, P. (2014). Monitoring of event-based mobilization of hydrophobic pollutants in rivers: Calibration of turbidity as a proxy for particle facilitated transport in field and laboratory. *Science of The Total Environment, 490*, 191-198.

Ruzycki, E. M., Axler, R. P., Host, G. E., Henneck, J. R., & Will, N. R. (2014). Estimating Sediment and Nutrient Loads in Four Western Lake Superior Streams. *JAWRA Journal of the American Water Resources Association*, *50*(5), 1138-1154, doi:10.1111/jawr.12175.

Ruzycki, E., Axler, R., Henneck, J., Will, N., & Host, G. (2011). Estimating mercury concentrations and loads from four western Lake Superior watersheds using continuous in-stream turbidity monitoring. *Aquatic Ecosystem Health & Management, 14*(4), 422-432.

Sadar, M.J., 1998, Turbidity Science. HACH, Technical Information Series-Booklet No. 11, 26 pp.

Schumm, S. A. (1963). Sinuosity of alluvial rivers on the Great Plains. *Geological Society of America Bulletin*, *74*(9), 1089-1100.

Scorpio, V., Aucelli, P. P., Giano, S. I., Pisano, L., Robustelli, G., Rosskopf, C. M., & Schiattarella, M. (2015). River channel adjustments in Southern Italy over the past 150years and implications for channel recovery. *Geomorphology, 251*, 77-90.

Shields Jr, F. D., Simon, A., & Steffen, L. J. (2000). Reservoir effects on downstream river channel migration. *Environmental Conservation*, *27*(01), 54-66.

Shields, A. (1936). Anwendung der Aehnlichkeitsmechanik und der Turbulenzforschungauf die Geschiebebewegung, Mitteilungen der Preussischen, Versuchsanstalt fur Wasserbau and Schiffbau, Berlin, Germany (English Translation: W. P. Ott and J. C. van Uchelen, California Institute of Technology, Publication No. 167., Pasadena, California).

Shutova, Y., Baker, A., Bridgeman, J., & Henderson, R. K. (2014). Spectroscopic characterisation of dissolved organic matter changes in drinking water treatment: from PARAFAC analysis to online monitoring wavelengths. *Water Research*, *54*, 159-169.

Siewe, S.S.S. (2003). Change detection of the landuse and landcover of the Fort Cobb reservoir watershed. Master's Thesis. Oklahoma State University.

Simon, A. & Klimetz, L.(2008).Relative magnitudes and sources of sediment in benchmark watersheds of the Conservation Effects Assessment Project, *Journal of Soil and Water Conservation 63*, 504-522.

Simon, A. & Rinaldi, M.: (2006). Disturbance, stream incision, and channel evolution: The roles of excess transport capacity and boundary materials in controlling channel response, *Geomorphology 79*, 361-383.

Slaets, J. I., Schmitter, P., Hilger, T., Lamers, M., Piepho, H.-P., Vien, T. D., et al. (2014). A turbidity-based method to continuously monitor sediment, carbon and nitrogen flows in mountainous watersheds. *Journal of Hydrology, 513*, 45-57.

Smith, D. G., Croker, G. F., & McFarlane, K. (1995). Human perception of water appearance: 1. Clarity and colour for bathing and aesthetics. *New Zealand journal of Marine and Freshwater Research, 29*(1), 29-43.

Soil Survey Division Staff (1993). Soil survey manual. Soil Conservation Service. U.S. Department of Agriculture Handbook 18.

Soil Survey Staff (2011). Natural Resources Conservation Service, United States Department of Agriculture. Soil Survey Geographic (SSURGO) Database. Available online: http://sdmdataaccess.nrcs.usda.gov/. Accessed 10 October 2011.

Starks, P. J., Steiner, J. L., & Stern, A. J. (2014). Upper Washita River experimental watersheds: Land cover data sets (1974–2007) for two southwestern Oklahoma agricultural watersheds. *Journal of Environmental Quality, 43*(4), 1310-1318.

Starks, P.J., Daniel, J.A., Moriasi, D.N., and Steiner, J.L.(2011a).Soils, crop production, and geology in the Fort Cobb Reservoir watershed, southwestern Oklahoma, Chap. 3 of Becker, C.J., ed., Assessment of conservation practices in the Fort Cobb Reservoir watershed, southwestern Oklahoma: U.S. Geological Survey Scientific Investigations Report 2010–5257, 10 p.

Starks, P.J., Rao, Mahesh, and Siewe, Siewe, 2011b, Land-cover analysis for the Fort Cobb Reservoir watershed, southwestern Oklahoma, 2005, chap. 5 of Becker, C.J., ed., Assessment of conservation practices in the Fort Cobb Reservoir watershed, southwestern Oklahoma: U.S. Geological Survey Scientific Investigations Report 2010–5257, 8 p.

Stasko, A. D., Gunn, J. M., & Johnston, T. A. (2012). Role of ambient light in structuring north-temperate fish communities: potential effects of increasing dissolved organic carbon concentration with a changing climate. *Environmental Reviews*, *20*(3), 173-190.

Steiner, J. L., Starks, P. J., Garbrecht, J. D., Moriasi, D. N., Zhang, X., Schneider, J. M., ... & Osei, E. (2014). Long-term environmental research: the upper washita river experimental watersheds, Oklahoma, USA. *Journal of Environmental Quality, 43*(4), 1227-1238.

Storm, D. E., Busteed, P. R. & White, M. J.: 2006, Fort Cobb Basin: Modeling and Land Cover Classification, Biosystems and Agricultural Engineering Department, Division of Agricultural Sciences and Natural Resources, Oklahoma State University.

Storm, D.E., White, M.J., and Stoodley, Scott. (2003). Fort Cobb Basin-Modeling and land cover classification, Final Report: Oklahoma Conservation Commission.

Sulzberger, B., & Durisch-Kaiser, E. (2009). Chemical characterization of dissolved organic matter (DOM): a prerequisite for understanding UV-induced changes of DOM absorption properties and bioavailability. *Aquatic Sciences*, *71*(2), 104-126.

Sun, H., Cornish, P. S., & Daniell, T. M. (2001). Turbidity-based erosion estimation in a catchment in South Australia. *Journal of Hydrology, 253*(1–4), 227-238, doi:http://dx.doi.org/10.1016/S0022-1694(01)00475-9.

Teixeira, E. C., & Caliari, P. C. (2005). Estimation of the concentration of suspended solids in rivers from turbidity measurement: error assessment. *Sediment Budgets, 1*, 151-160.

Thurman, E.M. 1985. *Organic geochemistry of natural waters*. Dordrecht: Martinus Njhoff/ Dr W. Junk Publishers.

Tobergte, A. G. (2012). Comparing lateral channel migration with historic and current geomorphic assessments, *Master's thesis*. Oklahoma State University.

Tomer, M. D., & Locke, M. A. (2011). The challenge of documenting water quality benefits of conservation practices: A review of USDA-ARS's conservation effects assessment project watershed studies. *Water Science and Technology*, *64*(1), 300-310

Trimble, S. W. (2008). The use of historical data and artifacts in geomorphology. *Progress in Physical Geography, 32*(1), 3-29.

Trimble, S. W., & Cooke, R. U. (1991). Historical sources for geomorphological research in the united states. *The Professional Geographer, 43*(2), 212-228.

USACE (2010). HEC-RAS River Analysis System. U.S. Army Corps of Engineers, Hydrologic Engineering Center, Davis, California.

USDA–ARS. 2013a. Ft Cobb Reservior Watershed 2005-2012 GIS datasets. Physiography-Geology [Database.] Available from: ftp://164.58.150.21/FT_Cobb_Reservoir_Watershed_2005-2012/GIS-DataSets/Physiography/Geology/ (Accessed March 8, 2016).

USDA–ARS. 2013b. Little Washita River Research Watershed GIS datasets: Reservoir hydrology. [Database.] Available from: ftp://164.58.150.21/Little_Washita_River_Research_Watershed_Other/GIS_Datasets/Hydrolog y/Resevoirs/. (Accessed March 8, 2016).

USDA-FSA (2003). Ortho Imagery, National Agriculture Imagery Program (NAIP). USDA-FSA Aerial Photography Field Office, Salt Lake City, Utah. Geospatial Data Gateway [online]. Available from: https://gdg.sc.egov.usda.gov/ (Accessed February 22, 2016).

USDA-FSA (2013). Ortho Imagery, National Agriculture Imagery Program (NAIP). USDA-FSA Aerial Photography Field Office, Salt Lake City, Utah. Geospatial Data

Gateway [online]. Available from: https://gdg.sc.egov.usda.gov/ (Accessed February 22, 2016).

USEPA. (2006). Wadeable Streams Assessment, A Collaborative Survey of the Nation's Streams, EPA 841-B-06-002, U.S. Environmental Agency, Office of Water, Washigton, DC.

USEPA. (2009). Environmental Impact and Benefits Assessment for Final Effluent Guidelines and Standards for the Construction and Development Category. In U. S. E. P. Agency (Ed.). 1200 Pennsylvania Avenue, NW, Washington, DC 20460: U.S. Environmental Protection Agency Office of Water (4303T).

USEPA. (1999). Guidance Manual for Compliance with the interim enhanced surface water treatment rule : Turbidity Provisions. United States Environmental Protection Agency.

USEPA. (2014). Effluent Limitations Guidelines and Standards for the Construction and Development Point Source Category, Final Rule. In U. S. E. P. Agency (Ed.), *EPA–HQ–OW–2010–0884; FRL–9906–51–OW; RIN 2040–AF44* (Vol. 40 CFR Part 450: , pp. 6): Federal Registar.

USEPA. (2016). Water Chemistry. Data from the National Aquatic Resource Surveys. National Aquatic Resource Surveys. United States Environmental Protection Agency. Available from: https://www.epa.gov/national-aquatic-resource-surveys/data-national-aquatic-resource-surveys (Accessed on March 29, 2016)

USGS. (2015). USGS National Hydrography Dataset (NHD) Best Resolution for Oklahoma 20151108 State or Territory Shapefile. Available from: http://viewer.nationalmap.gov/viewer/nhd.html?p=nhd (Accessed Feburary 27, 2016).

USGS. (2016a). The StreamStats program for Oklahoma. U.S. Geological Survey, U.S. Department of the Interior [online]. Available from: http://water.usgs.gov/osw/streamstats/oklahoma.html (Accessed Feburary 20, 2016).

USGS. (2016b). National Water Information System, Mean daily streamflow data. USGS 07325800 Cobb Creek near Eakly, OK. Available from: http://waterdata.usgs.gov/ok/nwis/dv/?site_no=07325800&agency_cd=USGS&referred_module=sw (Accessed May 15, 2016).

USGS. (2016c). National Water Information System. Daily Data. USGS 07325800 Cobb Creek near Eakly, OK, Available from: http://nwis.waterdata.usgs.gov/nwis/dv?site_no=07325800 (Accessed July 17, 2016).

Vanoni, V. A. (1964). Measurements of critical shear stress for entraining fine sediments in a boundary layer, KH-R-7, W. M. Keck Laboratory of Hydraulics and Water

Resources, Division of Engineering and Applied Science, California Institute of Technology, Pasadena, California.

Vogel, J. L., & Beauchamp, D. A. (1999). Effects of light, prey size, and turbidity on reaction distances of lake trout (Salvelinus namaycush) to salmonid prey. *Canadian Journal of Fisheries and Aquatic Sciences, 56*(7), 1293-1297.

Volk, C., Kaplan, L. A., Robinson, J., Johnson, B., Wood, L., Zhu, H. W., & LeChevallier, M. (2005). Fluctuations of dissolved organic matter in river used for drinking water and impacts on conventional treatment plant performance. *Environmental Science & Technology, 39*(11), 4258-4264.

Volk, C., Wood, L., Johnson, B., Robinson, J., Zhu, H. W. & Kaplan, L.(2002). Monitoring dissolved organic carbon in surface and drinking waters. *Journal of Environmental Monitoring 4*, 43-47.

Wallick, J. R., Lancaster, S. T., & Bolte, J. P. (2006). Determination of bank erodibility for natural and anthropogenic bank materials using a model of lateral migration and observed erosion along the Willamette River, Oregon, USA. *River Research and Applications, 22*(6), 631-649.

Warner, R. C., Schwab, P., & Marshall, D. (1998). SEDCAD 4 for Windows 95/98 & NT, Design Manual and User's Guide. *Civil Software Design, Ames, IA.*

Warner, R., & Sturm, T. (2002). Turbidity as a surrogate to estimate the effluent suspended sediment concentration of sediment controls at a construction site in the southeastern united states. In *Proceedings of the Federal Interagency workshop on Turbidity and Other Surrogates. Reno NV April, 2002.*

Wass, P. D., Marks, S. D., Finch, J. W., Leeks, G. J. L., & Ingram, J. K. (1997). Monitoring and preliminary interpretation of in-river turbidity and remote sensed imagery for suspended sediment transport studies in the Humber catchment. *Science of The Total Environment, 194–195*(0), 263-283, doi:http://dx.doi.org/10.1016/S0048-9697(96)05370-3.

Williamson, T. N., & Crawford, C. G. (2011). Estimation of suspended-sediment concentration from total suspended solids and turbidity data for kentucky, 1978-19951. *JAWRA Journal of the American Water Resources Association, 47*(4), 739-749.

Wilson, L.D. (2009), "Caddo County," Encyclopedia of Oklahoma History and Culture. Oklahoma Historical Society. Available from: www.okhistory.org (Accessed March 09, 2016).

Wissel, B., Boeing, W. J., & Ramcharan, C. W. (2003). Effects of water color on predation regimes and zooplankton assemblages in freshwater lakes. *Limnology and Oceanography, 48*(5), 1965-1976.

Worrall, F., Burt, T., & Shedden, R. (2003). Long term records of riverine dissolved organic matter. *Biogeochemistry, 64*(2), 165-178.

Worsfold, P.J. (2005). Spectrophotometry-Overview, In *Encyclopedia of Analytical Science* (Second Edition), edited by Paul Worsfold Alan Townshend Colin Poole, Elsevier, Oxford, 2005, Pages 318-321, doi; http://dx.doi.org/10.1016/B0-12-369397-7/00714-7.

Yallop, A. R., & Clutterbuck, B. (2009). Land management as a factor controlling dissolved organic carbon release from upland peat soils 1: Spatial variation in DOC productivity. *Science of the Total Environment, 407*(12), 3803-3813.

Yan, J., Wang, L., Fu, P. P., & Yu, H. (2004). Photomutagenicity of 16 polycyclic aromatic hydrocarbons from the US EPA priority pollutant list. *Mutation Research/Genetic Toxicology and Environmental Mutagenesis,557*(1), 99-108.

Yao, Z., Xiao, J., Ta, W., & Jia, X. (2013). Planform channel dynamics along the Ningxia–Inner Mongolia reaches of the Yellow River from 1958 to 2008: analysis using Landsat images and topographic maps. *Environmental Earth Sciences, 70*(1), 97-106.

Yue, P. (2006). TMDL development for Cobb Creek watershed and Fort Cobb lake. Final Report (FY99 Section 319(h) Grant # C9996100-07), June 26, 2006. Oklahoma Department of Environmental Quality.

Zabaleta, A., Martínez, M., Uriarte, J. A., & Antigüedad, I. (2007). Factors controlling suspended sediment yield during runoff events in small headwater catchments of the Basque Country. *CATENA, 71*(1), 179-190, doi:http://dx.doi.org/10.1016/j.catena.2006.06.007. APA. (2010).

APPENDICES

COLOR-DOC RAW DATA

Individual Sources

Table A.1. Color-DOC measurement data for set-I, Sphagnum peat moss. DOC = dissolved organic carbon; PCU = platinum cobalt unit; Abs = absorbance; ID = identification; max = maximum; PMA = peat moss sample set A followed by sample number; KHP = Potassium hydrogen phthalate

Peat Moss (PM): Set-I					
Sample ID	**Color (PCU)**	**DOC (mg/l)**	**Abs (455)**	**Abs (max)**	**Wavelength (max)**
PMA-1	400	68	0.258	2.878	288
PMA-2	357	61	0.230	2.629	289
PMA-3	319	59	0.206	2.417	290
PMA-4	281	49	0.181	2.132	289
PMA-5	245	44	0.158	1.898	287
PMA-6	203	37	0.131	1.601	281
PMA-7	163	27	0.105	1.313	281
PMA-8	121	23	0.078	0.966	282
PMA-9	82	15.	0.053	0.659	281
PMA-10	41	6.2	0.026	0.315	283

Standard Check:

KHP (100 mg/L) = 99 mg/L (measured)

Table A.2. Color-DOC measurement data for set-II, Sphagnum peat moss. DOC = dissolved organic carbon; PCU = platinum cobalt unit; Abs = absorbance; ID = identification; max = maximum; PMA = peat moss sample set B followed by sample number and KHP = Potassium hydrogen phthalate

Sphagnum Peat moss (PM): Set-II					
Sample ID	**Color (PCU)**	**DOC (mg/l)**	**Abs (455)**	**Abs (max)**	**Wavelength (max)**
PMB-1	396	71	0.256	2.907	289
PMB-2	360	66	0.232	2.663	292
PMB-3	316	56	0.203	2.439	288
PMB-4	278	49	0.179	2.166	287
PMB-5	246	44	0.159	1.879	287
PMB-6	200	34	0.129	1.601	284
PMB-7	161	28	0.104	1.284	283
PMB-8	122	21	0.079	0.997	281
PMB-9	84	15.2	0.054	0.656	281
PMB-10	42	6.7	0.027	0.33	281

Standard Check:

KHP (50 mg/L) = 47 mg/L (measured)

Table A.3. Color-DOC measurement data for set-III, Sphagnum peat moss. DOC = dissolved organic carbon; PCU = platinum cobalt unit; Abs = absorbance; ID = identification; max = maximum; PMA = peat moss sample set B followed by sample number and KHP = Potassium hydrogen phthalate

Sphagnum peat moss (PM): Set-III					
Sample ID	**Color (PCU)**	**DOC (mg/l)**	**Abs (455)**	**Abs (max)**	**Wavelength (max)**
PMC-1	394	69	0.254	2.911	292
PMC-2	355	62	0.229	2.606	293
PMC-3	315	53	0.204	2.402	292
PMC-4	276	49	0.178	2.146	286
PMC-5	238	41	0.154	1.868	288
PMC-6	200	35	0.129	1.638	278
PMC-7	163	28	0.105	1.3	282
PMC-8	121	21	0.078	0.977	281
PMC-9	87	14.4	0.056	0.662	281
PMC-10	44	6.3	0.028	0.313	281

Standard Check:

KHP (10 mg/L) = 9.2 mg/L (measured)

Table A.4. Color-DOC measurement for decomposing bark chips. DOC = dissolved organic carbon; PCU = platinum cobalt unit; Abs = absorbance; ID = identification; max = maximum; BC = bark chips followed by sample number; R = replicate sample and KHP = Potassium hydrogen phthalate

Decomposing bark chips (BC)					
Sample ID	**Color (PCU)**	**DOC (mg/l)**	**Abs (455)**	**Abs (max)**	**Wavelength (max)**
BC-1	437	43	0.282	2.98	290
BC-2	390	36	0.251	2.71	292
BC-2R	391	38	0.252	2.69	292
BC-3	346	33	0.223	2.55	288
BC-4	302	30	0.195	2.21	287
BC-4R	303	30	0.196	2.28	284
BC-5	259	26	0.167	1.91	283
BC-6	213	22	0.138	1.71	281
BC-6R	215	22	0.139	1.64	282
BC-7	170	16	0.109	1.33	282
BC-8	127	14	0.082	1.00	281
BC-8R	137	13	0.088	1.01	282
BC-9	82	7.6	0.053	0.70	281
BC-10	43	3.2	-	0.34	281
BC-10R	40	2.6	0.026	0.32	283

Standard Check:

KHP (100 mg/L) = 101 mg/L (measured)

Table A.5. Color-DOC measurement data for cotton burr compost. DOC = dissolved organic carbon; PCU = platinum cobalt unit; Abs = absorbance; ID = identification; max = maximum; CB = cotton burr compost followed by sample number; R = replicate sample and KHP = Potassium hydrogen phthalate

Cotton burr compost (CC)					
Sample ID	**Color (PCU)**	**DOC (mg/l)**	**Abs (455)**	**Abs (max)**	**Wavelength (max)**
CB-1	490	26	0.316	1.862	282
CB-2	437	24	0.282	1.723	281
CB-2R	438	23	0.282	1.756	281
CB-3	391	19	0.252	1.557	281
CB-4	339	17	0.219	1.366	281
CB-4R	339	16	0.219	1.362	281
CB-5	291	15	0.187	1.180	280
CB-6	242	14	0.156	0.990	281
CB-6R	241	14	0.156	0.994	280
CB-7	195	11	0.125	0.798	280
CB-8	144	5.6	0.093	0.596	280
CB-8R	144	6.3	0.093	0.598	280
CB-9	95	3.4	0.061	0.410	278
CB-10	46	0.5	0.030	0.226	279
CB-10R	48	1.5	0.031	0.228	278

Standard Check:

KHP (100 mg/L) = 97 mg/L (measured); KHP (10 mg/L) = 9.8 mg/L (measured)

Table A.6. Color-DOC measurement data for set-III, cow compost. DOC = dissolved organic carbon; PCU = platinum cobalt unit; Abs = absorbance; ID = identification; max = maximum; CM = cow compost, followed by sample number; R = replicate sample and KHP= Potassium hydrogen phthalate

Composted cow manure (CM)					
Sample ID	**Color (PCU)**	**DOC (mg/l)**	**Abs (455)**	**Abs (max)**	**Wavelength (max)**
CM-1	471	-	-	-	-
CM-2	382	-	-	-	-
CM-2R	379	-	-	-	-
CM-3	335	21	-	-	-
CM-4	286	19	0.185	1.459	287
CM-4R	288	18	0.185	1.493	284
CM-5	242	16	0.156	1.27	283
CM-6	206	14	0.133	1.073	281
CM-6R	205	13	0.132	1.041	282
CM-7	165	9.5	0.107	0.846	282
CM-8	128	7.5	0.082	0.619	281
CM-8R	128	6.9	0.082	0.627	282
CM-9	84	3.6	0.054	0.408	281
CM-10	42	2	0.027	0.71	281
CM-10R	43	1.8	0.028	0.71	283

Standard Check:

KHP (100 mg/L) = 94 mg/L (measured)

Heterogeneous Mixture

Table A.7. Measured DOC for individual source for heterogeneous mixture (set-I). DOC = dissolved organic carbon; Abs = absorbance; max = maximum; PM = peat moss; CM = cow manure; BC = bark chips and CC = cotton compost

Source	Measured DOC (mg/L)	Abs (max)	Wavelength (max)
PM	34	1.563	282
CM	15.	1.243	282
BC	16	1.247	281
CC	6.4	0.566	281

Table A.8. Color measurement for heterogeneous mixture of color-DOC sample on set-I source combination. All sources were in equal proportions for these samples. DOC = dissolved organic carbon; Abs = absorbance; max = maximum; PM = peat moss; CM = cow manure; BC = bark chips and CC = cotton compost

Source Combination	Measured Color (PCU)
PM + CM	216
PM + BC	175
PM + CC	170
CM + BC	173
CM + CC	174
BC + CC	133
PM + CM + BC	188
PM + CM + CC	195
PM + BC + CC	156
CM + BC + CC	160
PM+ CM + BC + CC	174

Table A.9. Measured DOC for individual source for heterogeneous mixture (set-II). DOC = dissolved organic carbon; Abs = absorbance; max = maximum; PM = peat moss; CM= cow manure; BC = bark chips and CC = cotton compost

Source	DOC Measured (mg/L)	Abs (max)	Wavelength (max)
PM	64	1.563	282
CM	19	1.243	282
BC	37	1.247	281
CC	5.6	0.566	281

Table A.10. Color measurement for heterogeneous mixture of color-DOC sample on set-II source combination. All sources were in equal proportions for these samples. DOC = dissolved organic carbon; PM = peat moss; CM = cow manure; BC = bark chips; CC = cotton compost and PCU = Platinum Cobalt Unit

Source Combination	Measured Color (PCU)
PM + CM	357
PM + BC	383
PM + CC	266
CM + BC	308
CM + CC	198
BC + CC	222
PM + CM + BC	349
PM + CM + CC	277
PM + BC + CC	291
CM + BC + CC	245
PM+ CM + BC + CC	291

Table A.11. Measured DOC for individual source for heterogeneous mixture (set-III). DOC = dissolved organic carbon; Abs = absorbance; max = maximum; PM = peat moss; CM = cow manure; BC = bark chips and CC = cotton compost

Source	**Measured DOC (mg/L)**	**Abs (max)**	**Wavelength (max)**
PM	64	2.821	289
CM	27	2.566	288
BC	32	2.588	288
CC	21	1.898	282

Table A.12. Color measurement for heterogeneous mixture of color-DOC sample on set-III source combination. All sources were in equal proportions for these samples. DOC = dissolved organic carbon; PM = peat moss; CM = cow manure; BC = bark chips; CC = cotton compost and PCU = Platinum Cobalt Unit

Source Combination	**Measured Color (PCU)**
PM + CM	464
PM + BC	388
PM + CC	461
CM + BC	408
CM + CC	480
BC + CC	402
PM + CM + BC	415
PM + CM + CC	462
PM + BC + CC	413
CM + BC + CC	427
PM+ CM + BC + CC	437

Figures

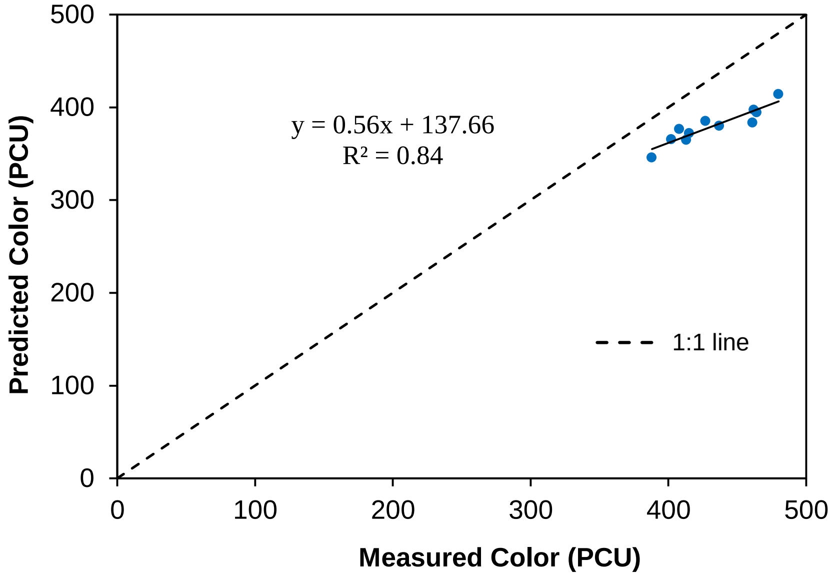

Figure A.1. Comparison between measured color and predicted color for heterogeneous sources of organic matter contained in colored water samples (set-III). The color unit is on Platinum Cobalt Unit (PCU). It was determined that the Hach test kits were likely not good for this data set due to being stored at too high of a temperature, so these data were not included in the validation.

VITA

Sagar Neupane

Candidate for the Degree of

Doctor of Philosophy

Thesis: ANTHROPOGENIC IMPACTS ON THE LANDSCAPE: INVESTIGATIONS IN WATER QUALITY AND CHANNEL STABILITY

Major Field: Biosystems and Agricultural Engineering

Biographical:

Education:

Completed the requirements for the Doctor of Philosophy in Biosystems and Agricultural Engineering at Oklahoma State University, Stillwater, Oklahoma in July, 2016.

Completed the requirements for the Master of Science in Civil Engineering at University of Idaho, Boise, Idaho in 2012.

Completed the requirements for the Bachelor of Civil Engineering at Pokhara University, Kaski, Nepal in 2006.

Experience:

August 2015-Current: Engineer In Training at Stantec Consulting Services, Cincinnati, OH

January 2012-July 2015: Graduate Research Associate, at Department of Biosystems and Agricultural Engineering, Oklahoma State University, Stillwater, OK

Professional Memberships:

American Society of Civil Engineers
Alpha Epsilon